ABIOTIC AND BIOTIC SEQUESTRATION OF SELENIUM IN ANOXIC COAL WASTE ROCK

A Thesis Submitted to the College of

Graduate and Postdoctoral Studies

In Partial Fulfillment of the Requirements

For the Degree of Master of Science

In the Department of Civil, Geological, and Environmental Engineering

University of Saskatchewan

Saskatoon

By

Sean Graham Deen

Permission to Use

In presenting this thesis/dissertation in partial fulfillment of the requirements for a Postgraduate degree from the University of Saskatchewan, I agree that the Libraries of this University may make it freely available for inspection. I further agree that permission for copying of this thesis/dissertation in any manner, in whole or in part, for scholarly purposes may be granted by the professor or professors who supervised my thesis/dissertation work or, in their absence, by the Head of the Department or the Dean of the College in which my thesis work was done. It is understood that any copying or publication or use of this thesis/dissertation or parts thereof for financial gain shall not be allowed without my written permission. It is also understood that due recognition shall be given to me and to the University of Saskatchewan in any scholarly use which may be made of any material in my thesis/dissertation.

Requests for permission to copy or to make other uses of materials in this thesis/dissertation in whole or part should be addressed to:

Head of the Department of Civil, Geological, and Environmental Engineering
University of Saskatchewan
57 Campus Drive
Saskatoon, Saskatchewan S7N 5A9
Canada

OR

Dean
College of Graduate and Postdoctoral Studies
University of Saskatchewan
116 Thorvaldson Building, 110 Science Place
Saskatoon, Saskatchewan S7N 5C9
Canada

Abstract

Waste rock dumps at coal mines in the Elk Valley are the primary source of selenium (Se) in the Elk River. The mobile Se oxyanions, Se(IV) and Se(VI), can be adsorbed to mineral phases or reduced biotically or abiotically to Se solid phases, such as Se(0). Microbial analyses and geochemical testing were conducted to determine if Se can be sequestered in anoxic coal waste rock by these mechanisms. Testing was conducted on a waste rock sample collected from the West Line Creek waste rock dump in the Elk Valley and a water sample collected from the rock drain flowing beneath the dump.

Microbial analyses included culturing with plate and broth media and 16S rRNA gene sequencing. The key finding from these analyses was that bacteria capable of reducing Se(VI) to Se(0) were present in the waste rock sample and bacteria capable of reducing Se(IV) to Se(0) were present in the rock drain water sample.

Geochemical tests included abiotic batch tests on waste rock and pure minerals, non-sterile batch tests on waste rock, and desorption batch tests on waste rock, as well as several solids analysis techniques, such as X-ray Absorption Spectroscopy and Energy Dispersive X-ray Spectroscopy. Batch tests were conducted at circumneutral pH in an anoxic glove box to simulate an anoxic zone of a waste rock dump. Batch testing on pure minerals present in the waste rock sample determined that siderite can reduce Se(VI) to Se(IV) and that siderite, pyrite, and sphalerite can adsorb Se(IV) and reduce Se(IV) to Se(0). Under sterile conditions, waste rock did not reduce Se(VI) but it did adsorb Se(IV) and reduce Se(IV) to Se(0). Under non-sterile conditions, Se(VI) was reduced to Se(IV) much faster than the sterile tests with siderite and Se(IV) was removed from solution by a combination of adsorption, biotic reduction, and abiotic reduction. Desorption batch testing showed that a fraction of sequestered Se was susceptible to desorption but that the fraction decreased over time. These findings suggest that sequestration of Se in anoxic coal waste rock is a viable method to decrease the amount of Se discharging from Elk Valley waste rock dumps.

Acknowledgements

I would like to thank my supervisors Dr. Lee Barbour and Dr. Jim Hendry for their support and guidance throughout my graduate studies. The advice and expertise of my advisory committee members, Dr. Matt Lindsay, Dr. Won Jae Chang, and Dr. Lisa Feldman, was also greatly appreciated. I am grateful for the microbiological training and support provided by Dr. Viorica (Ibi) Bondici. Without Ibi's help, the objectives of my thesis would not have been possible. Further, the lab expertise and willingness of Fina Nelson, Erin Schmeling, Tom Bonli, Jing Chen, Jianzhong Fan, and Sandeepraja Dangeti to collectively analyse well over a thousand aqueous and solid samples cannot go unmentioned. I would also like to acknowledge Dr. Darren Korber, who provided me access to his microbiology labs, equipment, and supplies.

I am very grateful for the financial assistance provided by my supervisors (NSERC-IRC funds to MJH (184573) and SLB (IRCPJ 428588-11)), the Department of Civil and Geological Engineering, the Saskatoon Branch of the Canadian Institute of Mining, Metallurgy and Petroleum, SRK Consulting (Canada) Inc., and BGC Engineering Inc. I am also thankful to Teck Resources Limited for providing technical expertise, allowing us to use samples collected from their waste rock dump, funding experiments, and giving me the opportunity to work on such an interesting research project.

Without the love and support of my wife, Chantelle, I would not have started my graduate program at the University of Saskatchewan, let alone finished it. I couldn't have done it without her. I would also like to acknowledge the encouragement I received from my fellow graduate students and friends, Matthew Buchynski, James Tipman, Terryn Kuzyk, Colleen Steele, Marcie Schabert, Mike Amos, and Jihun Kim.

Table of Contents

List of Tables

List of Figures

List of Abbreviations

BET – Brunauer–Emmett–Teller

BSE – Backscattered Electron

BSM – Basal Salt Media

CFU – Colony Forming Unit

EDS – Energy Dispersive X-Ray Spectroscopy

EXAFS – Extended X-ray Absorption Fine Structure

HPLC – High Performance Liquid Chromatography

IC – Ion Chromatography

ICP-MS – Inductively Couple Plasma Mass Spectroscopy

LCF – Linear Combination Fit

PIPES – 1,4-Piperazinediethanesulfonic acid

R2A – Reasoner's 2A media

RDP – Ribosomal Database Project

SEM – Scanning Electron Microscope

WDS – Wavelength Dispersive Spectroscopy

WLC – West Line Creek Waste Rock Dump

XANES – X-ray Absorption Near Edge Spectroscopy

XAS – X-ray Absorption Spectroscopy

XRD – X-ray Diffraction

1 Introduction

1.1 Background and Significance

Selenium (Se) is a naturally-occurring trace element essential for human and animal life (Beatty and Russo, 2014). It is also an environmental contaminant with a range of toxic effects (Lemly, 2004). Coal is naturally enriched with Se and, as a result, the mining, processing, and combustion of coal is one of the primary causes of Se release in the environment (Lemly, 2004). Elevated Se concentrations in the Elk River of southeast British Columbia, Canada are attributed to open pit coal mining along the valley (Figure 1-1; McDonald and Strosher, 1998; Wellen et al., 2015). Since the late 1990s, the concentration of Se immediately upstream of the mouth of the Elk River (at Lake Koocanusa) has exceeded 2 µg/L, the British Columbia Ministry of Environment water quality guideline for aquatic life (Beatty and Russo, 2014; Swanson, 2010). Teck Resources Limited (2014), the operator of five open pit steelmaking coal mines in the Elk Valley (Figure 1-1), is undertaking a large, multi-disciplinary research program to develop and implement measures to address the trend of increasing Se in Elk Valley. The research contained within this thesis was conducted in support of this research program.

The solubility, mobility, and bioavailability of Se are dependent on its oxidation state. In moderately to highly oxidizing conditions, Se is present as one of the oxyanions selenite ($Se^{IV}O_3^{2-}$) or selenate ($Se^{VI}O_4^{2-}$) which are soluble in water and thus mobile and bioavailable. The Se oxyanions are the dominant species of Se in well-oxygenated streams, runoff, and shallow infiltrating waters (Dungan and Frankenberger, 1999). The Se(IV) oxyanion strongly sorbs to some minerals (Balistrieri and Chao, 1987; Bar-Yosef and Meek, 1987; Rovira et al., 2008; Scheinost et al., 2008; Tachi et al., 1998). Conversely, Se(VI) adsorbs to fewer solids than Se(IV) and often by weaker bonds, which generally results in less attenuation during transport in groundwater (Balistrieri and Chao, 1987; Day et al., 2012; Hayes et al., 1987). Under reducing conditions, Se is found as elemental Se (Se(0)) which is insoluble, or one of the selenide anions (ie: Se(-I) and Se(-II)), which form a number of insoluble metallic compounds, such as FeSe and

$FeSe_2$ (Fernández-Martínez and Charlet, 2009; Lenz and Lens, 2009)). Given its redox-sensitive properties, the two key geochemical controls on the transport of Se are the adsorption of Se(IV) and precipitation of one of the reduced Se solid phases. Any Se removed from groundwater by one of these mechanisms will be immobilized. The removal of Se from solution and concomitant immobilization is referred to as sequestration herein.

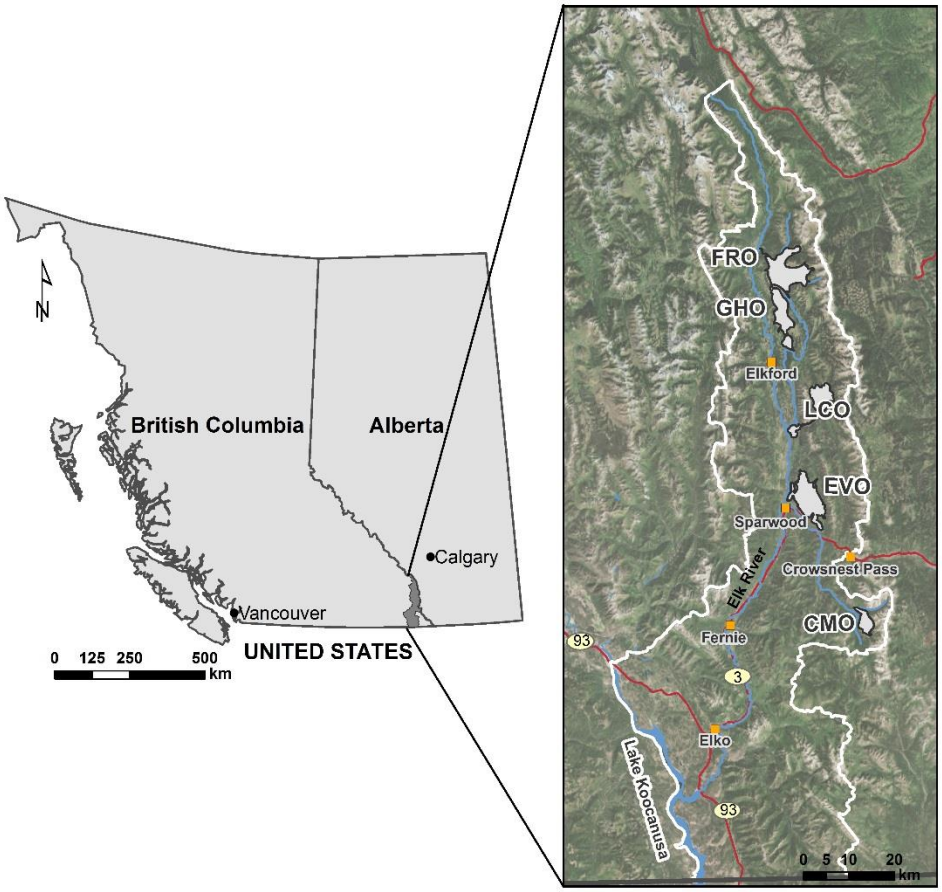

Figure 1-1: Location of five coal mining operations in the Elk Valley, British Columbia, Canada. The solid white line indicates the edge of the Elk River watershed (after Villeneuve et al., 2017).

Regional water quality modelling indicates that coal waste rock dumps in the Elk Valley are the source of approximately 80% of the Se load in the Elk River (Wellen et al., 2015). The primary source of aqueous-phase Se in the waste rock is the Se(-I,-II)-containing sulfide minerals pyrite (FeS_2) and sphalerite (ZnS) (Hendry et al., 2015). These minerals are oxidized in the waste rock dump by oxygen (O_2) (Essilfie-Dughan et al., 2017; Lussier et al., 2003; Wellen et al., 2015). Nitrate (NO_3^-) introduced to the waste rock during blasting may also oxidize the Se(-I,-II)-

containing minerals (Mahmood et al., 2017; Wellen et al., 2015). The oxidation of the sulfide minerals mobilizes incorporated Se(-I,-II) as Se(VI) (Day et al., 2012).

As a part of its Elk Valley Water Quality Plan, Teck Resources Limited (2014) is working to "identify a strategy and implement solutions to address increasing selenium" in the Elk River. This thesis investigates aspects of one potential solution - establishing water-saturated zones within the waste rock to remove Se from water migrating through the waste rock before it is discharged to the receiving environment. By limiting the ingress of O_2, water-saturated zones may allow natural biogeochemical controls to sequester Se within the waste rock. Such controls include the reduction of Se(VI) to Se(IV) or Se(0) by bacteria (Stolz and Oremland, 1999) and the adsorption and subsequent reduction of Se(IV) to Se(0) by the mineral phases such as pyrite (Bruggeman et al., 2005) and siderite (Badaut et al., 2012). The potential for these Se sequestration mechanisms to take place in anoxic coal waste rock was assessed by conducting microbiological and geochemical laboratory tests on one solid sample and one solution sample collected from a waste rock dump in the Elk Valley. The primary laboratory techniques employed in this thesis were batch testing and culturing. Batch testing was also conducted with Se(IV) and Se(VI) solutions buffered at pH 7 and pure mineral samples of siderite, pyrite, and sphalerite.

1.2 Objectives and Scope

This study investigated the potential for Se sequestration in coal waste rock under anoxic conditions by abiotic and biotic processes. The objectives of this thesis were to:

1. develop anoxic, abiotic laboratory procedures for batch testing;
2. assess the potential for adsorption, abiotic reduction, and biotic reduction of Se(IV) and Se(VI) in anoxic coal waste rock from the Elk Valley;
3. determine which, if any, of the Fe(II)-bearing or sulfide minerals known to be present in coal waste rock (siderite, pyrite, and sphalerite) can remove Se(IV) and Se(VI) from solution under anoxic conditions;
4. quantify abiotic Se(IV) sequestration in one coal waste rock sample using a sorption isotherm and reduction rates; and
5. determine the fraction of waste rock-sequestered Se that is susceptible to desorption.

The hypotheses of this study were that (1) Se(IV) and (2) Se(VI) could be removed from solution by a coal waste rock sample under anoxic conditions via (a) biotic mechanisms and (b) abiotic mechanisms. The conclusions of this study could assist Teck Resources Limited in selecting methods of ameliorating Se releases from coal waste rock dumps in the Elk Valley; however, the methods and key findings are not specific to coal waste rock dumps or to Se contamination and, thus, may be useful for others investigating complicated biogeochemical reaction mechanisms.

The scope of this study was limited to:

- characterization of the solids used in batch tests;
- isolation and identification of two bacteria isolated from the coal waste rock sample and two bacteria isolated from the rock drain water sample;
- laboratory batch tests on pure minerals and one coal waste rock sample;
- desorption batch tests to confirm presence of adsorbed Se on coal waste rock; and
- calculation of pertinent geochemical parameters for Se(IV) adsorption and reduction by the coal waste rock sample.

This study did not include:

- molecular or DNA analysis of microbial communities;
- creation of a hydrogeological or contaminant transport model; or
- an investigation into the risk of remobilization of sequestered Se.

1.3 Format of Thesis

This thesis was prepared as a manuscript-style thesis. It includes two manuscripts that present different aspects of the research program. Because journal restrictions on the manuscripts did not allow for a full review of pertinent literature, a detailed literature review is included (Chapter 2). The literature review provides geochemical and microbiological concepts important to this research, as well as the context for the necessity of the research. Abiotic laboratory procedures are developed (Objective 1) and used in conjunction with microbiological methods in the first manuscript (Chapter 3) to determine whether Se(IV) and Se(VI) can be adsorbed, abiotically reduced, or biotically reduced by waste rock (Objective 2). In the second manuscript (Chapter 4), the minerals in the waste rock sample that remove Se(IV) and Se(IV) from solution are determined

(Objective 3), abiotic Se(IV) removal from solution by the waste rock sample is quantified (Objective 4), and the fraction waste rock-sequestered Se that was susceptible to desorption is determined (Objective 5). Finally, major findings and conclusions developed in the two manuscripts are summarized in the Summary and Conclusions (Chapter 5).

2 Literature Review

The mechanisms of Se sequestration important to this study are adsorption of Se(IV) and Se(VI) to solid surfaces and reductive precipitation of Se solid phases, such as Se(0) and metallic Se(-I) and Se(-II) compounds. These mechanisms are described in more detail in the first two subsections of this chapter. This background provides the context for the following subsections, which highlight findings in pertinent literature studies.

2.1 Adsorption

Adsorption is a solute attenuation process that partitions solute ions between the aqueous and adsorbed phases resulting in slower rates of solute transport. Adsorption occurs as solute ions form either inner-sphere or outer-sphere complexes with the solid surface. Inner-sphere complexes are bonded chemically while outer-sphere complexes are bonded electrostatically. Inner-sphere complexes are stronger than outer-sphere complexes. Outer-sphere complexation is limited to ions with mineral surfaces of opposite charge while inner-sphere complexation occurs independently of the mineral and ion charges and is generally independent of most other ions in solution (Bostick et al., 2003; Langmuir, 1997). The Se oxyanions and the mineral surfaces of interest are net negative in neutral and alkaline solutions—pyrite and sphalerite have a net negative surface charge in solutions with a pH above 3 (Bebie et al., 1998; Curti et al., 2013; Weerasooriya and Tobschall, 2005) and siderite has a negative surface charge above pH 5.3 (Charlet et al., 1990). However, the Se(IV) oxyanion has been reported to form outer-sphere complexes with ferrous iron, Fe(II), sorbed to negative surfaces such as calcite (Chakraborty et al., 2010) and montmorillonite (Charlet et al., 2007). In addition to this, Se(IV) and Se(VI) adsorb to Fe(III)-oxyhydroxides, such as hematite and goethite (Hayes et al., 1987; Peak and Sparks, 2002; Rovira et al., 2008), which are produced by oxidation of pyrite in the coal waste rock (Hendry et al., 2015).

The number of adsorption sites on a mineral filled with a particular ion is dependent on the adsorption capacity of the mineral, the concentration of that particular ion in solution, and other

geochemical properties of the solution (e.g., temperature, pH, concentration of competing ions) (Appelo and Postma, 2005). The adsorption capacity of the mineral is determined by the total surface area available to the solute ions and the surface charge on the solid. If the concentration of the ion in question is small relative to the number of available adsorption sites, the relationship between solute ions and adsorbed ions is linear and independent of the number of adsorption sites. This is generally the case for trace elements such as Se. A partitioning, or distribution, coefficient (K_d, [(mg/kg adsorbent) / (mg/L solution)] or [L/kg]) is used to describe the linear relationship between the adsorbed and solute ions (Appelo and Postma, 2005).

Adsorption attenuates the rate of ion transport through groundwater systems. Although adsorption leads to a removal of solute ions from solution, the continuing transport of ions from a constant source concentration will eventually result in the filling of all available adsorption sites. At this point, ions will be transported through the system unattenuated. If the source of Se exceeds the number of available adsorption sites in a waste rock dump, adsorption of Se species by minerals within the waste dump will not be a potential mechanism for long-term Se sequestration on its own. The partitioning of Se species to mineral phases may, however, act to enhance other sequestration mechanisms, such as reductive precipitation (described in the following subsection).

2.2 Oxidation-Reduction (Redox) Reactions

Redox reactions involve the transfer of electrons from atoms of one redox element to atoms of another. The deficiency or surplus of electrons in a given atom is referred to as its oxidation state; Se(VI) is in a +6 oxidation state and is deficient of 6 electrons; Se(-II) is in a -2 oxidation state and has 2 excess electrons. The oxidation state of a Se atom has a significant effect on its properties. The Se oxyanions, $Se^{IV}O_3^{2-}$ and $Se^{VI}O_4^{2-}$, are soluble in water and, thus, mobile. Elemental Se (Se(0)) and metallic Se(-I) and Se(-II) compounds are insoluble and immobile (Fernández-Martínez and Charlet, 2009). When aqueous Se(IV) is reduced to Se(0), it precipitates as a solid. This process is called reductive precipitation. Other redox elements relevant to this study (and their redox states) include carbon (C; 4+, 0, 2-, 4-), hydrogen (H; 1+, 0), oxygen (O; 0, 2-), nitrogen (N; 5+, 3+, 0, 3-), iron (Fe; 3+, 2+, 0), and sulfur (6+, 4+, 0, 1-, 2-) (Langmuir, 1997). The relationship between two redox states of a single element is called a redox couple and is often expressed as a half reaction. An example redox couple is:

$$Fe^{2+} \leftrightharpoons Fe^{3+} + e^{-} \quad (2.1)$$

Free electrons do not exist on their own in real systems. They must be transferred to another element. An example of this is the reduction of $N^{V}O_3^-$ to elemental nitrogen, N(0), by Fe(II) (Appelo and Postma, 2005):

$$2NO_3^- + 12H^+ + 10e^- \leftrightharpoons N_2 + 6H_2O \quad (2.2)$$

$$10Fe^{2+} + 2NO_3^- + 12H^+ \leftrightharpoons 10Fe^{3+} + N_2 + 6H_2O \quad (2.3)$$

The Fe(III) ion is not soluble in most groundwater and typically precipitates out of solution (ie: $FeOOH_{(s)}$).

Redox reactions proceed in the direction that will bring the oxidation states of each redox species into equilibrium with the other redox species in solution. Each redox couple has a characteristic standard potential, E^0 (V). The overall redox potential of a solution, Eh (V), is a measurement of all rapid-reacting redox species in the solution. Increasing values of Eh represent an increase in oxidizing agents. If the Eh in a solution is greater than E^0 for a particular redox pair, the concentration of the oxidized species will be greater than the concentration of the reduced species in that solution. Using Equation (2.1) as an example, a solution Eh below the E^0 for the Fe(II)/Fe(III) redox couple would result in the Fe(II) concentration being greater than the Fe(III) concentration. In typical shallow groundwater, the O_2-H_2O redox pair has the highest E^0 and the organic carbon-bicarbonate redox pair has the lowest E^0 (Langmuir, 1997). As such, the ultimate oxidants and reductants in shallow groundwater are O_2 and organic hydrocarbons, respectively.

Coal waste rock dumps contain both oxidizing and reducing agents. Atmospheric O_2 and NO_3^- are the agents responsible for oxidizing, and thus increasing the mobility, of Se in the waste rock (Day et al., 2012; Mahmood et al., 2017). Reducing agents present in the waste rock include Fe(II) in siderite and pyrite, sulfide (S(-I,-II)) in pyrite and sphalerite, and organic carbon in coal. The establishment of saturated zones in the waste rock could effectively limit O_2 ingress and cause a decrease in the redox potential of water migrating through the saturated waste rock. It is predicted that Se(VI) and Se(IV) will be reduced to an insoluble Se species, such as Se(0), Se(-I), or Se(-II), in saturated, O_2-free waste rock.

2.3 Microbial and Geochemical Controls on Se Transport

The toxic effects of Se in aquatic environments make the microbial and geochemical controls on its mobility and bioavailability very important. In general, the focus of most studies has been limited to either biotic or abiotic sequestration mechanisms. As such, studies of abiotic and biotic mechanisms are described separately herein. However, the microbial and geochemical controls on Se are often intertwined in the environment. For example, Se is sequestered in the sediments of two Elk Valley lentic environments as abiotically adsorbed Se(IV) and biologically-produced Se(0) and Se(-II) (Martin et al., 2011). Similarly, both abiotic and biotic processes are important to the current study. As such, the microbiological and geochemical laboratory techniques described in this chapter were used to develop the methods described in Chapter 3.

In unsaturated soil and shallow groundwater systems, Se is present as soluble oxyanions and its mobility is controlled by adsorption processes. Several studies have investigated the adsorption of Se(IV) in the presence of other anions and O_2 (Balistrieri and Chao, 1987; Neal et al., 1987a, 1987b). Balistrieri and Chao (1987) used pure, synthetic goethite (α-FeOOH) as an adsorbent and found that the reactions reached equilibrium in 2 h and were completely reversible. The amount of Se(IV) adsorbed to the goethite was dependent on temperature, the presence of competitive ions, and pH. The amount of adsorbed Se(IV) increased by 10-25% when the batch test temperature was decreased from 32°C to 22°C. The amount of adsorbed Se(IV) decreased in the presence of low concentrations of phosphate (PO_4^{3-}) or high concentrations of bicarbonate (HCO_3^-). Sulfate (SO_4^{2-}), even at high concentrations, had no effect on Se(IV) adsorption. Finally, Se(IV) adsorption was much greater below pH 7 than above pH 8. This was attributed to the net negative surface charge of goethite above pH 7.7 (Balistrieri and Chao, 1987). In parallel experiments, Se(VI) adsorption was far less than that of Se(IV) below pH 7 and negligible above pH 7. The same trend was found by Hayes et al. (1987), who used X-ray Absorption Spectroscopy (XAS) to determine that Se(IV) adsorbed to goethite by forming strong, inner-sphere complexes with goethite, while Se(VI) formed weak outer-sphere complexes. Neal et al. (1987a, 1987b) conducted batch tests using alluvial soils with naturally high levels of Se and found the same pH-dependent adsorption trends as Balistrieri and Chao (1987). In addition to attributing increased Se(IV) adsorption at low pH to net positive mineral surface charges, Neal et al. (1987a) also suggested that the increased Se(IV) adsorption at low pH may be due to the presence of hydrolyzed Se(IV) ($HSeO_3^-$), which is less

negative than SeO_3^{2-}, and the increased solubility of Fe and Al, which may form Se(IV)-adsorbing colloids.

Prior to 1990, studies regarding the mobility and bioavailability of Se generally focused on the adsorption of Se(IV) and Se(VI) under oxidizing conditions. The importance of redox potential and the solubility of Se in its reduced forms became very important when toxic concentrations of Se were found in evaporation ponds and sediments of the Kesterson National Wildlife Refuge in California (Masscheleyn et al., 1990; White et al., 1991). Masscheleyn et al. (1990) investigated the influence of pH and Eh on Se oxidation state and solubility by conducting laboratory experiments on Se-contaminated sediment samples collected from the Kesterson Reservoir while White et al. (1991) focused efforts on the geochemical characterization of a natural redox barrier that removed Se from infiltrating Se-contaminated waters. Laboratory testing showed Se was only present as Se(-II,0) at -200 mV (Masscheleyn et al., 1990). The oxidation of Se(-II,0) to Se(IV) was concurrent with Fe(II) oxidation to Fe(III) oxidation at 0 mV. It was noted that oxidation of Se(-II) occurred at a much higher Eh than S(-II). The oxidation of Se(IV) to Se(VI) was subsequent to NO_3^- production at +200 mV and occurred by a slow reaction, which resulted in comparable concentrations of Se(IV) and Se(VI). This slow reaction time and coexistence of Se(IV) and Se(VI) is referred to as redox disequilibrium and was also noted in the field studies (White et al., 1991). Finally, when the redox potential was increased to +450 mV, Se(VI) became the dominant species and the total Se concentration increased, likely as a result of the desorption of adsorbed Se(IV) during oxidation to Se(VI). The laboratory tests with induced redox conditions showed that Se speciation and biochemistry are correlative with other redox-sensitive ions (e.g., Fe(II), NO_3^-) in addition to pH and Eh (Masscheleyn et al., 1990); however, the strength of this correlation resulted from the induced redox potential of the system and does not suggest that the oxidation state of aqueous Se is solely dependent on the other redox species in solution. White et al. (1991) found that all Se(IV) and Se(VI) injected into an Se reducing formation was reduced to Se solid phases in 10 to 25 d but no Se(IV) or Se(VI) reduction occurred in closed vials that contained identical solutions under the same redox conditions. As such, Se immobilization was attributed to the solid substrate and attached microbial communities in the Se reducing formation rather than dissolved redox species.

The Se contamination at the Kesterson National Wildlife Refuge also prompted research into microorganisms in the environment that reduce Se oxyanions. Microorganisms reduce Se oxyanions as a means of detoxification, respiration, and synthesis of essential compounds. Examples of essential compounds are the amino acids selenocysteine and selenomethionine, which contain Se(-II) taken up by assimilatory reduction of aqueous Se oxyanions (Stolz and Oremland, 1999). Respiration and detoxification generally produce Se(0) by dissimilatory reduction, which results in the accumulation of Se nanosopheres outside of the cell envelope (Stolz et al., 2006). Biologically-produced Se nanospheres are red, and when allowed to accumulate, can act as an indicator for Se reduction by microbial colonies cultured on plate media (Hunter and Manter, 2009; Oremland et al., 2004). Using Se(VI)-enriched media, Maiers et al. (1988) determined that Se(VI)-reducing bacteria were present in 7 of 7 soil samples, 12 of 13 sediment samples, and 1 of 24 water samples collected near the Kesterson Reservoir. Burton et al. (1987) determined more than 50% of bacteria isolated from the Kesterson Reservoir were resistant to 10 mM Se(IV) while less than 5% of bacteria isolated from the Volta Reservoir, a non-polluted reservoir near the Kesterson Reservoir, were resistant to 10 mM Se(IV). Of 30 bacterial species isolated, all 30 reduced Se(IV) to Se(0) and 3 reduced Se(VI) to Se(0). Bacteria capable of reducing Se oxyanions have been isolated from other environments characterized by high Se concentrations (Oremland et al., 1990; Staicu et al., 2015; Switzer Blum et al., 2001), as well as environments with relatively low concentrations of Se (Ike et al., 2000; Steinberg and Oremland, 1990). In summary, Se(IV)-reducing bacteria are more common than Se(VI)-reducing bacteria and bacteria capable of Se reduction are more abundant in Se-contaminated environments than in environments free of contamination. Stolz and Oremland (1999) suggest that "bacteria capable of dissimilatory selenate reduction are abundant in nature" and that dissimilatory reduction is the most environmentally significant reduction process for Se oxyanions.

2.4 Relevant Se Sequestration Studies

Years after contamination of the groundwater at the Kesterson National Wildlife Refuge, White et al. (1991) found that migration of Se species through the reducing groundwater system below the contaminated reservoir was very limited and that "the potential of regional contamination from Se at Kesterson [was] an unlikely possibility". This study serves as an example of Se sequestration in a reducing geological formation. In addition to effectively controlling Se contamination,

geological formations characterized by reducing conditions may be effective as engineered Se containment systems for the long-term storage or disposal of Se-laden waste. An example of this application is the siting of high-level radioactive waste disposal systems that contain ^{79}Se, a radioactive isotope of Se and fission product of ^{235}U. The ^{79}Se is likely to be present as Se oxyanions and, with a half-life of around one million years, is expected to be "responsible for the highest dose [of radiation] to man over a period of tens of thousands of years" (Bruggeman et al., 2005). Investigations have found that geologic formations containing Fe(II), such as the Boom clay layer in Belgium (Bruggeman et al., 2005) or Tuff in Japan (Tachi et al., 1998), may be suitable sites for waste disposal. This has led to a great deal of research on Se sorption and reduction by Fe(II)-containing minerals, such as pyrite and siderite. The experimental details and key findings of some relevant studies are summarized in Table 2-1.

The adsorption and reduction of Se(IV) and Se(VI) by pyrite have been studied and documented extensively while studies on Se sequestration by siderite are limited to Se(IV). Pyrite can effectively adsorb Se(IV) and reduce Se(IV) to Se(0) and, possibly, Se(-I) or Se(-II) (Breynaert et al., 2008; Charlet et al., 2012; Naveau et al., 2007). The reduction of Se(VI) by pyrite occurs much slower than the reduction of Se(IV) and has only been confirmed in laboratory studies that have been kinetically enhanced by conducting batch tests at high temperatures (80°C; Curti et al., 2012) or with synthetic, nano-composite pyrite (Charlet et al., 2012). The electron donor for Se(IV) reduction is the S_2^{2-} in pyrite and not the Fe(II) (Han et al., 2012). In two sets of batch tests with siderite, Se(IV) was adsorbed and reduced to Se(0) (Badaut et al., 2012; Scheinost et al., 2008; Scheinost and Charlet, 2008). Badaut et al. (2012) determined the reduction of Se(IV) at the surface of siderite to be the most important process in the removal of Se(IV) from solution. The aforementioned studies on siderite did not conduct any batch tests with Se(VI).

Table 2-1: Key Findings of some relevant Se sorption and reduction studies.

Study	Experiment	Key findings
(Tachi et al., 1998)	Batch and through diffusion sorption tests: - Atmosphere: N_2, < 1 ppm O_2, room temp - Solution: deionized water, with 0.1 mM NaCl, 0.1-1 mM Se(IV), pH: varied 2-13 - Solid: Tuff (75-355 µm, 57 m^2/g), 400 g/L; natural and synthetic minerals, 25-50 g/L; 5 mm thick tuff for diffusion test - Time length: 14 d batch tests, 30 d diffusion tests	- Tuff sorbed 90% of Se below pH 8, decreases to 30% with increasing pH - Pyrite and Fe-oxyhydroxide sorbed 90% of Se below pH 8, decreases to 10% with increasing pH - Other minerals sorbed less Se but showed the same trend of decreasing sorption with increasing pH - Fe minerals most important for Se(IV) sorption - At pH 8: $K_{d,batch}$ = 23 L/kg, $K_{d,diff}$ = 1.1 L/kg - normalized by surface area of pores > 20 nm, $K_{d,batch} \approx K_{d,diff}$
(Bruggeman et al., 2005)	- Atmosphere: 99.6% N_2, 0.4% CO_2, ~2 ppm O_2, 22°C - Solution: synthetic and actual Boom clay water ($CaCO_3$ saturated), with 5-10 µM Se(IV), pH: 8.2-8.3 - Solid: natural pyrite (<125 µm), 2.5-10 g/L; Boom clay, 250 g/L - Time length: 2-9 months	- K_d = 660 – 151 445 L/kg, 60-99% removal after 2 months, tests did not appear to be at equilibrium; - given transport rates through clay, this is expected to be sufficient for ^{79}Se containment - Addition of HS^- hampered reduction of Se(IV) to Se(0) - Suggests Se(IV) reduction by pyrite is "initiated by an adsorption reaction"
(Naveau et al., 2007)	- Atmosphere: N_2, < 1 ppm O_2, CO_2, 25°C - Solution: deionized water with 50 mM $NaClO_4$, 0.1 mM Se(IV) or Se(-II), pH: varied 2-10 - Solid: natural and synthetic pyrite (1.1 and 0.8 m^2/g, respectively), 8 g/L - Time length: 24 h	- Uptake of Se(-II) and Se(IV) nearly identical - Synthetic: 95% adsorption for pH < 5, ~5% for pH > 7 - Natural: 65% adsorption for pH = 2, <15% for pH > 7 - XAS[1] revealed that Se(IV) reduction associated with S(-II) oxidation rather than Fe(II) oxidation - All Se on surfaces was reduced solid phase - did not differentiate between Se(0), Se(-I), and Se(-II)
(Charlet et al., 2007)	- Atmosphere: N_2, < 1 ppm O_2, 25°C - Solution: deionized water with 50 mM $CaCl_2$, 5 mM Fe(II), 0.5 mM Se(IV), pH: 6.5 - 7.6 - Solid: synthetic montmorillonite, 20 g/L - Time length: 30 d	- 10-15% of Fe sorbed to clay, < 5% Se sorbed, sorption only monitored for 10 h. - ~40% sorbed Se(IV) reduced to Se(0) in 6 h, ~75% reduced in 30 d - reduced Se only present as Se(0)

Table 2-1: Key Findings of some relevant Se sorption and reduction studies (Continued).

Study	Experiment	Key findings
(Scheinost et al., 2008; Scheinost and Charlet, 2008)	- Atmosphere: N_2, < 1 ppm O_2, 23°C - Solution: deionized water with 5 mM $CaCl_2$, 1 mM Se(IV), pH: 8.3 - Solid: Synthetic siderite (3 µm), 20 g/L - Time length: 24 h	- After 24 h, ~60% Se present as precipitated Se(0), ~39% Se(IV) adsorbed to surface, 0.6% of Se(IV) in solution - Fe(II) is the electron donor for Se(IV) reduction - reduction by siderite slower than the other tested Fe(II) minerals, attributed to lower surface area of siderite
(Breynaert et al., 2008)	- Atmosphere: 95% N_2, 5% H_2, < 2 ppm O_2, - Solution: deionized water with 6.14 mM Se(IV), pH: 6.5-8.5 - Solid: Natural pyrite (<100 µm, <10 µm; 0.88, 4.42 m^2/g), 20 g/L - Time length: 2-3 weeks	- K_d = 3.6 – 15.9 L/kg (100 µm), 14.1 - 172.9 L/kg (10 µm) - K_d lowered by HCl pretreatment and increased pH - Oxidation of FeS_2 to FeOOH may enhance Se(IV) sorption - H_2 does not enhance Se(IV) reduction - Supports the Se(IV) adsorption and subsequent reduction to Se(0) mechanism proposed by Bruggeman et al. (2005)
(Chakraborty et al., 2010)	- Atmosphere: N_2, < 1 ppm O_2, CO_2 - Solution: deionized water with 4.1 mM $NaHCO_3$, 4.9 mM $CaCl_2$, 0.06 or 0.4 mM Fe(II), 0.12 or 0.24 mM Se(IV), pH: 7.0 - Solid: natural calcite (100-140 µm), 2.5 g/L - Time length: 1 and 24 h	- Fe(II) quickly adsorbed onto calcite surface (minutes) and slowly incorporated into crystal lattice (weeks) - Fe(II) in lattice protected from oxidation, not effective for reducing Se(IV) - up to 45% of sorbed Se reduced to Se(0) on calcite with high adsorbed Fe(II) content, <5% without adsorbed Fe(II). - 2% Se(IV) sorbed in 72 h without Fe(II), 6% sorbed in 1 h with Fe(II), and 20% sorbed with Fe(II) in 24 h
(Kang et al., 2011)	- Atmosphere: O_2-free glove box, 25°C - Solution: deionized water with 10 mM NaCl, 1.5 mM Se(IV), pH: 4.5, 6 (acetate, phosphate buffered) - Solid: natural pyrite (90-120 µm, 0.11 m^2/g), 7.5 g/L - Time length: 7 and 33 d	- Se reduction in first 7 d was minor at pH 4.5, 6 - Reduction from 12-33 d was pseudo-first order reaction - 7-15% Se(IV) removal at pH 4.5-5.1 - Inferred that Fe(II) is adsorbed to pyrite and reduces Se on surface - Acid addition to maintain pH required throughout experiment, attributed to formation of $Fe(OH)_3$

Table 2-1: Key Findings of some relevant Se sorption and reduction studies (Continued).

Study	Experiment	Key findings
(Badaut et al., 2012)	- Atmosphere: 85% N_2, 10% CO_2, 5% H_2, <1 ppmv O_2 - Solution: deionized water with 0.1 M NaCl, 0.05 M $NaHCO_3$, 0.74 mM Se(IV), pH: 7.3, imposed redox potential: -400 mV NHE - Solid: synthetic siderite (1-10 µm), 75 g/L - Time length: 24 h	- 35% removal of Se from solution in 10 m, 83% in 8 h, and 94% in 24 h - At 20 h, 60% of Se(IV) was reduced to Se(0); ~35% of Se removed from solution in the experiment was due to Se(IV) adsorption to siderite - Adsorption of Se(IV) occurs before reduction of Se(IV) to Se(0)
(Charlet et al., 2012)	- Atmosphere: N_2, < 2 ppm O_2 - Solution: deionized water with 50 mM acetate buffer, 20 mM $NaClO_4$, 0.4 mM Se(IV), 0.5 mM Se(VI), pH: 6.0 - Solid: synthetic pyrite/greigite mixture (< 150 nm), 4.28 g/L - Time length: 14 d	- >90% Se(IV) adsorbed at pH 6 in 30 m, 40-60% at pH 8-9, reduction enhanced with 0.1 mM Fe(II), complete reduction after 14 d - 25-40% Se(VI) reduction after 14 d, Fe(II) addition only enhanced reduction at pH 8-9 - aqueous Se(VI) is inert on iron sulfides - majority of reduced Se as $FeSe_2$, attributed to presence of greigite
(Han et al., 2012)	- Atmosphere: 95% N_2, 5% H_2 - Solution: deionized water with 3.1 mM Se(IV) or Se(VI), pH: 8.0 - Solid: Synthetic pyrite (0.5 -1 µm, 15.9 m^2/g), 1 g/L - Time length: 30 d	- Aqueous analyses not conducted, removal not calculated - Surface Fe(II) not involved with Se reduction, XAS[1] suggests S_2^{2-} oxidized to $S_4O_6^{2-}$ or $S_2O_3^{2-}$ in Se(IV) reduction
(Baik et al., 2013)	- Atmosphere: Ar, 25°C - Solution: deionized water with 0.1 M $NaClO_4$, 10-3-1 mM Se(IV), 0 - 50 mg/L Fe(II), pH: varied - Solid: Natural chlorite (5.15 m2/g), 10 g/L - Time length: 7 d	- Sorption increased with increasing pH and Fe(II) - Fe(II) sorption ~30% at pH ≤ 5, 100% at pH ≥ 9 - Se(IV) sorption followed Langmuir isotherm - <10% of Se sorbed with Fe(II) ≤ 0.5 mg/L - >80% of Se sorbed with Fe(II) ≥ 5 mg/L, pH ≥ 8 - 100% of Se sorbed with Fe(II) ≥ 50 mg/L, pH ≥ 6 - XANES[1] found no Se(IV) reduction at pH 5, most Se(IV) reduced to Se(0) at pH 9 - Fe(II) oxidation resulted in goethite

Table 2-1: Key Findings of some relevant Se sorption and reduction studies (Continued).

Study	Experiment	Key findings
(Curti et al., 2013)	- Atmosphere: N_2, < 5 ppm O_2, 80°C - Solution: deionized water with 0 or 1 mM NaHS, 10 mM Se(IV) or Se(VI), pH: ~8.0 - Solid: Natural pyrite (0.5 g chips, <250 µm, and <63 µm), 8 g/L - Time length: 2 or 8 months	- <16% of Se(IV) and Se(VI) was sorbed to pyrite - ~50% sorbed Se as Se(0) after 2 months, 100% Se(0) after 8 months - Sorption and reduction of Se(VI) occurred at significantly slower rates than Se(IV) reduction - X-ray Fluorescence and XAS[1] found highly concentrated Se clusters (µm scale) containing Se(0), Se(IV), and Se(VI) - Photoreduction during XAS[1] occurred in samples treated with NaHS
(Finck and Dardenne, 2016)	3 experiments (Fe(II), S(-II), FeS) - Atmosphere: Ar - Solution: deionized water with: (A) Se(IV):Fe(II) of 1:4, pH: 5, (B) Se(IV):S(-II) of 1:2, pH: 5, (C) 13 mM Se(IV), pH: 7.3 - Solid: Synthetic Mackinawite, 10 g/L (C only) - Time length: 4 d, 3 h, 7 d (for A, B, C)	Conducted XANES[1], EXAFS[1], and XRD[1] on samples - In (A), partial Se(IV) reduction occurred, pH down to 2.8 - Precipitate included Se(0) and $Fe_2(SeO_3)_3 \cdot H_2O$ - In (B), all Se(IV) reduced to Se(0) rapidly, pH up to 13 - Results suggest S(-II) oxidized to S(0) but no S(0) found - Filtrate (0.45 µm filters) was yellow, colloidal S(0) washed out. - In (C), Se(0) and FeS_2 on FeS surface, pH up to 11.5 - Se(IV) reduction occurred by S(-II) oxidation to S(-I)
(Jung et al., 2016)	- Atmosphere: N_2 - Solution: deionized water with 10 mM PO_4 buffer, 0.11 mM Se(IV), 0-5 mM Na_2S, pH: 4.0, 7.0, 11.0 - Also tested effect of ultraviolet (UV) light - Solid: none - Time length: 60 min	- Complete Se(IV) reduction to Se(0) with S(-II):Se(IV) > 10 at pH 7 - Se(IV) reduction occurred in < 5 min at pH 4 and 7 and did not occur at pH 11, suggesting H2S is the reactant rather than S^{2-} or HS^-: $HSeO_3^- + 2H_2S + H^+ \rightarrow Se^0 + 2S^0 + 3H_2O$ - UV light did not affect removal efficiency, but it did affect reaction products by changing S valence state - Se_8 produced without UV, Se_3S_5 produced with UV: $3HSeO_3^- + 6S_2^{2-} + 15H^+ \rightarrow Se_3S_5^0 + 7S^0 + 9H_2O$

[1] XAS – X-ray Absorption Spectroscopy; XANES – X-ray Absorption Near Edge Spectroscopy; EXAFS – Extended X-ray Absorption Fine Structure; XRD – X-ray Diffraction.

Although Se is commonly reported as being present in sphalerite, uptake of Se(IV) or Se(VI) has not been studied in detail (Lenz and Lens, 2009; Price, 2009; Yamamoto et al., 1984). In batch tests conducted with 25 g/L synthetic ZnS and ~8 mg/L Se(VI) solutions at circumneutral pH, 60% of Se(VI) was removed from solution in 7 d (Yllera De Llano et al., 1996). Removal was attributed solely to adsorption as no change in Se oxidation state was observed. No studies have investigated whether Se(VI) also adsorbs to natural sphalerite or if sphalerite can remove Se(IV) from solution. To the author's knowledge, the proposed study will be the first to investigate the removal of Se(IV) and Se(VI) from solution by natural sphalerite.

In general, Se(IV) is much more effectively sequestered by abiotic mechanisms than Se(VI). Fortunately, biotic Se(VI) reduction, or bioreduction, can be an effective mechanism for large scale Se sequestration. Field trials conducted in two locations in western Canada in the Elk Valley have shown that anaerobic bioreactors can treat Se-laden, mine-affected water (Baldwin et al., 2015; Luek et al., 2014). Further, *in situ* Se(VI) bioreduction has been reported at two different coal mines in British Columbia. Kennedy et al. (2015) found that Se bioreduction occurring in suboxic portions of unsaturated coal reject piles was sufficient to maintain "low to non-detectable release rates to the surrounding environment". Also, bioreduction has been effective in the sequestration of Se in water-saturated coal waste rock (Bianchin et al., 2013), and unsaturated phosphate waste rock (Hay et al., 2016). While all three of these studies show the potential for bioreduction of Se(VI) to Se(IV) in mine waste, they did not investigate the mechanisms that removed Se(IV) from the mine waste pore water. The mechanism that removes Se(IV) from solution determines how Se is sequestered and how likely it is to be remobilized. This is apparent in a study conducted by Knotek-Smith et al. (2006), who used a combination of microbial and geochemical techniques to determine that Se bound to Fe was at much less of a risk of remobilization than the biologically-produced Se solid phases. As such, this study has determined the mechanisms that remove Se(VI) and Se(IV) from the pore water of saturated, anoxic coal waste rock.

2.5 Summary

The sequestration of Se in saturated coal waste rock may be the result of several mechanisms. The mechanisms investigated in this study are the bioreduction, adsorption, and abiotic reduction of Se(VI) and Se(IV). Bacteria capable of reducing Se(IV) and Se(VI) to insoluble Se(0) have been isolated from many Se-contaminated environments and are expected to be present in the waste

rock (Stolz and Oremland, 1999). Pyrite and siderite, which are both present in the waste rock, adsorb Se(IV) and reduce it to Se(0) under anoxic conditions (Badaut et al., 2012; Breynaert et al., 2008). Pyrite was also shown to reduce Se(VI) to Se(0), but only in kinetically-enhanced laboratory experiments (Charlet et al., 2012; Curti et al., 2013). Synthetic ZnS has been shown to adsorb Se(VI) (Yllera De Llano et al., 1996) but no studies have determined whether Se(IV) or Se(VI) adsorb to or are reduced by natural sphalerite. Given the various pathways that Se(VI) can be removed from solution and sequestered in the waste rock, a combination of microbial and geochemical laboratory techniques were required to determine the biotic and abiotic mechanisms that remove Se(VI) and Se(IV) from saturated, coal waste rock.

3 Biotic and Abiotic Sequestration of Selenium in Anoxic Coal Waste Rock

This manuscript was submitted to Mine Water and the Environment on May 7, 2017. It has been reformatted from its original form for inclusion in this thesis. The contributing authors are Sean G. Deen, Viorica F. Bondici, Joseph Essilfie-Dughan, S. Lee Barbour, and M. Jim Hendry. As the lead author, I planned the experiments with support of Drs. Barbour, Hendry, and Bondici. I sterilized all the materials for the batch tests, prepared the batch tests, sampled the batch tests, cultured selected samples, and prepared the XANES sample for Dr. Essilfie-Dughan. I prepared the plate media and assisted Dr. Bondici to isolate, subculture, and prepare the bacteria for sequencing. Dr. Bondici processed the 16S rRNA gene sequencing results and produced the phylogenetic tree. The XANES analysis was conducted and interpreted by Dr. Essilfie-Dughan. With the support of Drs. Barbour and Hendry, I interpreted the results of the abiotic batch tests.

In this study, a method for separating biotic and abiotic mechanisms of Se sequestration was developed. The method was used to determine whether Se(IV) and Se(VI) can be sequestered abiotically and biotically by coal waste rock under anoxic, laboratory conditions. The method developed in this manuscript satisfies the first objective of this thesis. The results and findings discussed in this manuscript partially satisfy the second objective of this thesis.

3.1 Abstract

Mobile Se oxyanions ($Se^{VI}O_4^{2-}$ and $Se^{IV}O_4^{2-}$) can be sequestered by biotic or abiotic reduction to non-mobile species or by adsorption to mineral surfaces. Microbial analyses and geochemical batch testing with samples collected from a coal waste rock dump in the Elk Valley, British Columbia, Canada were conducted to assess whether Se can be sequestered in anoxic, waste rock by these mechanisms. Bacteria that reduce Se(IV) and Se(VI) to Se(0) were isolated from the waste rock and determined to be affiliated with the genera *Erwinia* and *Pseudomonas*. Isolates that reduce Se(IV) to Se(0) were present in a water sample collected from an underlying rock drain.

They were affiliated with the genus *Arthrobacter*. The production of Se(0) was confirmed by X-ray Absorption Near Edge Spectroscopy of red precipitate isolated from a broth media containing rock drain water. No adsorption or reduction of Se(VI) was observed in anoxic, abiotic (sterile) batch tests conducted with waste rock and a 1.0 mg/L Se(VI) solution whereas Se(IV) was adsorbed by the waste rock and subsequently reduced to Se(0) in abiotic batch tests with a 0.7 mg/L Se(IV) solution. In non-sterile batch tests using waste rock and rock drain water (0.39 mg/L Se(VI)), Se(VI) was biologically reduced to Se(IV), which was subsequently removed from solution by a combination of bioreduction, adsorption, and possibly abiotic reduction. This study suggests that, under anoxic conditions, Se sequestration in waste rock may occur via biotic reduction of Se(VI) to Se(IV) followed by adsorption of Se(IV) and abiotic and biotic reduction of Se(IV) to Se(0).

3.2 Introduction

Selenium is both an essential micronutrient for animal, plant, and human life and a toxic environmental contaminant at elevated concentrations (Lenz and Lens, 2009). The toxic effects of Se, as well as its mobility and bioavailability, are defined by its oxidation state. Se is typically present in surface water and shallow groundwater as the soluble, mobile oxyanions $Se^{VI}O_4^{2-}$ and $Se^{IV}O_3^{2-}$ (Dungan and Frankenberger, 1999). The mobile nature of the Se oxyanions make aquatic environments, and the fish and wildlife associated with them, particularly susceptible to Se bioaccumulation and its concomitant toxic effects (Lemly, 2004; Lenz and Lens, 2009). Cases of Se contamination of fish and aquatic wildlife are often associated with irrigation drainage, landfill leachate, and waste associated with the mining and processing of coal and metals (Lemly, 2004).

Mobile species of Se can be removed from water by adsorption onto solids or precipitation when reduced to insoluble species by abiotic or biotic processes. The Se(IV) oxyanion strongly adsorbs on minerals, such as clays (Bar-Yosef and Meek, 1987), Fe-oxyhydroxides (Duc et al., 2003; Rovira et al., 2008; Su and Suarez, 2000), pyrite (Kang et al., 2011; Tachi et al., 1998), and siderite (Scheinost et al., 2008). The adsorption of the Se(VI) oxyanion occurs to a much lesser extent than the Se(IV) oxyanion, often via weak electrostatic bonds (Balistrieri and Chao, 1987; Hayes et al., 1987). Once adsorbed, Se(IV) and Se(VI) can be reduced to Se(0) in abiotic reactions with Fe(II) or Fe(II)-bearing minerals (Charlet et al., 2012, 2007; Chen et al., 2009; Myneni, 1997). Removal

of Se(IV) and Se(VI) oxyanions from solution by microorganisms via reduction to insoluble Se(0) and Se(-II), often referred to as bioreduction, occur by three primary mechanisms: (1) incorporation into amino acids or other essential compounds; (2) detoxification; and (3) respiration (Stolz and Oremland, 1999). The most environmentally significant form of Se bioreduction is respiration, which occurs in the presence of electron acceptors, such as organic carbon and Fe(II), and the absence of more favourable electron acceptors, such as O_2 and NO_3^- , which can also be removed from solution by microorganisms (Herbel et al., 2000; Knotek-Smith et al., 2006; Maiers et al., 1988; Oremland et al., 1989; Stolz and Oremland, 1999). Examples of this process have been observed in the Goddard Marsh and Fording River Oxbow in the Elk Valley, where Se is sequestered in the sediments as Se(0) and Se(-II) while the overlying water column maintains a Se(VI) concentration >20 µg/L (Martin et al., 2011). Artificial bioreduction systems can also be created to treat Se-contaminated water (Lenz et al., 2008) or enhance abiotic immobilization systems (Knotek-Smith et al., 2006). Previous field studies have reported sequestration of mobilized Se by adsorption of Se(IV) on Fe(III) oxyhydroxides in coal tailings (Ziemkiewicz et al., 2011) and bioreduction of Se(VI) to insoluble Se species in a mine pit backfilled with water saturated waste rock (Bianchin et al., 2013) and in unsaturated coarse coal reject piles (Kennedy et al., 2015). While these studies confirm that Se sequestration can occur within mine waste facilities, the sequestration processes (biotic and/or abiotic) and their possible underlying mechanisms were not investigated.

The Elk Valley, south-eastern British Columbia, Canada has been a major steelmaking coal mining region in Canada since the late 1960s (Goodarzi et al., 2009; Lussier et al., 2003). The Elk River, located in the Elk Valley, (Figure 1-1) contains elevated concentrations of Se. For example, the concentration of Se at a monitoring station at the mouth of the Elk River (Figure 1-1) has exceeded the British Columbia Ministry of Environment water quality guideline for aquatic life of 2 µg/L since late 1990s (Beatty and Russo, 2014; Swanson, 2010). The dominant source of this Se load can be attributed to waste rock dumps at five coal mining operations in the Elk Valley (Figure 1-1; McDonald and Strosher, 1998; Wellen et al., 2015).

The primary sources of aqueous-phase Se in the Elk Valley waste rock are the sulfide minerals pyrite (FeS_2) and sphalerite (ZnS), which contain 21% of solid-phase Se (Hendry et al., 2015). Oxidation of Se(-II)-containing pyrite and sphalerite by O_2 (Essilfie-Dughan et al., 2017), and

possibly NO_3^- introduced to the waste rock during blasting (Mahmood et al., 2017) generates mobile Se(IV) and Se(VI) oxyanions that enter the Elk River (Day et al., 2012; Hendry et al., 2015). Excess carbonate minerals in the waste rock, including siderite ($FeCO_3$) and ankerite ($CaMg_{0.5}Fe_{0.5}(CO_3)_2$), maintain a circumneutral pH in the waste rock dumps (Biswas et al., 2016).

One possible management mechanism to control the discharge of Se-rich waters from the waste rock to receiving waters could be the establishment of anoxic zones. These anoxic zones could include mined-out pits filled with saturated waste rock or constructed water-saturated zones at the base of the oxic waste rock dumps through which the Se-rich dump drainage must migrate before discharging to receiving waters. The development and assessment of such Se management initiatives require an understanding of the potential Se sequestration mechanisms within the waste rock. As such, the objectives of the current study were to assess the potential for adsorption, abiotic reduction, and bioreduction of Se(IV) and Se(VI) in anoxic coal waste rock from the Elk Valley. These objectives were attained using sterile and non-sterile batch tests and culture-dependent microbial methods on samples of waste rock and associated rock drain water. The presence of bacteria capable of reducing Se(VI) and Se(IV) to Se(0) was confirmed using culture-dependent methods. Adsorption and abiotic reduction of Se(IV) and Se(VI) were quantified in anoxic, sterile batch tests. The minerals associated with sequestered Se were identified using aqueous and solid analytical techniques. In addition to assisting with the development and assessment of Se management initiatives at waste rock dumps in the Elk Valley, the findings of this study may be of value in controlling Se contamination from other sources including irrigation drainage, landfill leachate, and waste associated with the mining and processing of metals. Furthermore, the methods described in this study are not specific to Se contamination or the mechanisms of Se sequestration. There are many environmental contaminants controlled by both abiotic and biotic controls that are investigated using experiments designed to detect biotic and abiotic reactions simultaneously; however, abiotic batch tests in combination with culture-dependent methods can be beneficial to research programs focussed on understanding complex reaction mechanisms.

3.3 Materials and Methods

3.3.1 Site Description and Sample Characterization

Samples of waste rock and water from the waste rock drain outlet were collected from the WLC waste rock dump, Elk Valley, British Columbia, Canada (Figure 1-1). The dump was constructed at the Line Creek Mine between 1981 and 2012 (Mahmood et al., 2017; Villeneuve et al., 2017). As of 2011, it contained 210 M m^3 of waste rock, covered an area of about 2.7 km^2, and had average and maximum heights of 115 and 255 m, respectively (Villeneuve et al., 2017). Boulders segregate from the waste rock during end dumping and form a coarse permeable basal drain below the waste rock dump referred to as a rock drain. The WLC rock drains convey O_2-rich water from upstream of the dump as well as water draining from the dump downstream to Line Creek, a tributary of the Elk River (Villeneuve et al., 2017). Between 2002 and 2012, the annual volume of water discharged from the rock drain was on the order of 1 M m^3. This annual water discharge was estimated to carry about 900 kg/a of dissolved Se out of the dump (Hendry et al., 2015). Currently the discharge water is being treated at the WLC Active Water Treatment Facility (Teck Resources Limited, 2016).

A rock drain water sample was collected from the rock drain outflow in September 2014 as part of a routine sampling campaign. Key constituents of the drain water sample included (as mg/L): Ca, 302; Mg, 174; Fe, 0.09; Se, 0.39; SO_4^{2-}, 1032; NO_3^-, 21.1; and alkalinity (as $CaCO_3$), 256. The pH of the sample was 7.8. Although the dissolved O_2 content of the water sample was not measured at the time of sampling, the average O_2 content at the rock drain outflow was measured to be 73.3±2.1% of saturation (mean ± standard deviation, n = 21; Sean Carey, McMaster University, personal communication) in June 2012. As such, the rock drain water sample was assumed to be oxic at time of sampling and allowed to equilibrate under atmospheric conditions at laboratory temperature (22±2°C) prior to use in the experiments described below.

The solid waste rock sample tested in this study was collected in 2012 as part of a dump sampling program described by Hendry et al. (2015). It was collected from borehole LCO-WLC-12-02a at a depth of 53.7 m below ground surface from a zone of oxic, unsaturated waste rock placed in the dump between 1990 and 1994 (Mahmood et al., 2017). The gravimetric water content of the sample was 4% (Barbour et al., 2016). Immediately after collection, the sample was vacuum sealed

and stored at laboratory temperature prior to geochemical characterization by Hendry et al. (2015). The pyrite and sphalerite concentrations in the sample were determined to be 1265 mg/kg and 415 mg/kg, respectively using LECO analyses (Hendry et al., 2015) and XRD analyses showed that siderite and ankerite made up 1% and 5% of the sample, respectively (Table A-1 in Appendix A). The remainder of the sample was made up of quartz and clay minerals. As part of the current study, the sample was further characterized using Electron Microprobe Wavelength Dispersive Spectroscopy Analysis (WDS) to confirm the presence of ankerite, which is difficult to distinguish from dolomite using XRD. These measurements showed that the ankerite contained an average Ca:Mg:Fe:Mn cation ratio of 1.10:0.46:0.43:0.01 and the siderites an average Ca:Mg:Fe:Mn cation ratio of 0.03:0.09:0.87:0.01. The XRD and WDS analyses are presented in Appendix A. Prior to testing and analyses of the solid sample, it was air dried and ground with an agate mortar and pestle. The ground sample had a specific surface area of 3.5 m^2/g as measured by the Brunauer-Emmett-Teller (BET) method.

In addition to batch testing on the waste rock sample, batch tests were also conducted on quartz to represent an inert solid. The quartz sample was prepared by grinding synthetic silica sand (99.7% SiO_2, U.S. Silica, Ottawa, Illinois) with a tungsten carbide swing mill. The specific surface area of the ground quartz was measured to be 0.86 m^2/g using the BET method.

3.3.2 Overview of Methods and Analyses

Three sets of experiments were undertaken to investigate the biotic and abiotic controls on Se as summarized in Table 3-1. Biotic and abiotic processes were assessed using standard culture-dependent microbial analyses and sacrificial, sterile batch testing, respectively. The combined effect of biotic and abiotic processes was investigated using non-sterile batch tests. Analyses conducted in each set of experiments are presented in Table 3-1. Solution analyses included pH measurements, elemental quantification of Se, Fe, and Mn by Inductively Coupled Plasma Mass Spectrometry (ICP-MS), NO_3^- quantification by Ion Chromatography (IC), and Se speciation quantification by High Performance Liquid Chromatography (HPLC) coupled with ICP-MS. The methods' detection limit for Se, Fe, Mn, and NO_3^- were 0.5, 2, 0.02, and 50 µg/L, respectively. Solid analyses included mineral characterization by XRD, semi-quantitative elemental analysis and collection of backscattered electron (BSE) images by Electron Microprobe Energy Dispersive X-ray Spectroscopy (EDS), imaging by Scanning Electron Microscopy (SEM), Se redox

speciation by XANES, and elemental quantification of Se by ICP-MS. Prior to ICP-MS analysis, solids were dissolved in hydrofluoric and nitric acids in a procedure modified from Jenner et al. (1990). Details of the XRD, EDS, and XANES analyses are provided in the Appendix 1.

Table 3-1: Summary of experiments conducted.

Experiment	Technique	Conditions	Analyses
Microbial Analyses			
Isolation and identification of Se-reducers	Culturing on agar media	22±2°C, oxic	16S rRNA Gene Sequencing
Confirmation of reduced Se	Culturing in broth media	22±2°C, oxic	XANES, EDS, SEM, XRD, ICP-MS
Sterile Geochemical Tests			
Control	Abiotic batch tests	33±2°C, N_2 glove box, sterile	ICP-MS, IC, Plating
Se adsorption and reduction	Abiotic batch tests	33±2°C, N_2 glove box, sterile	ICP-MS, IC, HPLC, Plating, XRD, EDS
Non-sterile Combined Biogeochemical Tests[1]			
Se(IV) and Se(VI) sequestration	Batch tests	33±2°C, N_2 glove box, not sterile	ICP-MS, IC, HPLC, Plating, XRD, EDS

[1] Non-sterile combined biogeochemical tests are presented with the sterile geochemical batch tests at the end of Section 3.4.2.

3.3.3 Se Bioreduction

The potential for Se bioreduction by the culturable microbial community in the waste rock and rock drain water was assessed using a culture-dependent method. Although not all the bacteria in the samples are culturable, culture-dependent methods make it possible to determine the capabilities of different microbial isolates. Sterile phosphate-buffered saline solution was used for sample suspension and serial dilutions used for culturing. The dilution range, which provided countable bacterial colonies, was pre-determined by plating the samples using eight tenfold serial dilutions. The fourth to eighth dilutions were selected to plate samples in duplicate on both Se(IV)- and Se(VI)-amended basal salt media (BSM). This medium was produced using a recipe modified from that described by Maiers et al. (1988) and Ike et al. (2000) and contained (in g/L): $(NH_4)_2SO_4$, 0.3; $CaCl_2 \cdot 2H_2O$, 0.2; $MgSO_4 \cdot 7H_2O$, 0.143; NaCl, 5.85; KH_2PO_4, 0.05; K_2HPO_4, 0.05; yeast

extract, 0.5; 60% sodium lactate syrup, 1.9; agar, 15; and 1 mL trace mineral salt solution. The trace mineral salt solution contained (in g/L): H_3BO_3, 0.6; $Co(NO_3)_2$, 0.15; $CuSO_4$, 0.08; $MnCl_2 \cdot 4H_2O$, 0.99; and $Zn(O_2CCH_3)_2$, 0.35. After the medium was sterilized (single 20 m autoclave wet cycle, 121°C, 120 kPa), 10 mL of filter-sterilized (0.02 µm, Whatman, Inc.) 100 mM Se(IV) or Se(VI) solution was added to the media to yield 1 mM Se. The Se(IV) and Se(VI) solutions were made with Na_2SeO_3 and Na_2SeO_4 salts (Sigma-Aldrich, St Louis, MO, USA), respectively. Cultured plates were sealed with plastic paraffin film and kept at room temperature for a minimum of two weeks prior to enumeration.

A common product of Se bioreduction is red elemental Se nanospheres (Stolz and Oremland, 1999). The accumulation of the red nanospheres in Se-reducing colonies grown on solid media causes the colony or centre of the colony to appear red and allows for visual confirmation of Se bioreduction (Oremland et al., 2004). Four red colonies from Se(IV)-enriched BSM plates were subcultured on Se-free BSM plates to confirm the colonies were only red in the presence of Se. These bacterial colonies were subcultured on Se(IV)- and Se(VI)-enriched media to determine if they could reduce Se(IV) and Se(VI). Two bacterial colonies were isolated from each of the waste rock and rock drain water samples. These isolated bacterial colonies were subjected to DNA extraction using an EZ-10 Spin Column Bacterial Genomic DNA Mini-Preps Kit (Bio Basic Canada, Markham, ON) following the manufacturer's recommended protocol. Polymerase chain reaction (PCR) amplification of the 16S rRNA gene was performed using a 27F (5'-AGAGTTTGATCMTGGCTCAG) and 1492R (5'-GGWTACCTTGTTACGACTT) primer set, yielding an amplicon approximately 1400 base pairs long. The Econotaq Plus Master Mix (Lucigen Corporation, Middleton, WI) was used for a 50-µL reaction mixture and the final concentration of the primers was 1 µM. The thermal cycling profile was set according to the Econotaq recommended settings. The PCR amplicons were sequenced at Génome Québec (McGill University, Montreal, Canada). Identification and phylogenetic analyses were carried out according to Bondici et al. (2013). For taxonomic identification, the 16S rRNA gene sequences were compared to all the type strains within the Ribosomal Database Project (RDP) database (Cole et al., 2009). A phylogenetic tree was constructed by the neighbour-joining method using MEGA with 1000 bootstrap replicates (Tamura et al., 2011).

An enriched broth media was prepared to isolate red Se(0) particles for subsequent analysis. The media was created by dissolving the BSM ingredients, with the exception of the agar, in the drain water sample in two 500 mL high-density polyethylene bottles. The bottles were sealed during incubation. To limit the potential toxicity impacts of the elevated Se(IV) concentrations, Na_2SeO_3 salt was added to the broth in two 2 mM increments and two 5 mM increments. After 28 d, a total of 15 mM of Se(IV) was added to each of the bottles. The media was then incubated an additional 14 d, transferred to 50 mL Falcon centrifuge tubes, and centrifuged at 4400 rpm for 20 m.

3.3.4 Abiotic and Non-Sterile Batch Tests

All batch test solids, solutions, and bottles were sterilized to eliminate biotic processes from the batch tests. The ground waste rock and quartz samples were sterilized by exposing them to 30 kGy of ^{60}Co gamma radiation (Chemistry Department, University of Saskatchewan) and autoclaving them in two 30 min dry (gravity, 121°C, 120 kPa) cycles 24 h apart. Prior to autoclaving, the ground samples were split into 120 mg subsamples, transferred to glass crimp top batch test bottles, allowed to equilibrate with the atmosphere in a nitrogen (N_2) glove box (MBraun, <100 ppmv O_2) for 2 d, and crimp-sealed with silicon septa. Dry autoclave cycles were used and the solids kept in sealed bottles during autoclaving to minimize oxidation of the minerals during the sterilization process. Concerns that the reduced minerals of interest in the solid waste rock sample may be oxidized during sterilization were addressed by performing the same sterilization procedures on pure-phase mineral samples of pyrite, sphalerite, and siderite. Characterization of these materials before and after sterilization confirmed that no measurable oxidation occurred. Details of the materials tested and analyses conducted are provided in the Appendix A. The autoclaved batch test bottles were reintroduced to the glove box prior to the addition of batch test solutions. The solutions were passed through a 0.02 µm syringe filter during addition to the batch test bottles. The bottles were then resealed with sterile septa. Multiple batch tests with identical solutions were conducted to allow separate bottles to be sacrificially sampled on each sampling day, thus eliminating the risk of contaminating the batch tests during sampling.

Batch tests were conducted in the N_2 glove box. The rock drain water and deionized water (Millipore Milli-Q 18.2 MΩ) used in the experiments were bubbled with N_2 for 1 h prior to being introduced into the glove box. Each abiotic batch test contained 120 mg ground waste rock or quartz and 16 mL of one of five solutions: Se-free deionized water (control), deionized water with

1.0 mg/L Se(VI), deionized water with 0.7 mg/L Se(IV), deionized water with 86 mg/L Se(IV), or rock drain water. The Se(VI) and Se(IV) solutions were made using Na_2SeO_4 and Na_2SeO_3 salts, respectively. All solutions were adjusted to and buffered at pH 7 with 50 mM PIPES (1,4-Piperazinediethanesulfonic acid), sodium hydroxide pellets, and 1 M hydrochloric acid.

All sampling was conducted in the glove box. The days at which samples were collected and details of the sampling program are presented in Table 3-2. Immediately prior to sampling, each bottle was shaken, opened in the glove box, and, after the majority of the solid had settled out (generally after 30 min), the supernatant was decanted into a new 10 mL syringe and passed through a 0.2 µm filter. The pH of each sample was measured with an electrode (Thermo Scientific Orion ROSS Ultra pH/ATC Triode, accuracy: 0.03 pH units, precision: 0.01 pH units) after it was filtered but before it was split into subsamples for ICP-MS, IC, and HPLC analyses. Solution samples were removed from the glove box after they were split into subsamples for analyses. Subsamples requiring preservation were immediately preserved after removal of the glove box while the remainder of the samples were kept sealed until analysis. On the final day (see Table 3-2), four bottles were combined into composite solution and solid samples. Selected solid samples were rinsed with degassed deionized water three times and air dried in the glove box. Dried solid samples remained in the glove box until analysis.

Table 3-2: Batch test sampling days.

Batch Test Solution	**Sample Days**
Control – no Se	0[1,2], 1[3], 4, 10[1], 22[3,4]
1.0 mg/L Se(VI)	0[1,2], 1[3], 4[1,2], 6, 14, 21[1,2], 30, 42, 60, 82, 100[2,3,4]
0.7 mg/L Se(IV)	0[1,2], 1[3], 3[2], 6, 10[1], 14, 20[2], 29[1], 41, 46, 60, 66, 81[2,3,4]
86 mg/L Se(IV)	0[1,2], 61[1,4]
Drain water (sterile)	0[1,2], 1[3], 4, 7, 14[1], 21[2], 30, 42[1], 47[5], 53, 60, 82, 100[2,3,4]
Drain water (non-sterile)	0[1,2], 1[3], 4[1,2], 7, 14, 21[1,2], 30, 42, 47[2], 53[2], 60[2], 67, 82, 100[2,3,4]

[1] Sampled in triplicate
[2] Sample analyzed by HPLC for Se speciation
[3] Sample plated to assess sterility/CFU enumeration
[4] Four samples combined for composite sample
[5] Sampled in duplicate

Plating was conducted on the abiotic batch tests sampled on days 1 and 81 or 100 to confirm their sterility. Approximately 1 mL of the solutions to be cultured was aliquoted into sterile 1.5 mL Eppendorf tubes prior to the solids settling. The samples, as well as two tenfold serial dilutions, were plated in duplicate on Se(IV)-amended BSM, Se(VI)-amended BSM, and Reasoner's 2A (R2A) media (Difco BD, Sparks, MD, USA). Plates were sealed with plastic paraffin film and incubated in the glove box for a minimum of 16 d prior to bacterial colonies counts. The absence of colonies on cultured plates was interpreted as confirmation of batch test sterility.

In addition to the sterile abiotic batch tests, one set of batch tests was conducted using non-sterile waste rock and rock drain water to simulate the potential effects of combined abiotic and biotic processes on Se removal. With the exception of sterilization and plating procedures, the non-sterile batch tests were conducted using the same preparation and sampling procedures as the abiotic batch tests. The ground samples were not irradiated or autoclaved and the rock drain water not filtered. The day 1 and 100 batch tests were plated using the same procedure as the sterile batch tests with the exception of increasing the number of plated dilutions from three to five to account for the higher number of bacteria present in the non-sterile batch tests. These non-sterile batch test results were compared to the abiotic test results to determine the impact of viable bacteria on the concentration of Se in solution.

3.4 Results and Discussion

3.4.1 Se Bioreduction

Plating on Se-amended media was conducted to determine whether viable bacteria capable of reducing Se(IV) and Se(VI) to Se(0) were present in the waste rock and drain water. Three days after cultivation, white bacterial colonies with red centres developed on the Se(IV)-amended plates cultured with the waste rock solid and the rock drain water. Bacterial colonies were also present on the Se(VI)-amended plates cultured with waste rock, but not on those cultured with the rock drain water. After 8 d, the colonies on Se(IV)-amended plates were mostly red while the colonies on the Se(VI)-amended plates were red in the centre and yellow on the edges. No colonies were observed on the Se(VI)-amended plates cultured with rock drain water, suggesting the absence of Se(VI)-reducing bacteria or a very small population of Se(VI)-reducing bacteria relative to the Se(IV)-reducing population.

Two colonies from each of the samples cultured on Se(IV)-amended media under aerobic conditions were isolated. Isolated colonies were sub-cultured on Se-free media, which resulted in the development of yellow colonies within 3 d for colonies originating from waste rock and 10 d for colonies originating from drain water. These results confirm that the colonies only appeared red when Se was available for reduction and that their growth was not dependent on the presence of Se. Isolates grown on Se-free media were sub-cultured on Se(IV)- and Se(VI)-amended media. Colonies grown on the Se(IV)-amended media were similar in size, shape and colour to those originally selected for isolation. On Se(VI)-amended media, colonies originating from the waste rock sample were yellow with red centres after 8 d while colonies originating from drain water remained yellow, consistent with those that developed on the Se-free plates. The presence of viable Se(IV)- and Se(VI)-reducing bacteria in the waste rock sample and Se(IV)-reducing bacteria in the drain water sample suggest there is potential for Se(IV) and Se(VI) bioreduction to occur within the WLC waste rock dump provided the necessary nutrients and favourable geochemical conditions exist.

Sequence analyses of almost full-length 16S rRNA gene sequence showed the isolates originating from the waste rock sample, WR1 and WR2, were closely related to species of *Erwinia* and *Pseudomonas*, respectively (Figure 3-1). The isolates obtained from the drain water sample, DW1 and DW2, were closely related to species of *Arthrobacter*. Pairwise comparison of the 16S rRNA gene sequences (~1400 base pairs) showed that the drain water isolates were 100% identical to each other. Percent identities of the three distinct isolates to the type strains present within the RDP database were as follows: WR1 97% to *Erwinia amylovora*, WR2 99% to *Pseudomonas brenneri*, and DW1 and DW2 99% to *Arthrobacter subterraneus* and *Arthrobacter tumbae*.

Several species of *Pseudomonas* originating from Se-contaminated environments can reduce Se(IV) or Se(VI) to Se(0) under aerobic and anaerobic laboratory conditions (Macy et al., 1989; Oremland et al., 1989). *Pseudomonas stutzeri* can reduce Se(VI) to Se(IV) and Se(IV) to Se(0) similarly to the pseudomonad WR2 isolated and cultured in this study (Kuroda et al., 2011; Lortie et al., 1992). Also, *P. aeruginosa* (Macy et al., 1989), *P. fluorescens* (Garbisu et al., 1996; Steinberg et al., 1992), and *P. moraviensis* (Staicu et al., 2015) reduce Se(IV) to Se(0). Reduction of Se(VI) by some *Pseudomonas* species is inhibited by NO_3^-, which was present in the rock drain

water sample. *Pseudomonas fluorescens* and some other pseudomonads can remove NO_3^- from solution by denitrification (Hunter and Manter, 2009; Lortie et al., 1992; Steinberg et al., 1992).

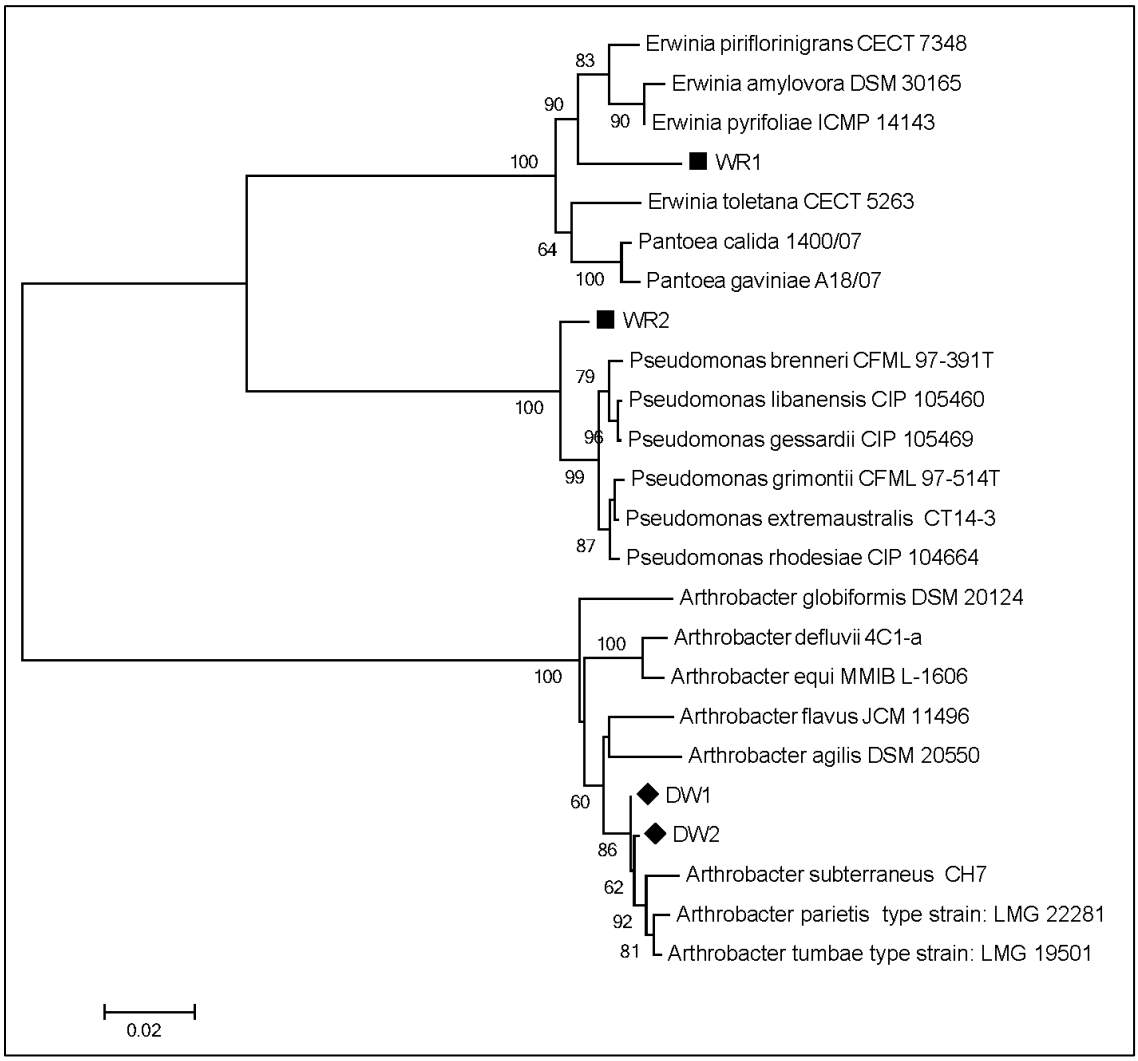

Figure 3-1: Neighbour-joining phylogenetic tree of four bacterial isolate sequences and reference 16S ribosomal sequences. Bootstrap values greater than 60 are indicated at the nodes. Isolates were named according to the location of isolation: WR (waste rock), DW (drain water). Bar represents 0.02 substitutions per nucleotide position.

In contrast to *Pseudomonas*, the ability of *Arthrobacter* to remediate Se-contaminated sites or to treat Se-contaminated waters has not been studied extensively. While several studies identified species of *Arthrobacter* in Se-reducing environments (Maiers et al., 1988; Yang et al., 2016), only two reported Se reduction by an *Arthrobacter* species. One *Arthrobacter* species isolated from a reservoir in California with low Se concentrations reduced Se(IV) to Se(0) but not Se(VI) (Burton et al., 1987). A second species isolated from a coal mine-affected marsh in the Elk Valley reduced

both Se(IV) and Se(VI) to Se(0) (Yang et al., 2016). Although the latter species was retrieved from an environment similar to that of DW1 and DW2, it is unlikely to be the same species as DW1 and DW2 given the absence of Se(0) on the Se(VI)-amended media cultured with DW1 and DW2. Finally, we found no information on the Se tolerance or reduction capacity of *Erwinia*; the *Erwinia* genera consists of facultative anaerobic plant pathogens, such as *E. amylovora*, responsible for fire blight in fruit trees (Zhao, 2014). Given this difference in capabilities and the marginal sequence homology (97% to known 16S rRNA sequences) for WR1 and *E. amylovora*, WR1 is a putatively novel species.

Broth media was prepared to allow the isolation of reduced Se precipitate from the media for analysis. The broth media appeared pink after 6 d and a red precipitate accumulated at the bottom of the bottles after 17 d. The addition of Se(IV) to the enriched broth resulted in the accumulation of additional red precipitate. The collected XANES spectrum, EDS spectrum, and SEM images corresponding to the red precipitate are presented in Figure 3-2. Linear Combination Fitting (LCF) analysis of the XANES spectrum (Figure A-3 and Table A-4 in Appendix A) indicates that Se(IV), Se(0), and Se(-II) make up 70.2±3.3%, 13.5±1.0%, and 16.3±1.1%, respectively of the Se present in the isolated red precipitate. The presence of Se(0) and Se(-II) shows that Se(IV) reduction did occur in the broth media. The Se(IV) content was attributed to the precipitation of $CaSeO_3$, which was supersaturated in the broth (Seby et al., 2001). The sub-micron particles visible in the SEM images (Figures 3-2c and 3-2d) are of comparable size and shape to other Se(0) nanospheres (Hockin and Gadd, 2006; Lenz et al., 2008; Oremland et al., 2004; Yang, 2011). Further, the largest peaks of the red precipitate XRD pattern (Figure S3) are consistent with trigonal elemental Se measured by Keller et al. (1977). The precipitation of Se(0) nanospheres in the broth confirms the red hue that developed at the centre of the bacterial colonies on Se-amended plate media was solid-phase Se(0) and that both Se(IV) and Se(VI) can be sequestered as solid Se(0) by bacteria present in the WLC waste rock dump.

In addition to being supersaturated with $CaSeO_3$, the broth was also supersaturated in calcite ($CaCO_3$), and hydroxyapatite ($Ca_{10}(PO_4)_6(OH)_2$; Geochemist's Workbench Spec8; data not presented). The presence of these Ca and phosphate compounds is supported by the EDS spectrum (Figure 3-2b) and the ICP-MS results, which determined that the digested precipitate was comprised of 20% Ca, 14.9% Se, and 6.8% P, by weight. There is no indication of these minerals

or any other minerals in the XRD pattern (Figure A-2). Conversely, XRD analysis of Se(0)-containing bioreactor sludge by Lenz et al. (2008) suggests the presence of calcite and brushite ($CaHPO_4.2H_2O$) but not Se(0). Although the form and importance of P and Ca in the precipitate is unclear, their co-precipitation with Se may act as a marker indicating precipitation of Se(0) when EDS is used to characterize sequestered Se on waste rock.

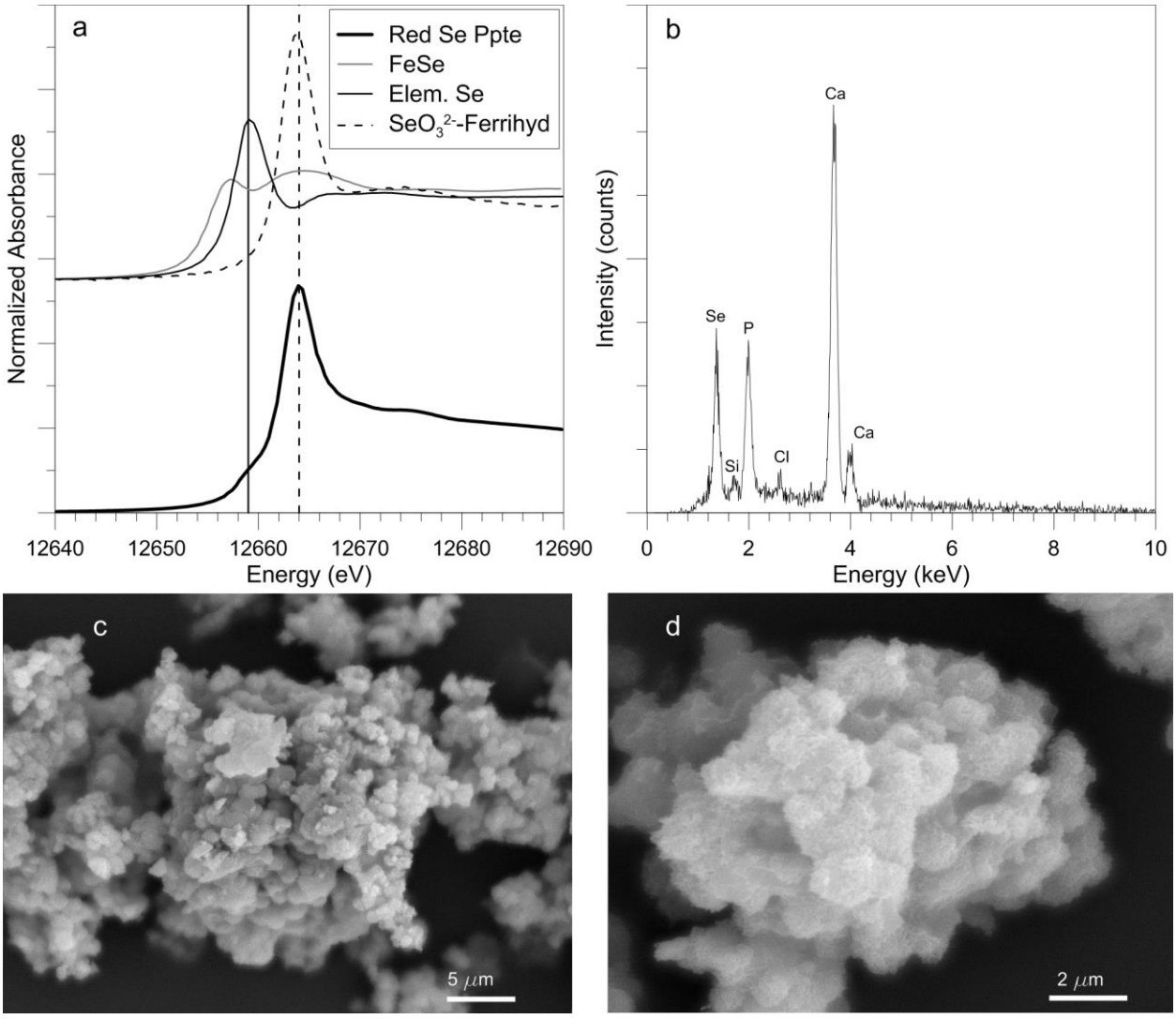

Figure 3-2: XANES spectrum (a), EDS Spectrum (b), and SEM images (c and d) of the red precipitate isolated from the broth media.

3.4.2 Abiotic Batch Tests

The absence of colonies on the plates cultured from the control, 0.7 mg/L Se(IV), and 1.0 mg/L Se(VI) abiotic batch tests confirms that the batch tests were sterile. All but one of the plates

cultured from the abiotic rock drain water batch tests were also free of colonies. Eleven colonies (the equivalent of 110 Se-reducing, colony forming units per millimetre; CFU/mL) with red centres grew on one of the Se(IV)-amended BSM plates cultured with the undiluted day 100 abiotic drain water batch test. The presence of Se(IV)-reducing colonies on the one plate has been attributed to contamination of the abiotic rock drain water batch tests during the addition of filtered solution because the glassware and ground samples for all four sets of abiotic batch tests were sterilized together. Plating of the day 1 non-sterile batch test yielded $1.5x10^7$ and $7.5x10^4$ CFU/mL on R2A and Se(IV)-amended plates, respectively. The R2A count decreased to $8.5x10^4$ CFU/mL in the day 100 batch test and the Se(IV)-amended media count remained at $7.5x10^4$ CFU/mL. These values are much higher than that of the contaminated abiotic batch test and, as such, changes in solution chemistry due to biological activity should be much more evident in the non-sterile batch test results. Furthermore, since not all abiotic drain water batch tests were expected to be contaminated, any biotic processes should yield inconsistent results when compared to the non-contaminated samples. The colonies that developed on the abiotic and non-sterile batch test-cultured plates were not investigated further nor was the cause of the absence of colonies on all Se(VI)-amended plates cultured in the glove box.

Abiotic batch tests conducted using inert quartz yielded no change in solution chemistry. In the quartz batch tests, the standard deviations of measured Se and NO_3^- concentrations were < 7% of the mean when the batch test concentrations were more than two times the detection limit. The concentrations of Fe and Mn were 0.069±0.086 and 0.0078±0.0029 mg/L, respectively. While variation in these values is greater than the sensitivity of ICP-MS, no patterns with time were observed and the mean values are much lower than that of the waste rock batch tests (Figures 3-3, 3-4, and 3-5). These data confirm that changes in the solution chemistry of the waste rock batch tests can be attributed to reactions related to the waste rock.

The evolution of pH and the redox elements (i.e. Se, Fe, and Mn) measured in the Se-free (control), 1.0 mg/L Se(VI), and 0.7 mg/L Se(IV) batch tests on waste rock with time are presented in Figures 3-3, 3-4, and 3-5, respectively. The solutions in each of these batch tests were prepared with deionized water and buffered at pH 7. The Se concentration in the control batch test solutions increased from 0.004 mg/L on day 0 to 0.030 mg/L on day 4. This increase has been attributed to the dissolution of Se salts that precipitated in the waste rock pore space during air drying. No

measurable change in Se concentration was measured in the 1.0 mg/L Se(VI) batch tests nor in the oxidation state of the aqueous Se. An increase of ~0.03 mg/L relative to the initial 1.0 mg/L is less than the precision of the ICP-MS measurements. In the 0.7 mg/L Se(IV) batch tests, 40% of the Se(IV) was removed from solution on the first day and the remainder by day 81 (Figure 3-6). The concentration of Se(VI) increased initially and remained around 0.030 mg/L, following the same trend as Se in the control batch tests (Figure 3-3). The initial uptake of Se(IV) by the waste rock is attributed to adsorption and the long term uptake is attributed to reduction from Se(IV) to insoluble Se(0). Siderite and pyrite remove Se(IV) from solution by these two mechanisms (Bruggeman et al., 2005; Kang et al., 2011; Scheinost et al., 2008).

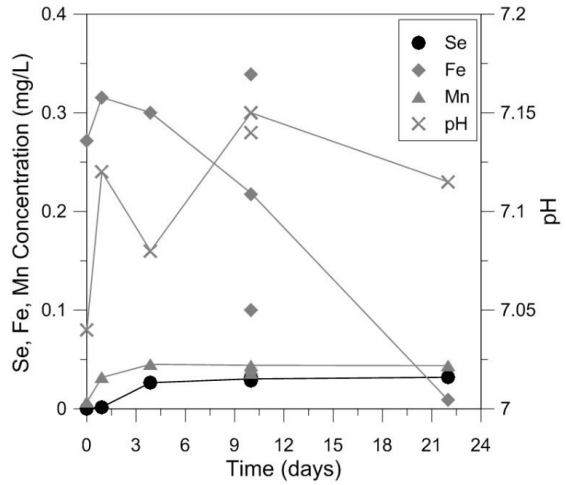

Figure 3-3: Measured pH and Se, Fe, and Mn concentrations in sterile, Se-free (control) waste rock batch tests. Points represent single measurements. Lines pass through the average measurement of a given day.

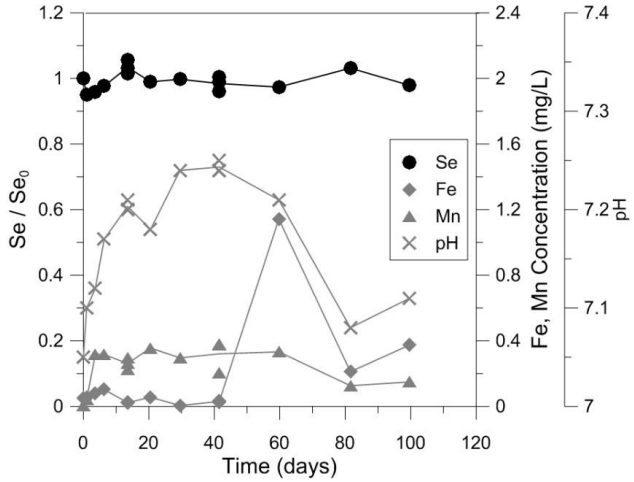

Figure 3-4: Relative Se concentrations, Fe concentrations, Mn concentrations, and pH in sterile, 1.0 mg/L Se(VI) waste rock batch test solutions. Se/Se_0 refers to fraction of initial Se concentration.

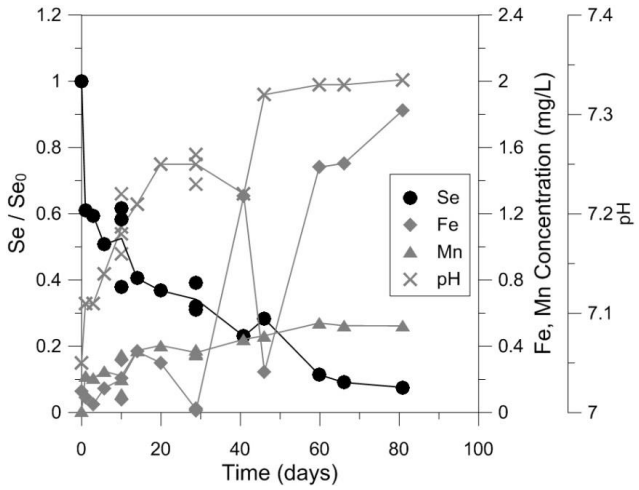

Figure 3-5: Relative Se concentrations, Fe concentrations, Mn concentrations, and pH in sterile, 0.7 mg/L Se(IV) waste rock batch test solutions.

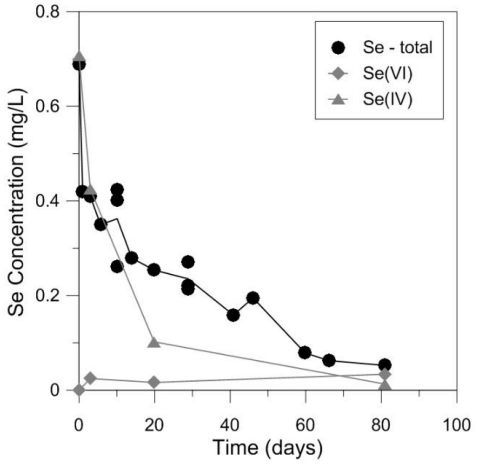

Figure 3-6: Concentrations of total Se measured by ICP-MS and Se(IV) and Se(VI) measured by HPLC-ICP-MS in sterile, 0.7 mg/L Se(IV) waste rock batch test solutions.

In each of the waste rock batch tests, the increases in pH and the concentrations of Fe and Mn in the first 2 to 4 d are attributed to dissolution of the carbonate minerals siderite and ankerite. The solubility of Fe(III) is very low at neutral pH with the precipitation of goethite or other Fe-oxyhydroxides (Appelo and Postma, 2005). The cause of the decreasing Fe concentration with time in the control batch tests is not clear – it may have resulted from the oxidation of Fe(II) to Fe(III) by trace amounts of O_2 (Figure 3-3). The increase in Fe concentration in the Se(VI) batch tests after day 42 is attributed to the reduction of insoluble Fe(III) to soluble Fe(II) and, thus, reflected a decreasing redox potential in the batch tests (Figure 3-4). As such, the high

concentrations of Fe in the Se(IV) batch tests relative to the control and Se(VI) batch tests suggest a lower redox potential and that Se(IV) was reduced to Se(0) (Figure 3-5). After day 29, the increase in Fe concentration was accompanied by an increase in pH and Mn concentration, confirming the source of Fe(II) and the associated low redox potential was the carbonate minerals in the waste rock. No explanation for the anomalous Fe concentration measurement in the 60 d 1.0 mg/L Se(VI) batch test (Figure 3-4) was determined and, because of its anomalous nature, will not be considered further.

The impact of sample heterogeneity and the precision of analyses on trends in pH and the concentrations of Se, Fe, and Mn are apparent in Figures 3-3, 3-4, and 3-5, especially on days where batch tests were sampled in triplicate (see Table 3-2 for list of triplicate sampling days). In most cases where sampling was conducted in triplicate, variations in pH and elemental concentrations were not great enough to obfuscate overall concentration-time trends. One example of this is the day 10 triplicate Se and Mn measurements in the control batch tests (Figure 3-3). The Fe concentrations, however, varied greatly. The variation in Fe on day 10 was likely due to a combination of analytical error and differences in the rate of Fe(II) oxidation to Fe(III) in the three different batch tests. The effects of sample heterogeneity on reaction commencement time and rate are evident during rapid changes in solution chemistry, such as when Se(IV) was reduced to Se(0) and Fe(III) was reduced to Fe(II) (Figure 3-5). In this case, the Fe concentration increased between days 29 and 41, decreased between days 41and 46, and then increased again after day 46. The opposite trend was measured in the Se concentrations. These apparent fluctuations are attributed to differing reaction rates in the batch tests and not actual fluctuations in any single batch test. While the use of identical, sacrificial batch tests can make it difficult to differentiate reactions from heterogeneity, it allows us to confirm that the batch test results are repeatable. For example, the equilibrium Se concentration of 0.032±0.005 mg/L was measured in all six of the control batch tests sampled after day 3.

The sequestration of Se by the waste rock as Se(0) precipitate and Se(IV) sorbed to Fe minerals is supported by the EDS spectra (Figure 3-7). In preparation for EDS, the waste rock was subjected to sterile, 61 d, 86 mg/L Se(IV) batch tests, which resulted in the solid Se concentration increasing from 4.9 to 510 mg/kg. Given that over 99% of the Se on the analyzed waste rock was derived from the batch testing, all Se measured by EDS was assumed to be the result of Se sequestration

rather than naturally-occurring Se in the waste rock minerals. In the BSE images corresponding to the EDS spectra (Figure 3-7), relatively light elements (e.g., Si, Al, Mg, and Na) appear darker than heavier elements (e.g., Se, Fe, and Ca). In Figure 3-7a, two high-Se locations, c1 and c2, were present on a silicate (grey) mineral. At c1, Se was associated with Ca and P consistent with bioreduced Se(0) (Figure 3-2a) indicating that Se(0) was present at c1. At c2, Se(IV) was sorbed to Fe minerals. The ratio of Fe to S at c2 suggests a combination of pyrite and siderite or an Fe(III)-oxyhydroxide. Given that Fe(III)-oxyhydroxides are a common secondary mineral associated with pyrite in the waste rock (Hendry et al., 2015), it is likely that one or more Fe(III)-oxyhydroxides were present at c2; however, we cannot confirm this statement because EDS analyses cannot identify the oxidation state of Fe nor can it detect the presence of carbonate, hydroxides, or oxides. At c3 and c4, Se was associated with Ca and P, as well as the Fe-minerals chalcopyrite and siderite, respectively. This adds evidence to the hypothesis that reduction of Se(IV) to Se(0) by pyrite "involves an adsorption step" (Bruggeman et al., 2005). Adsorption and reduction of Se(IV) by chalcopyrite (c3) has been found to be very similar to pyrite (Naveau et al., 2007). Sequestration of Se at c4 is attributed to adsorption of Se(IV) and subsequent reduction to Se(0) by siderite, which was observed by Scheinost et al. (2008).

The initial Se(VI) concentration in the abiotic and non-sterile rock drain water batch test solutions was 0.39 mg/L. Consistent with the control and Se(VI) batch tests (Figures 3-3 and 3-4), the concentration of Se increased by ~0.03 mg/L and there was no change in aqueous Se oxidation state (Figure 3-8). In the non-sterile batch tests, all Se(VI) was reduced to Se(IV) between days 47 and 53 and 97% of Se was removed from solution by day 67 (Figure 3-9). The reduction of Se(VI) to Se(IV) is attributed to biotic processes given the absence of Se(VI) reduction in the abiotic batch tests. This is supported by the presence of Se(VI) reducing bacteria in the waste rock sample isolated using culture-dependent methods. Confirmation of reduction of Se(VI) to Se(IV) in the non-sterile batch test solutions highlights the importance of abiotic sequestration of Se(IV) in waste rock dumps where aqueous Se is predominantly present as Se(VI). After the Se was reduced to Se(IV) in the non-sterile drain water batch tests, it was removed from solution much faster than that of the sterile 0.7 mg/L Se(IV) batch tests, suggesting that bioreduction of Se(IV) to Se(0) occurred concurrently with adsorption of the Se(IV) to the waste rock and abiotic reduction to Se(0).

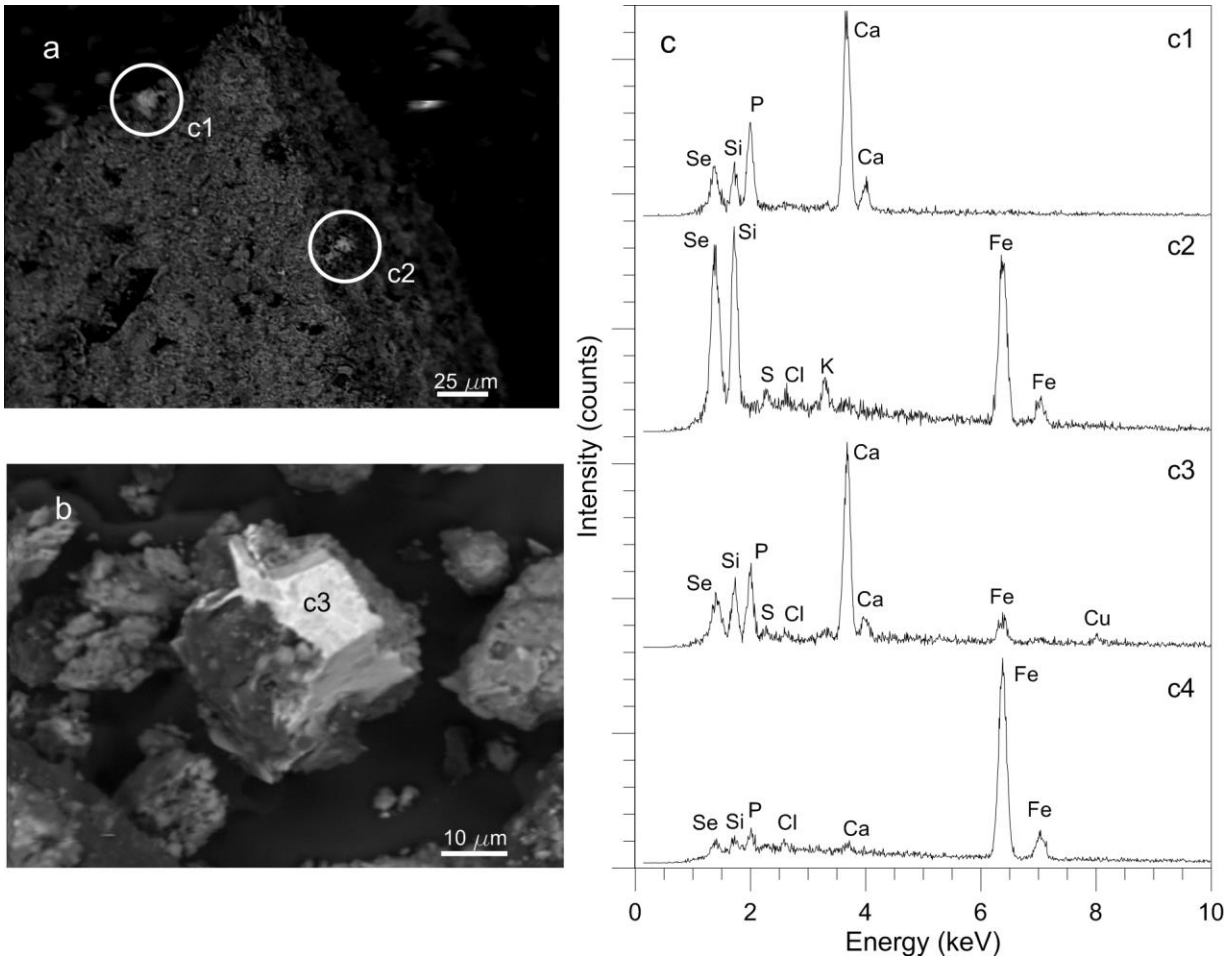

Figure 3-7: BSE images (a, b) and EDS spectra (c) collected from waste rock reacted for 61 d in sterile 86 mg/L Se(IV) batch tests. The corresponding BSE image for EDS spectrum c4 is not presented.

A large shift in redox potential prior to Se removal was apparent in the non-sterile rock drain water batch tests (Figure 3-9). The initial high NO_3^- concentration is characteristic of oxidizing conditions (Hockin and Gadd, 2006; Masscheleyn et al., 1990) while the high Fe concentration after day 47 is characteristic of reducing conditions (Couture et al., 2015; Kang et al., 2011). The reduction of Se(VI) to Se(IV) only in the absence of NO_3^- is consistent with other studies that have shown that NO_3^- inhibits Se(VI) reduction and is preferentially reduced by several Se(VI)-reducing bacterial species (Oremland et al., 1989; Steinberg et al., 1992). Three of the Se-reducing isolates collected from waste rock and drain water samples are affiliated with NO_3^- reducers in the genera *Pseudomonas* (Steinberg et al., 1992) and *Arthrobacter* (Eschbach et al., 2003). Abiotic NO_3^- reduction by Fe(II) or organic carbon occurs very slowly or not at all unless in the presence of a catalyst (Parmentier et al., 2014; Picardal, 2012); however, complete removal of NO_3^- from

the drain water did occur in some abiotic batch tests (Figure 3-8). Given the inconsistency of NO_3^- removal and the presence of bacterial contamination determined by plating, NO_3^- removal from the abiotic batch tests is attributed to biotic processes.

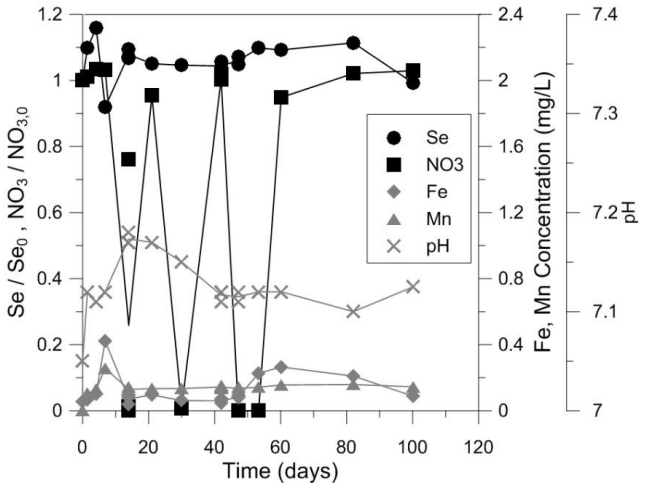

Figure 3-8: Relative Se and $\mathbf{NO_3^-}$ concentrations, Fe and Mn concentrations, and pH in sterile rock drain water batch test solutions (0.39 mg/L Se(VI), 21.1 mg/L $\mathbf{NO_3^-}$).

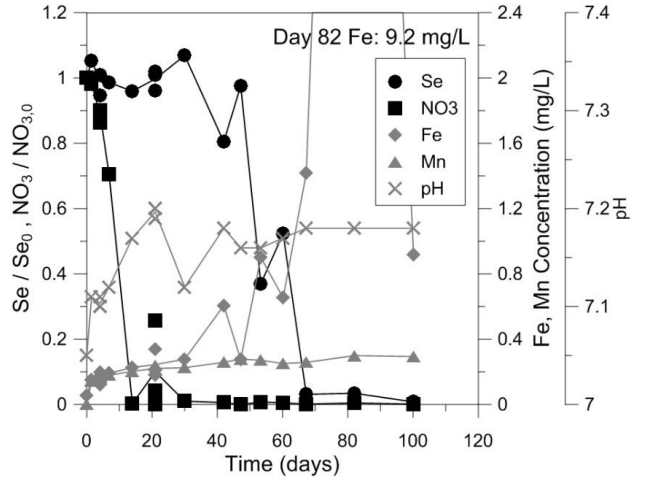

Figure 3-9: Relative Se and $\mathbf{NO_3^-}$ concentrations, Fe and Mn concentrations, and pH in non-sterile rock drain water batch test solutions (0.39 mg/L Se(VI), 21.1 mg/L $\mathbf{NO_3^-}$).

3.5 Conclusions

Laboratory experiments showed the potential for biotic and abiotic Se sequestration in coal waste rock from the WLC dump, Elk Valley, British Columbia, Canada under anoxic conditions. Bacterial isolates affiliated with the genera *Erwinia* and *Pseudomonas* that can reduce Se(IV) and Se(VI) to Se(0) were present in the solid waste rock sample. Further, isolates affiliated with the

genus *Arthrobacter* that can reduce Se(IV) to Se(0) were present in water sampled from an associated rock drain. Under anoxic, abiotic conditions, 40% of the initial 0.7 mg/L Se(IV) was removed from solution in 1 d by adsorption to the solid waste rock sample and the remainder was removed by reduction to insoluble Se(0) by day 81. Adsorption of Se(IV) to pyrite, siderite, and/or Fe oxyhydroxide, and abiotic reduction of Se(IV) to Se(0) by siderite and chalcopyrite were confirmed with EDS. Conversely, under the same environmental conditions, Se(VI) was not removed from solution. Finally, non-sterile batch tests confirmed that bacteria in the waste rock reduce Se(VI) to Se(IV) under anoxic conditions without the addition of nutrient amendments, which allowed subsequent bioreduction, adsorption and abiotic reduction of Se(IV). These results confirm Se sequestration within the WLC dump would be possible if the dump was anoxic. The sequestration of Se under anoxic conditions should be a viable method to decrease the concentration of Se in water migrating through the coal waste rock dumps in the Elk Valley before it discharges to the Elk River and its tributaries. Additional research to develop specific design and management criteria for the development of such anoxic zones is warranted. It should include the determination of Se(IV) adsorption isotherms for waste rock and reaction rates for the reduction of dissolved O_2, NO_3^-, Se(VI), and Se(IV).

4 Geochemical Controls on Selenium Sequestration in Anoxic Coal Waste Rock

This manuscript will be submitted to Mine Water and the Environment once Chapter 3 is published. It has been reformatted from its original form for inclusion in this thesis. The contributing authors are Sean G Deen, Joseph Essilfie-Dughan, S Lee Barbour, and M Jim Hendry. As the lead author, I developed the experiments with support of Drs. Barbour and Hendry, prepared the samples and materials for sterile lab work, conducted and sampled the batch tests, and interpreted the results with the support of Drs. Barbour and Hendry. The XANES analysis was conducted and interpreted by Dr. Essilfie-Dughan.

In this study, the method developed in the previous chapter was used to conduct abiotic batch tests on the minerals siderite, pyrite, and sphalerite in parallel with coal waste rock to determine the minerals in waste rock responsible for abiotic Se sequestration and confirm the abiotic Se sequestration mechanisms. Further abiotic batch tests were conducted on coal waste rock to quantify Se(IV) sequestration by adsorption and reduction. Finally, desorption batch tests were conducted to determine the fraction of waste rock-sequestered Se that is susceptible to desorption. The findings in this manuscript satisfy thesis objectives 3, 4, and 5 and may be of value to mine operators to incorporate effective saturated zones in waste rock zones and, ultimately, curb Se releases to the Elk River and its tributaries.

4.1 Abstract

The mechanisms of abiotic sequestration of Se(VI) and Se(IV) in water-saturated, anoxic, coal waste rock were identified using sterile batch testing on a waste rock sample collected from the Elk Valley, Canada and on pure mineral samples corresponding to minerals present in the waste rock (i.e., siderite, pyrite, and sphalerite). Only siderite was shown to remove Se(VI) from solution and only after 42 d. This removal was attributed to the reduction of Se(VI) to Se(IV) followed by adsorption to siderite or further reduction to Se(0). The waste rock and mineral samples all removed Se(IV) from solution. Pyrite removed all Se(IV) from solution in 1 d via adsorption and

reduction to Se(0) and Se(-I/-II) by S_2^{2-}. Siderite removed Se(IV) from solution by adsorption initially (≤1 d) and then by slower reduction to Se(0) over a period of 91 d. Removal of Se(IV) by sphalerite was minor relative to the other samples and had a minimal effect on Se sequestration in the waste rock. The waste rock sample removed Se(IV) from solution in two stages: day 1 removal was attributed to adsorption and reduction by pyrite and siderite; longer-term (up to 91 d), constant-rate removal was attributed to reduction to Se(0) by siderite. The initial (1 d) removal of Se(IV) by waste rock was characterized using a distribution coefficient (K_d) of 15.5 L/kg. Longer-term Se(IV) pseudo-zero order removal rates were between 0.063 and 0.55 μM/d (0.0050 and 0.043 mg/L·d). Desorption tests on waste rock showed that about one third of the Se sequestered by waste rock on day 1 could be desorbed with deionized water whereas Se sequestered after day 1 could not be desorbed using SO_4^{2-} and PO_4^{3-} solutions. These findings show that abiotic Se sequestration can occur in saturated, anoxic zones in coal waste rock dumps.

4.2 Introduction

Selenium is a trace element that is toxic to animal and human life at relatively low concentrations. Surface coal mining can release Se to aquatic environments (Beatty and Russo, 2014; Hendry et al., 2015; Lemly, 2004; Palmer et al., 2010; Swanson, 2010; Wellen et al., 2015). The concentrations of Se in the Elk River, which flows through the Elk Valley, a major coal-producing region of Canada have been increasing with time (Teck Resources Limited, 2014). The increasing Se concentrations are attributed to drainage from the waste rock dumps at five open-pit coal mining operations in the Elk Valley (Dessouki and Ryan, 2010; Wellen et al., 2015).

The sources of leachable Se in the coal waste rock dumps in the Elk Valley are the trace amounts of Se(-I) and Se(-II) incorporated into the primary sulfide minerals pyrite (FeS_2), sphalerite (ZnS), and chalcopyrite ($CuFeS_2$) (Hendry et al., 2015). Blasting, removal, and storage of waste rock in dumps allow the ingress of O_2, which reacts with water and the Se(-I,-II)-containing sulfide minerals to produce selenate (Se(VI), SeO_4^{2-}) and selenite (Se(IV), SeO_3^{2-}) (Day et al., 2012; Essilfie-Dughan et al., 2017; Hendry et al., 2015). Although some of the oxidized Se is sequestered in the dumps as Se(IV) sorbed to Fe oxyhydroxides (Hendry et al., 2015), the majority of the oxidized Se leaches from the dumps as Se(VI) (Day et al., 2012; Hendry et al., 2015).

The presence of saturated or near-saturated zones will limit the rate of O_2 ingress into waste rock, which, when combined with other O_2 consumption mechanisms, can result in the presence of sub-oxic to reducing conditions (Appelo and Postma, 2005; Mahmood et al., 2017; Schabert, 2016). Under these conditions, the Se(VI) produced under oxic conditions will be susceptible to biological reduction (Bianchin et al., 2013; Kennedy et al., 2015). Although abiotic reduction of Se(VI) can occur in the presence of green rust (Myneni, 1997), nanocomposite pyrite-greigite (Charlet et al., 2012), and pyrite at 80°C (Curti et al., 2013), the results presented in Chapter 3 suggest that abiotic Se(VI) reduction does not occur in anoxic, water-saturated Elk Valley coal waste rock. Once the Se(VI) is reduced to Se(IV), the Se can be removed from solution by adsorption to mineral phases (Fe oxyhydroxides: Balistrieri and Chao, 1987; Rovira et al., 2008; Hendry et al., 2015; pyrite: Bruggeman et al., 2005; Kang et al., 2011; siderite: Badaut et al., 2012; Scheinost et al., 2008; and clays: Bar-Yosef and Meek, 1987) or by reduction to non-soluble, non-mobile reduced Se solid phases. These Se solid phases include elemental Se (Se(0)) and Se(-I,-II)-containing mineral phases such as $FeSe_2$ or FeSe (Fernández-Martínez and Charlet, 2009). Reduction of Se(IV) has been shown to occur both biotically (Stolz and Oremland, 1999) and abiotically (Chen et al., 2009; Myneni, 1997). While Bianchin et al. (2013) and Kennedy et al. (2015) showed that sub-oxic coal waste rock can sequester Se, they did not investigate the mechanisms responsible for removing dissolved Se(IV) from migrating groundwater. Overall, there is a paucity of knowledge on the impact of abiotic reactions on the sequestration of Se in anoxic environments.

The goal of the current study was to improve upon our understanding of abiotic sequestration of Se from coal waste rock in the Elk Valley under anoxic conditions. The objectives of this study were to: (1) determine which, if any, of the Fe(II)-bearing or sulfide minerals known to be present in coal waste rock can remove Se(IV) and Se(VI) from solution under anoxic conditions; (2) identify the abiotic mechanisms that sequester Se in anoxic, water-saturated waste rock; (3) quantify abiotic Se sequestration on waste rock with time; and (4) assess the fraction of waste rock-sequestered Se susceptible to desorption.

These objectives were attained by conducting abiotic, anoxic batch tests and desorption batch tests. Abiotic batch tests were conducted using Se(IV) and Se(VI) solutions with one Elk Valley waste rock sample and the minerals siderite, pyrite, and sphalerite. In addition to determining which of the key minerals in the waste rock were effective in the removal of Se(IV) and Se(VI) from

solution, analysis of the mineral batch tests provided insights into the complex geochemical reactions in anoxic waste rock. Sequestration of Se by the waste rock sample was quantified using a sorption isotherm for short-term removal and a range of reduction rates for long-term removal. XANES analysis was used to identify sequestration mechanisms and desorption batch testing was used to evaluate the potential for desorption of sequestered Se from the waste rock sample. Although the focus of our study was on water-saturated coal waste rock, we believe that the developed methods and findings could be extended to other anoxic saturated and anoxic-suboxic unsaturated waste rock derived from mining activities.

4.3 Materials and Methods

4.3.1 Solid Samples and Solution Preparation

Abiotic batch tests were conducted on a coal waste rock sample and three minerals present within the waste rock: siderite, pyrite, and sphalerite. The waste rock sample was collected from the WLC coal waste rock dump located at the Teck-operated Line Creek open pit coal mine in the Elk Valley, British Columbia, Canada (Figure 1-1). The procedure for the collection of the waste rock samples is presented in Hendry et al. (2015). The siderite content of the waste rock sample (by weight) was determined to be ~1% using XRD (Table A-1) and the pyrite and sphalerite contents were determined to be 0.13%, and 0.04%, respectively, using LECO analysis (Hendry et al., 2015). The sources of the mineral samples used in batch tests are presented in Table 4-1. The sphalerite sample was determined to have an Fe content of 0.2% by weight using WDS analysis. The waste rock and mineral samples were air dried and crushed with an agate mortar and pestle prior to batch testing. The specific surface area of each of the samples was measured by the BET method (Table 4-1). A comparison of the specific surface area of the mineral samples to similar mineral samples used in other studies from the literature is presented in Appendix A.

Batch test solutions were prepared with deionized (Millipore Milli-Q 18.2 MΩ) water that was bubbled with N_2 for 1 h and equilibrated with the atmosphere in a N_2 glove box (MBraun, <100 ppmv O_2, 33±2°C) for 2 d prior to solution preparation. The Se(VI) and Se(IV) batch test solutions were prepared with Na_2SeO_4 and Na_2SeO_3 salts, respectively (Sigma-Aldrich, St. Louis, MO, USA), buffered with 50 mM PIPES (Sigma Aldrich), and adjusted to pH 7 with hydrochloric acid and sodium hydroxide. The Se(VI) and Se(IV) batch test solutions used in this study are presented

in Table 4-2. Desorption batch testing was conducted with deionized water, 1000 mg/L SO_4^{2-}, and 100 mg/L PO_4^{3-} solutions. The SO_4^{2-} and PO_4^{3-} solutions were prepared with $MgSO_4 \cdot 7H_2O$ and Na_2HPO_4 salts (Sigma Aldrich), respectively.

Table 4-1: Sources and surface areas of the ground mineral and waste rock samples used in the batch tests.

Sample/Mineral	Ideal Formula	BET surface area (m^2/g)	Source
Waste rock	-	3.5	Collected from WLC at Line Creek Operations, British Columbia, Sample 30385a
Siderite	$FeCO_3$	0.52	Collected from Mt. St. Hilaire Quebec, purchased from Ward's Science
Pyrite	FeS_2	0.35	Synthetic, purchased from Sigma Aldrich
Sphalerite	ZnS	0.13	Natural, University of Saskatchewan Minerals Collection; Specimen no. 2621-N2

4.3.2 Abiotic Batch Test Method

All batch tests were prepared, stored, and sampled in a N_2 glove box. A sterile, anoxic, sacrificial batch testing method was used to study abiotic processes in the absence of biotic reactions. Each sacrificial batch test consisted of 120 mg of ground waste rock or mineral sample and 16 mL of solution. The ground samples were exposed to 30 kGy of ^{60}Co gamma irradiation prior to being placed in 30 mL glass crimp top batch test bottles. The bottled solid samples were then equilibrated with the glove box atmosphere for 2 d, sealed with silicon septa, removed from the glove box, dry autoclaved (gravity, 30 m, 121°C, 120 kPa) twice (24 h apart), and returned to the glove box. Septa were removed when the syringe filter-sterilized (0.02 µm, Whatman) solution was added and were replaced immediately after addition of the solution. To minimize the risk of contamination, only one bottle was open at a time. Bottles were shaken vigorously for ~5 s once resealed. Replicate batch tests were prepared and sampled sacrificially to eliminate the risk of contaminating future samples during sampling. Several batch tests (Table 4-2) were cultured on Se-amended Basal Salt and R2A plate media (media and method described in Chapter 3) to confirm the batch tests were

sterile and, thus, abiotic. The absence of microbial colonies on all plates cultured with batch tests in this study (data not presented) confirmed that all cultured batch tests were sterile.

The batch test solutions, solids, and the sampling days are presented in Table 4-2. Batch tests using the 1.0 mg/L Se(VI), 0.7 mg/L Se(IV), and 15 mg/L Se(IV) solutions were conducted on the waste rock and mineral samples. The other solutions listed in Table 4-2 were only used in waste rock batch tests. Each mineral-solution set with a contact time longer than 1 d was sampled in triplicate twice to confirm the consistency of geochemical measurements in identical batch tests. The procedure for sampling in the glove box included shaking the glass bottles vigorously for ~5 s, removing the septa, allowing the solid samples to settle out for ~30 min, decanting the supernatant into a syringe, and filtering the supernatant (0.2 µm, Whatman). The pH of the filtered samples was measured with a Thermo Scientific Orion Ross Ultra pH/ATC Triode (accuracy: 0.03 pH units, precision: 0.01 pH units) in the glove box. Samples were preserved for chemical analysis as required immediately after their removal from the glove box. All samples were analyzed for Se, Fe, and Zn concentrations using ICP-MS methods. The oxidation state of Se in selected samples (Table 4-2) was determined by HPLC coupled with ICP-MS using a method modified from the method described by Tonnietto et al. (2010). The limits of detection for Se, Fe, Zn, Se(VI), and Se(IV) were 0.5, 2, 0.5, 10, and 10 µg/L, respectively. The HPLC-ICP-MS measurements were used to determine the concentrations of Se(IV) and Se(VI) relative to each other. The total Se concentrations measured by ICP-MS were used in time series plots for determining trends. The concentration of SO_4^{2-} in the samples was measured by IC. The addition of the PIPES buffer yielded a background SO_4^{2-} concentration of ~1700 mg/L and measurement precision of ~90 mg/L, which was too imprecise to detect changes in the concentration of SO_4^{2-} in most of the batch tests. As such, these results are not presented nor discussed in detail.

Table 4-2: Timing of sample collection and associated analyses during abiotic batch testing.

Batch Test		Sample Days
1.0 mg/L Se(VI)	- Waste rock	0[1,2], 1[3], 4[1,2], 6, 14, 21[1,2], 30, 42, 60, 82, 100[2,3,4]
	Siderite	0[1,2], 1, 4[2], 7[1], 14, 21[2], 30[1], 42, 60, 71[5], 82, 100[2,3,4]
	Pyrite	0[1,2], 1, 4[2], 7[1], 14, 21[2], 30[1], 42, 60, 82[5], 100[2,4]
	Sphalerite	0[1,2], 1[3], 4[2], 7, 14[1], 21[2], 30, 42[1], 60, 82, 100[2,3,4]
0.7 mg/L Se(IV)	- Waste rock	0[1,2], 1[3], 3[2], 6, 10[1], 14, 20[2], 29[1], 41, 46, 60, 66, 81[2,3,4]
	Siderite	0[1,2], 1, 3[2], 6[1], 10, 14, 20[1,2], 29, 41, 60, 81[2,4], 99
	Pyrite	0[1,2], 1, 3[2], 6[1], 10, 14, 20[1,2], 29, 41, 60, 81[2,4]
	Sphalerite	0[1,2], 1[3], 3[2], 6, 10[1], 14, 20[2], 29[1], 41, 46, 60, 81[2,3,4], 99
15 mg/L Se(IV)	- Waste rock	0[1,2], 1[1], 3[2], 6, 10, 14[1], 20[2], 30[1], 42, 60[2,6], 90[1]
	Siderite	0[1,2], 1, 3[1,2], 6, 10, 14[1], 20[1,2], 30, 42, 60[2,6], 90[1]
	Pyrite	0[1,2], 1, 3[1], 6, 10, 14, 30[1], 42, 60[6], 90[1]
	Sphalerite	0[1,2], 1[1], 3[2], 6, 10, 14[1], 20[2], 30[1], 42, 60[2,6], 90[1]
1.3 mg/L Se(IV)	- Waste rock	0[1,2], 1[1,7], 5[2], 13, 27, 35[2,8]
2.3 mg/L Se(IV)	- Waste rock	0[1,2], 1[1,7], 3[2], 6, 19, 29, 41, 59[2,8]
3.9 mg/L Se(IV)	- Waste rock	0[1,2], 1[1,7], 3[2], 6, 19, 29, 41, 59[2,8]
0.20 mg/L Se(IV)	- Waste rock	0[5], 1[1]
0.43 mg/L Se(IV)	- Waste rock	0[5], 1[1]
0.93 mg/L Se(IV)	- Waste rock	0[5], 1[1]
2.3 mg/L Se(IV)	- Waste rock	0[5], 1[1]
4.5 mg/L Se(IV)	- Waste rock	0[5], 1[1]
8.9 mg/L Se(IV)	- Waste rock	0[5], 1[1]

[1] Sampled in triplicate

[2] Sample analyzed by HPLC-ICP-MS for Se redox speciation

[3] Sample plated to assess sterility/CFU enumeration

[4] Four samples combined for composite sample

[5] Sampled in duplicate

[6] Five samples combined for composite sample; solids were dry and analyzed by XANES

[7] Sampled in triplicate; solids were dried and subjected to deionized water batch test

[8] Six batch tests sampled; solids were dried; desorption batch testing conducted on three using a 1000 mg/L SO_4^{2-} solution and three using a 100 mg/L PO_4^{3-} solution

4.3.3 XANES Analyses

XANES analyses were conducted to determine the redox speciation of the Se sequestered by the mineral phases (pyrite, siderite, and sphalerite) and the waste rock sample. The samples for XANES analyses were collected from the 15 mg/L Se(IV) batch tests on day 60. Five replicate batch tests were sampled and combined to produce 600 mg solid samples of each of the four solids. The solid samples were triple rinsed with deionized water, air dried in the glove box, mounted in Teflon® sample holders, and contained by triple layers of Kapton® tape to minimize exposure to the atmosphere during the XANES data collection. The samples were transported and stored under N_2 gas in a vacuum-sealed container for the XANES experiments. The Se K-edge XANES measurements were conducted at the Hard X-ray Micro-Analysis (HXMA-06ID-1) beamline at the Canadian Light Source (CLS), Saskatoon, Canada. The incident white beam was monochromatized with double Si(111) crystals. To remove higher harmonics in the incident beam, the second monochromator was detuned to 50% of the fully tuned beam intensity. A monochromator step size of 0.25 eV was used in the XANES region during the data collection. The XANES data for the samples was collected in fluorescence mode using a 32-element solid-state germanium detector. Twelve layers of Al foil were placed between the sample and the detector to reduce scattering as well as fluorescence from Fe and thus enhance the Se fluorescence signal reaching the detector.

To determine redox speciation of Se in the samples, XANES data were also collected on Se reference standards of known oxidation states [Na_2SeO_4: Se(VI); Na_2SeO_3: Se(IV); elemental Se powder: Se(0); and FeSe: Se(-II)]. No XANES data was collected on a Se(-I) reference standard (i.e., $FeSe_2$), which has a similar XANES spectrum to Se(-II). As such, Se corresponding to the FeSe standard will be referred to as the more general Se(-I/-II). The data for the reference standards were collected in transmission mode using helium-filled gas ionization chambers. XANES data for both the samples and reference standards were collected at ambient temperature and pressure with the simultaneous measurement of a Se reference foil spectra for energy calibration. Multiple XANES scans (4 for each sample and 2 for each reference standard) were collected and averaged to increase the signal-to-noise ratio. To prevent beam-induced changes to the Se redox speciation, each scan was collected at a different spot on the sample.

The XANES data reduction and analyses were conducted with ATHENA (Demeter v. 0.9.25) XAS analysis software (Ravel and Newville, 2005). Data reduction included the standard procedures of energy calibration, averaging of scans, background subtraction, and per atom normalization. To determine the fraction of Se redox species present in each sample, LCF analysis was then used to fit the Se K-edge XANES spectra of each sample to that of the reference standards. All the LCF analyses were conducted over an energy range of 12640 to 12690 eV.

4.3.4 Desorption Batch Tests

Waste rock solids for desorption batch tests were collected from the abiotic batch tests conducted using 1.3 mg/L, 2.3 mg/L, and 3.9 mg/L Se(IV) solutions. Three samples from each solution set were sampled after 1 d and six samples were sampled after 35 or 59 d (Table 4-2). To reflect this, the six sets of samples were named 1.3/1, 2.3/1, 3.9/1, 1.3/35, 2.3/59, and 3.9/59. All solid samples were triple rinsed with deionized water and air dried in the glove box prior to desorption batch testing. Desorption batch tests were conducted in triplicate for 1 d. Deionized water was used in desorption batch tests with samples 1.3/1, 2.3/1, and 3.9/1 and the 1000 mg/L SO_4^{2-} and 100 mg/L PO_4^{3-} solutions were used with samples 1.3/35, 2.3/59, and 3.9/59. Although the waste rock samples and batch test bottles were not sterilized prior to desorption batch testing, biotic effects on Se desorption in the batch tests were assumed to be negligible given the relatively short (1 d) incubation time and absence of nutrients and carbon source.

4.4 Results

4.4.1 Mineral Batch Tests

Siderite was the only mineral that removed Se(VI) from solution during the batch tests. There were no measureable changes in the Se concentrations in the 1.0 mg/L Se(VI) batch tests with pyrite or sphalerite (Table 4-3). The concentration of Se in the 1 mg/L Se(VI) batch tests began to decrease linearly after day 42 and 90% of Se was removed by day 100 (Figure 4-1a). The calculated reaction rate and corresponding coefficient of determination (R^2) are presented with in Table 4-4. No Se(IV) was detected in the Se(VI) batch tests with siderite, pyrite, or sphalerite. The Se redox speciation (HPLC-ICP-MS) results are presented in Table B-1 in Appendix B.

Table 4-3: Summary of Se removal from solution during batch tests.

Solid	1.0 mg/L Se(VI)	0.7 mg/L Se(IV)	15 mg/L Se(IV)
Siderite	0% removal in 42 d, 90% removal by 100 d	>95% removal by 6 d[1]	13% removal in 1 d, 99.7% removal by 91 d
Pyrite	No measureable Se removal[1]	95% removal in 1 d[1]	>95% removal in 1 d
Sphalerite	No measureable Se removal[1]	0% removal in 1 d, 27% removal by 99 d	Removal of Se(IV) was slow, minimal[1]
Waste rock	No measureable Se removal[1]	40% removal in 1 d, 97% removal by 99 d	<10% removal in 1 d, 40% removal by 99 d[1]

[1] Figures depicting these experimental data are presented in Figures B1 to B6 in Appendix B

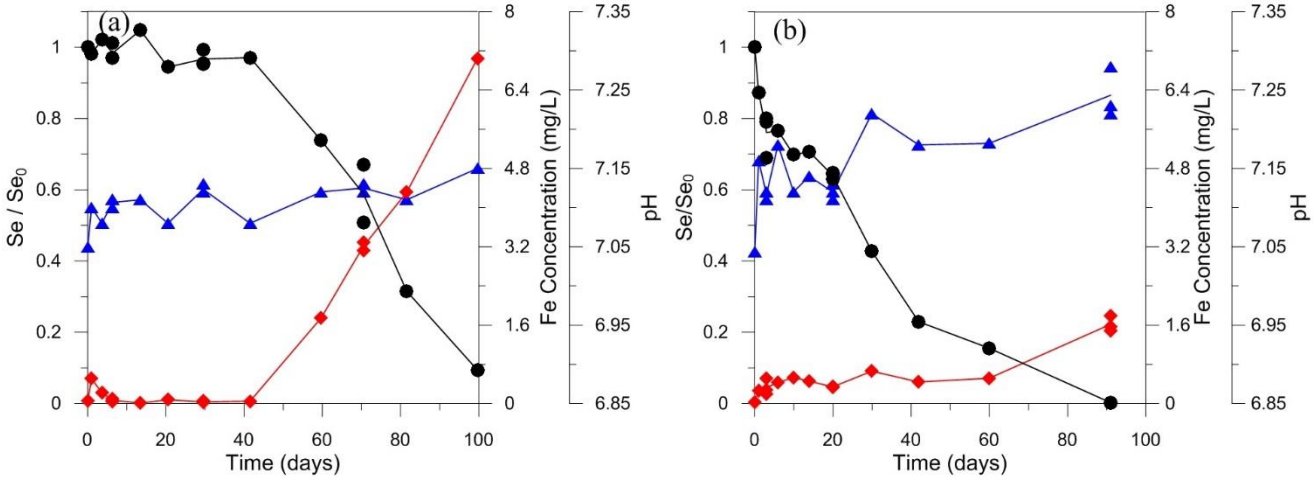

Figure 4-1: Relative Se concentrations (black circles), Fe concentrations (red diamonds), and pH (blue triangles) in sterile batch testing using 1.0 mg/L Se(VI) (a) and 15 mg/L Se(IV) (b) solutions with siderite. Se/Se_0 refers to fraction of initial Se concentration.

Results of the sterile, abiotic batch tests using 0.7 mg/L Se(IV) and 15 mg/L Se(IV) with mineral samples are summarized in Table 4-3 and Figures 4-2a and 4-2b. Se(IV) was removed from solution at different rates by each mineral. For example, in the 15 mg/L Se(IV) batch tests, pyrite removed 99.5% of Se from solution in 1 d, siderite removed ~13% in 1 d and 99.7% in 91 d, and sphalerite removed ~10% in 91 d (Figure 4-2a). In the 0.7 mg/L Se(IV) batch tests, pyrite removed 95% of Se from solution in 1 d, siderite removed 95% in 6 d, and sphalerite removed 5% of the initial 0.7 mg/L Se(IV) in 3 d and ~30% in 99 d (Figure 4-2b). The calculated reaction rates, and the corresponding R^2 values, for each of the minerals are presented in Table 4-4. The relatively constant rate of removal of Se(IV) from the 15 mg/L solution by siderite was fit with a zero order reaction rate while the exponentially decreasing rate of removal of Se(IV) from the 0.7 mg/L

solution by sphalerite was fit with a first order reaction rate. The formulas for these reactions are also presented in Table 4-4. Removal of Se(IV) in the early stages of the 15 mg/L batch tests with sphalerite was not well quantified because the changes in Se concentrations were less than the ~5% precision of the Se measurements. Because Se(IV) removal by pyrite was complete within 3 d in the 15 mg/L batch tests, a minimum reaction rate was calculated for the 99.6% Se(IV) removal that occurred in the 1 d batch tests assuming a pseudo-first order reaction in accordance with the findings of Kang et al. (2011). The increase in Se concentration in the 0.7 mg/L Se(IV) batch tests with pyrite after 6 d resulted from an increase in Se(VI) rather than Se(IV); the Se(IV) concentrations measured in the 0.7 mg/L Se(IV) pyrite batch test solutions are reflective of 94 to 100% Se(IV) removal (redox speciation data is presented in Table B-1). The observed increase in Se(VI) concentrations was not investigated.

Table 4-4: Reaction rates for Se(IV) and Se(VI) removal from batch test solutions.

		Reaction Order	**Reaction Rate (k)**		**R^2**
			μM/d	d^{-1}	
Siderite	+ Se(VI) (1 mg/L)	Zero[1]	0.20		0.93
	+ Se(IV) (15 mg/L)	Zero	2.4		0.95
Pyrite	+ Se(IV) (15 mg/L)	First[2,3]		>5.5	---
Sphalerite	+ Se(IV) (0.7 mg/L)	First[2]		0.0028	0.82
Waste rock	+ Se(IV) (0.7 mg/L)	Zero	0.063		0.95
	+ Se(IV) (2.3 mg/L)	Zero	0.37		0.97
	+ Se(IV) (3.9 mg/L)	Zero	0.28		0.91
	+ Se(IV) (15 mg/L)	Zero	0.55		0.94

[1] Zero order reactions follow the formula $Se_t = Se_0 - kt$
[2] First order reactions follow the formula $\ln Se_t = \ln Se_0 - kt$
[3] Assumed pseudo-first order in accordance with Kang et al. (2011).

The evolution of pH and concentrations of Fe and Se with time for the 1.0 mg/L Se(VI) and 15 mg/L Se(IV) batch tests with siderite are presented in Figures 4-1a and 4-1b, respectively. In both sets of batch tests, the pH and Fe concentrations increased on day 1. In the 1.0 mg/L Se(VI) batch test (Figure 4-1a), the Fe concentrations decreased to <0.1 mg/L after day 3 but then increased steadily after day 42. This increase was concurrent with the decrease in Se concentrations. The

concentrations of Fe in the 15 mg/L Se(IV) batch tests (Figure 4-1b) did not decrease after day 1, but increased concurrently with the decreasing Se concentrations.

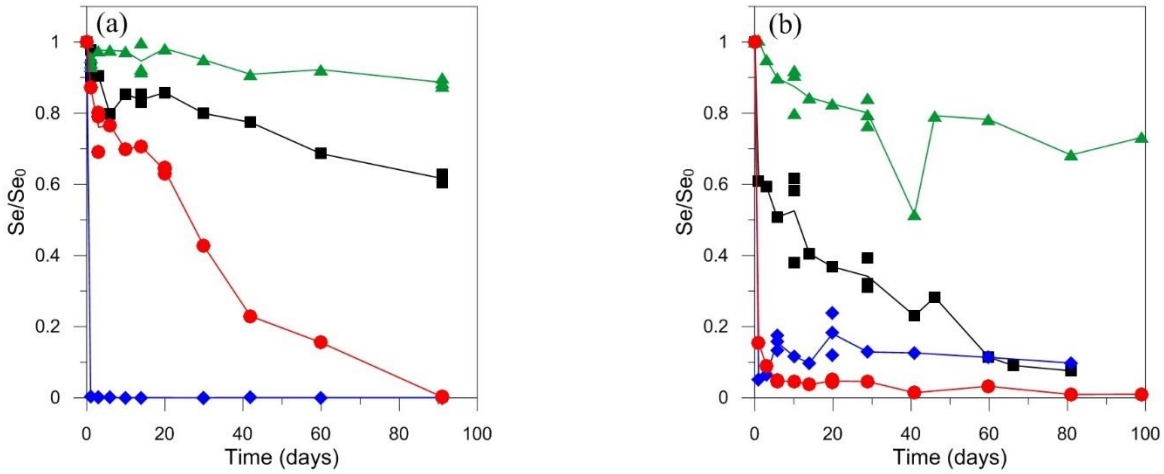

Figure 4-2: Relative concentrations of Se in sterile batch test using 15 mg/L Se(IV) (a) and 0.7 mg/L Se(IV) (b) solutions with solid samples of siderite (red circles), pyrite (blue diamonds), sphalerite (green triangles), and waste rock (black squares).

The evolution of pH and concentrations of Fe and Se with time for the 15 mg/L Se(IV) batch tests with pyrite is presented in Figure 4-3. The Fe concentration measured in the batch test sampled on day 1 was 39 mg/L, which was the highest Fe concentration measured in the batch tests. A decrease in pH and ~250 mg/L increase in SO_4^{2-} in the 1 d batch test (SO_4^{2-} results not presented) were also measured. These changes were also observed in the 0.7 mg/L Se(IV) and 1.0 mg/L Se(VI) batch tests with pyrite, but to a much lesser extent (Figures B2 and B3, respectively); the maximum Fe concentration in these two sets of batch tests was 1.7 mg/L.

In the 0.7 mg/L Se(IV) batch tests with sphalerite, the Zn concentrations increased as the Se concentrations decreased (Figure 4-4). A similar trend of increasing Zn concentration also occurred in the first 42 d of 15 mg/L Se(IV) batch tests with sphalerite (Figure B-5). In contrast to the trends of decreasing pH and increasing SO_4^{2-} noted in the batch tests with pyrite, no measureable changes in the SO_4^{2-} concentrations were observed and the pH increased only in the 15 mg/L Se(IV) batch tests with sphalerite. There was no trend in the Fe concentration in the batch tests with sphalerite and the average Fe concentration in these batch tests was 0.08 mg/L (results not shown).

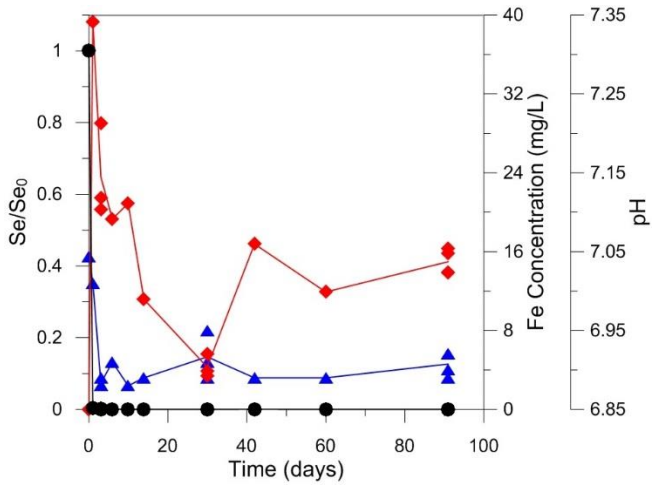

Figure 4-3: Relative Se concentrations (black circles), Fe concentrations (red diamonds), and pH (blue triangles) in sterile batch testing using a 15 mg/L Se(IV) solution with pyrite.

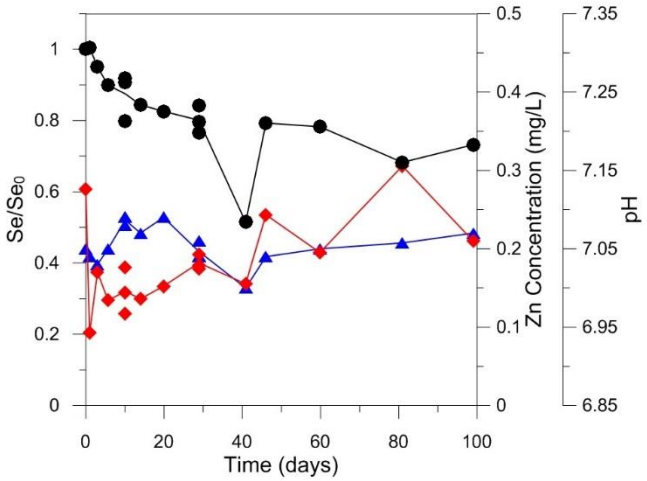

Figure 4-4: Relative Se concentrations (black circles), Zn concentrations (red diamonds), and pH (blue triangles) in sterile batch testing using a 0.7 mg/L Se(IV) solution with sphalerite.

4.4.2 Waste Rock Batch Tests

Consistent with pyrite and sphalerite, waste rock did not remove Se(VI) from solution and consistent with all three minerals, waste rock did remove Se(IV) from solution (Table 4-3). The Se(IV) removal rates for waste rock were slower than those observed for pyrite and siderite, but faster than the rate for sphalerite (Figures 4-2a and 4-2b). Similar to siderite, Se(IV) removal by waste rock was fastest on day 1 and the Se(IV) removal rate was constant after day 1. This trend was most evident in the 0.7 mg/L Se(IV) batch tests (Figure 4-2b), where 40% of the Se(IV) was removed on day 1 and ~97% by day 81. After day 60, the majority of the Se in solution was Se(VI), indicating that the Se remaining in solution on day 81 did not reflect incomplete Se(IV) removal

by waste rock. There was no change in the concentration or oxidation state of Se in the 1.0 mg/L Se(VI) batch tests with waste rock (Figure 4-5a and Table B-1).

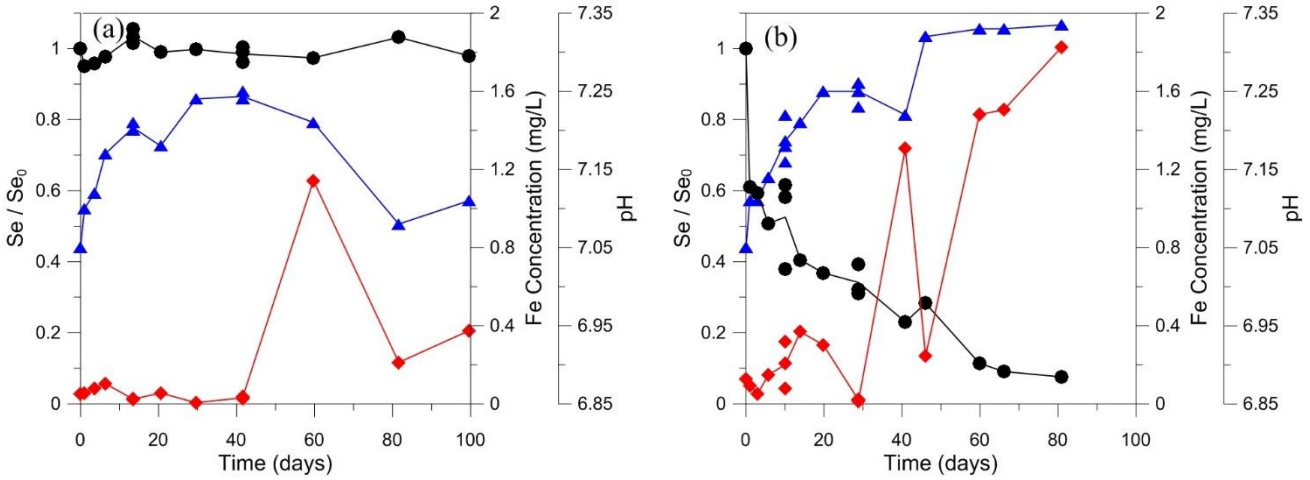

Figure 4-5: Relative Se concentrations (black circles), Fe concentrations (red diamonds), and pH (blue triangles) in sterile batch testing using 1.0 mg/L Se(VI) (a) and 0.7 mg/L Se(IV) (b) solutions with waste rock.

The Fe concentrations and pH increased with time in the 0.7 mg/L and 15 mg/L Se(IV) batch tests with waste rock (Figures 4-5b and B6), following the same trends observed in the 15 mg/L Se(IV) batch tests with siderite (Figure 4-1b). Trends of low Fe concentrations and increasing pH in the initial 42 d of the 1.0 mg/L Se(VI) batch tests with siderite and waste rock (Figure 4-1a and Figure 4-5a, respectively) were observed. After day 42, however, the Fe concentrations increased more slowly in the waste rock batch tests than in the siderite batch tests; the Fe concentrations in the Se(VI) batch tests remained below the Fe concentrations measured in the siderite batch test at the onset of Se(VI) removal. Elevated Zn concentrations characteristic of the sphalerite batch tests were not observed in the waste rock batch tests.

The two-stage trend in Se(IV) removal observed in the 0.7 mg/L and 15 mg/L Se(IV) batch tests with waste rock (Figure 4-6) was consistent with the 15 mg/L Se(IV) batch tests with siderite (Figure 4-1b). This two-stage trend was presumed to be due to an initial adsorption reaction followed by a kinetically-controlled reduction reaction. The longer-term Se(IV) removal rates for waste rock are presented in Table 4-4. The Se(IV) removed from solution by waste rock in the 1 d batch tests is presented in the form of an adsorption isotherm in Figure 4-7. The linear sorption isotherm distribution coefficient (K_d; the ratio of the concentration of Se on the waste rock to the concentration of Se in solution) was found to be 15.5±0.9 L/kg (±0.9 L/kg represents 1 standard

deviation) based on the results of 17 single day batch tests. The measurement at 13.9 mg/L did not follow the same trend as the other the 17 measurements and, thus, was considered an outlier and not used in the K_d calculation.

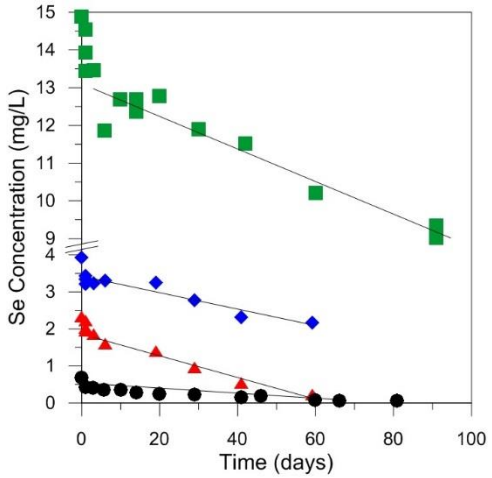

Figure 4-6: Concentrations of Se in sterile batch test using 0.7 mg/L (black circles), 2.3 mg/L (red triangles), 3.9 mg/L (blue diamonds), and 15 mg/L (green squares) Se(IV) solutions with waste rock. Lines were fitted to the measurements taken after day 1 and excluding day 81 measurement of the 0.7 mg/L Se(IV) batch test.

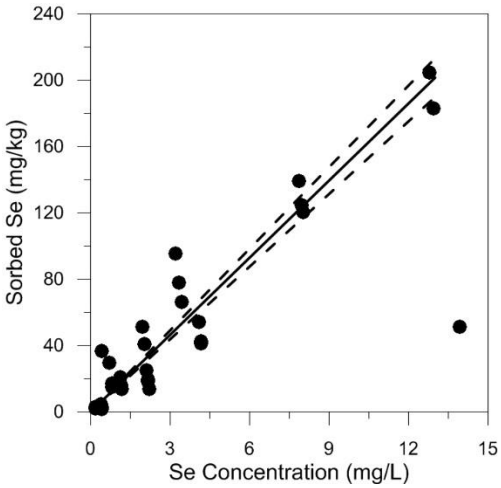

Figure 4-7: Linear sorption isotherm for Se(IV) removal from solution by waste rock in 1 d abiotic batch tests. The solid line represents a K_d of 15.5 L/kg. The dashed lines represent one standard deviation (±0.9 L/kg). The outlier measurement at 13.9 mg/L was not included in the K_d calculation.

4.4.3 XANES Results

The normalized Se K-edge XANES spectra of the samples collected from the 15 mg/L Se(IV) batch tests on day 60 are presented in Figure 4-8a along with corresponding spectra of the reference

standards. The spectra have well-defined absorption edges. The Se K-edge excitation potential for Se in the ground state (Se(0)) is 12 658 eV and increases or decreases with the oxidation state. The observed increase in edge energy of the Se reference standards (Se(-II) to Se(VI); Figure 4-8a) is a consequence of the Se in the higher oxidation states having fewer electrons than protons, which results in the energy states of the electrons being slightly lower and an increased absorption edge energy (Kelly et al., 2008; Pickering et al., 1995). Qualitative comparison of the Se K-edge XANES spectra of samples to that of reference standards shows that Se predominantly occurs as a mixture of Se(IV) and Se(0) in all the four samples tested (Figure 4-8a). Visual comparisons of the XANES spectra show that the Se on the pyrite sample is predominantly Se(0) while the waste rock sample it is predominantly Se(IV).

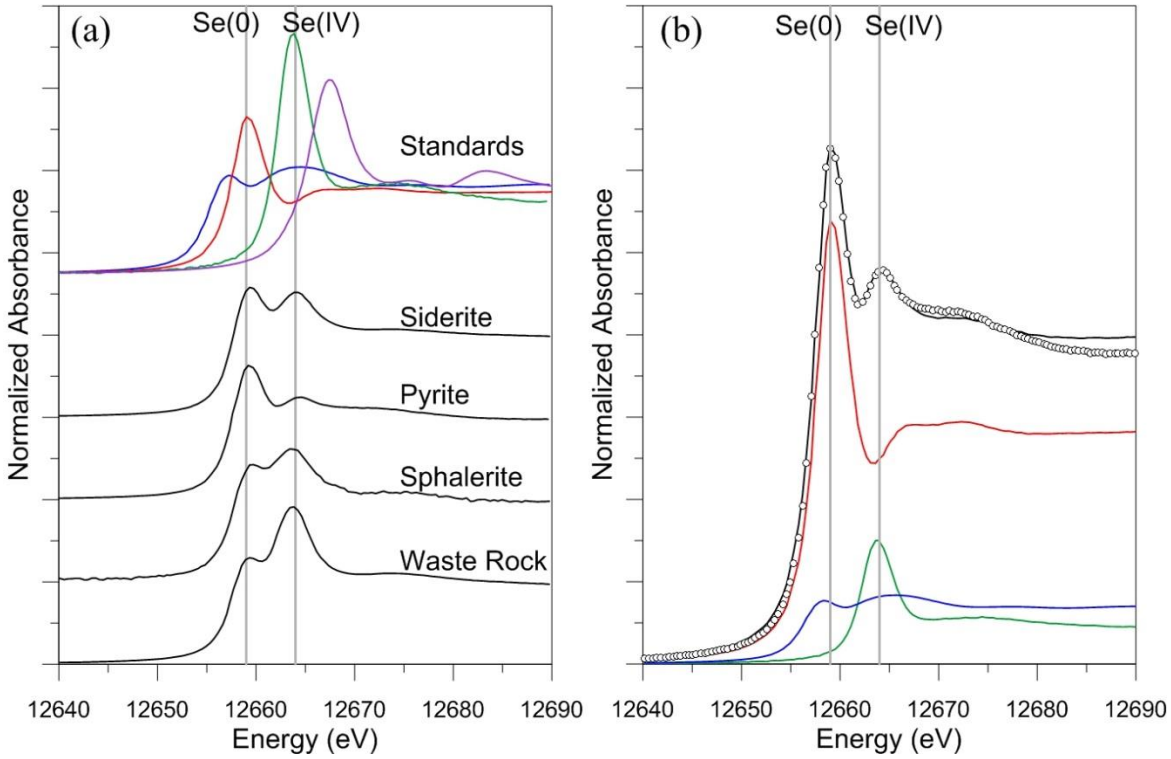

Figure 4-8: XANES spectra of reference compounds and samples of minerals and waste rock collected from the 15 mg/L Se(IV) batch tests on day 60 (a); experimental (open circles) and LCF fit (black) for the Se K-edge XANES spectrum of the pyrite sample (b). Standards (in order of ascending edge energies) are represented by the following colours: FeSe [Se(-II)] – blue; elemental Se [Se(0)] – red; Na_2SeO_3 [Se(IV)]) – green; Na_2SeO_4 [Se(VI)]) – purple.

The results of the LCF analyses of the Se K-edge XANES spectra are presented in Table 4-5. Figure 4-8b is an illustrative example LCF fit for the Se K-edge XANES spectrum of the pyrite sample denoting the fractional contributions of reference compounds spectra used to generate the

fitted spectrum. The LCF fit percentages presented in Table 4-5, correspond to the respective normalized reference spectra required to yield a good match between simulated and experimental XANES spectra of the samples with the R-factor providing a measure of the goodness of the fit (smaller R-factor values indicate better fits). Since the totals were not constrained during LCF fit analysis, the total values also reflect the goodness of fit, with better fits represented by total values closer to 100%. The quantitative analyses results indicate that some of the Se(IV) removed from solution by mineral and waste rock samples was sequestered as Se(0) over the 60 d experimental period. Pyrite, the mineral that removed Se(IV) from solution the fastest (Figure 4-2a), had the highest fraction of reduced Se species and was the only sample to sequester Se as Se(-I/-II) in addition to Se(IV) and Se(0) (Table 4-5).

Table 4-5: Quantitative redox speciation of Se on mineral phases and coal waste rock from LCF analysis of Se K-edge XANES spectra.

Sample	Se (IV)[1]	Se (0) [1]	Se (-I/-II) [1]	Total	R-factor[2]
Se(IV)-Pyrite	12.9 (±0.4)	70.7 (±1.0)	16.3 (±1.3)	99.9	0.001
Se(IV)-Siderite	27.5 (±0.9)	72.3 (±2.0)	-	99.8	0.003
Se(IV)-Sphalerite	32.7 (±0.6)	67.4 (±1.7)	-	100.1	0.004
Se(IV)-Waste Rock	41.7 (±0.9)	59.0 (±2.0)	-	100.7	0.003

[1] Entries represent percentage ± estimated standard deviation from the fit
[2] The R-factor is defined as $\sum(I_{obs}-I_{calc})^2/N$, where I_{obs} and I_{calc} are the observed and calculated normalized intensities, respectively, and the summation is over N data points

4.4.4 Desorption Batch Tests

Desorption batch tests were conducted on waste rock collected from short-term (1 d) and long-term (35 or 59 d) abiotic batch tests containing 1.3, 2.3, or 3.9 mg/L Se(IV) solutions (Figure 4-9, Table B-2). Only Se(IV) was detected in the desorption solutions (Table B-1). The Se solution concentrations increased from <0.01 to 0.11±0.04 mg/L (mean ± standard deviation) in the desorption batch tests in the 1.3/1, 2.3/1, and 3.9/1 sample sets (Figure 4-9a). The Se solution concentrations in the desorption batch tests in the 1.3/35 and 3.9/59 sample sets did not differ greatly (0.12±0.04 mg/L), but desorption batch tests with the 2.3/59 sample set yielded lower solution concentrations (0.03±0.02 mg/L). In Figure 4-9b, it is apparent that increasing the amount of Se on the waste rock during the 59 d batch test does not increase the amount of Se that can be desorbed by any of the desorption solutions used. The fraction of sequestered Se desorbed in each

of these experiments is presented in Figure B-7 and Table B-2. The 1.3/35 batch tests using the PO_4^{3-} solution yielded 2 times more desorbed Se(IV) than those using the SO_4^{2-} solution. The differences in the SO_4^{2-} and PO_4^{3-} desorption test results for sample sets 2.3/59 and 3.9/59 were less than the standard deviation of the measurements. Thus the two different solutions desorbed approximately the same amount of Se(IV) from these two sample sets.

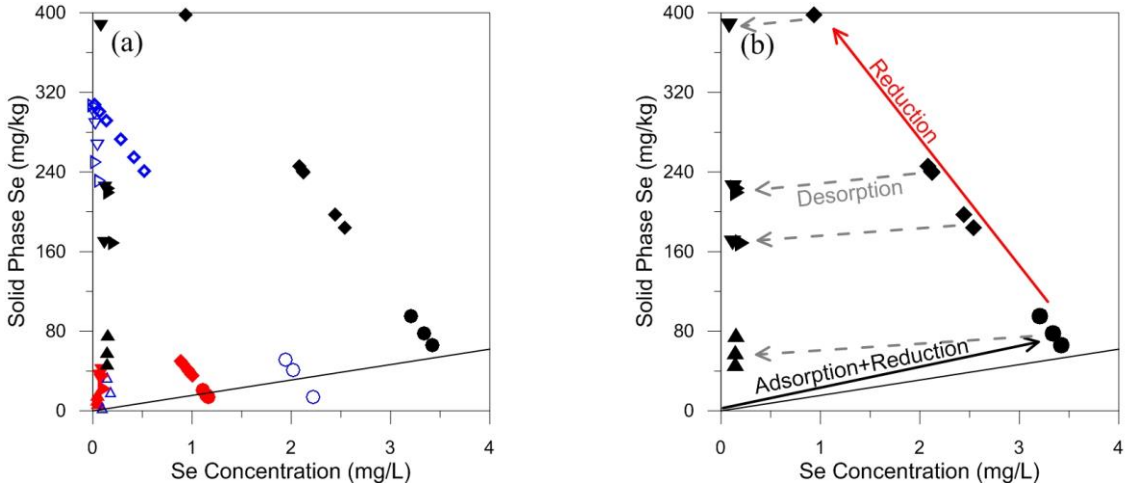

Figure 4-9: Calculated solid phase Se and measured aqueous Se in abiotic batch tests with 1d (circles) and 35/59 d (diamonds) contact times and desorption batch tests using deionized water (triangles pointed up), $\mathbf{SO_4^{2-}}$ (triangles pointed down), and $\mathbf{PO_4^{3-}}$ (triangles pointed right). The sequestered Se in batch tests using 1.3, 2.3, and 3.9 mg/L Se(IV) solutions in waste rock are presented by red, blue open, and black symbols, respectively (a). Abiotic and desorption batch test results for the 3.9 mg/L Se(IV) solution are also shown in (b) with arrows and text describing the reaction mechanisms presented by the plot. The line represents a K_d of 15.5 L/kg.

4.5 Discussion

4.5.1 Se Sequestration by Minerals

Siderite was the only mineral that removed Se(VI) from solution. The 42 d delay prior to removal suggests that Se(VI) did not adsorb to the surface of siderite. The increase in Fe concentrations and decrease in Se(VI) concentrations are consistent with the presence of reducing conditions. Under reducing conditions, Fe is present as soluble Fe(II), rather than insoluble Fe(III), thus a high Fe concentration is an indicator of reducing conditions (Appelo and Postma, 2005). The development of reducing conditions at the onset of Se(VI) removal suggests that the Se(VI) was reduced to Se(IV) or a reduced Se solid phase by the reducing agent Fe(II). No Se(IV) was detected in any of the Se(VI) batch test solutions (Table B-1), but the rate of Se(IV) removal by siderite

was more than 10 times faster than the rate of Se(VI) removal (Table 4-4), thus Se(IV) was unlikely to accumulate in the batch test solutions if produced.

The rate of Se(IV) removal from solution by siderite was greatest on day 1 and the rate of removal remained relatively constant after day 1 (Figure 4-1b). The day 1 removal is attributed primarily to adsorption of Se(IV) to the siderite surface and the longer-term constant rate of removal is attributed to the reduction of Se(IV) to Se(0). The presence of Se(IV) and Se(0) on the siderite sample analyzed with XANES supports these two mechanisms of Se sequestration. The constant Se(IV) removal rate over the large range in Se(IV) concentrations measured suggests that Se(IV) reduction can be described by a pseudo-zero order reaction. Reducing conditions, as indicated by increasing Fe concentrations, developed around day 42 in all three sets of siderite batch tests (Figures 4-1a, 4-1b, and B2), but Se(IV) reduction occurred much sooner than Se(VI) reduction. The immediate reduction of Se(IV) may be attributed to the reduction of adsorbed Se(IV) rather than aqueous Se(IV). Since no Se(VI) was adsorbed to the siderite, reduction of Se(VI) did not occur until sufficient reducing conditions developed in the batch test solutions. The reduction of adsorbed Se(IV) to Se(0) was determined to be the primary mechanism of Se(IV) reduction by siderite in batch tests conducted by Badaut et al. (2012).

Pyrite did not adsorb or reduce Se(VI) (Table 4-3, Figure B-3), consistent with the findings of laboratory experiments of Bruggeman et al. (2002) and Han et al. (2012). However, the majority of Se(IV) was removed from the batch test solutions by pyrite within 1 d (the first sampling event). Despite the lower specific surface area of the pyrite sample relative to siderite (Table 4-1), a property that generally correlates to less Se(IV) adsorption (Tachi et al., 1998) and slower Se(IV) reduction rates (Scheinost and Charlet, 2008), the Se(IV) removal by pyrite was faster, suggesting that the difference in removal rates was not a result of differences in specific surface area. Although the trends in the concentrations of Se with time cannot be used to discern whether Se(IV) was adsorbed or reduced to a Se solid phase, the presence of Se(IV), Se(0), and Se(-I/-II) on the pyrite sample analyzed with XANES suggests both of these sequestration mechanisms contributed to the Se removal. This finding is consistent with Bruggeman et al. (2005) and Breynaert et al. (2008) who determined that Se(IV) was adsorbed to pyrite prior to its reduction to Se(0). In addition, the precipitation of Fe selenides (FeSe, $FeSe_2$, Fe_7Se_8) has been observed to occur in batch tests containing aqueous Se(IV) and pyrite (Charlet et al., 2012; Diener et al., 2012), as well as other

Fe(II) minerals that exhibit fast Se(IV) reduction kinetics (Scheinost et al., 2008). Both Charlet et al. (2012) and Diener et al. (2012) observed that $FeSe_2$, rather than FeSe, precipitated in batch tests containing pyrite and Se(IV). These findings suggest that the Se(-I/-II) fraction of Se sequestered by the pyrite sample was present as $FeSe_2$. Kang et al. (2013) suggest that Fe selenides precipitate after Se(0) and only once aqueous Se(IV) is depleted. As such, the absence of Se(-I/-II) in the XANES analysis results of the other samples, all of which removed Se(IV) from 15 mg/L Se(IV) solution at a much slower rate than pyrite, is expected.

The decreased pH and increased concentrations of Fe and SO_4^{2-} in the 15 mg/L Se(IV) batch tests with pyrite (Figure 4-3) at 1 d suggest that pyrite oxidative dissolution occurred. These changes were greater in the 15 mg/L Se(IV) batch tests than the 0.7 mg/L Se(IV) batch tests (Figure B-2), suggesting that the oxidizing agent responsible for the pyrite oxidation was Se(IV). The high concentrations of SO_4^{2-} and Fe show that S_2^{2-} in the pyrite was oxidized to SO_4^{2-} and Fe(II) was not oxidized to Fe(III). As such, S_2^{2-} was the primary electron donor for Se(IV) reduction in the pyrite batch tests. Preferential oxidation of the S_2^{2-} in pyrite during Se(IV) reduction is consistent with the spectroscopic findings of Naveau et al. (2007) and Han et al. (2012).

Measureable removal of Se(IV) from the 0.7 mg/L Se(IV) batch tests by sphalerite commenced after day 1, suggesting that its removal was caused by reduction to a Se solid phase rather than adsorption to the sphalerite surface (Figure 4-4). However, Se(0) and Se(IV) were both present in the sphalerite sample analyzed by XANES (Table 4-5), suggesting both reduction and adsorption occurred. Unlike reduction rates calculated in the siderite batch test results (Figures 4-1a and 4-1b), the rate of Se(IV) removal in the sphalerite batch tests decreased with increasing time, suggesting that the reduction rate is dependent on reactant concentration or the redox potential of the batch test solution. However, the lack of trends in pH or Fe concentrations in these batch tests suggest the rate was not limited by the redox potential but possibly by the availability of a reducing agent. Given the low Fe content of the sphalerite sample (0.2% by weight) and low concentration of Fe in the sphalerite batch test solutions (average 0.08 mg/L), Fe(II) was not likely to be the reducing agent. Concurrent increases in Zn concentrations and decreases in Se concentrations suggest that the rate-limiting step in Se(IV) removal is sphalerite dissolution, which yields aqueous Zn and the reducing agent $HS^-/H_2S_{(aq)}$ in the following reactions (Crundwell, 2013; Parkhurst and Appelo, 1999):

$$ZnS + H^+ \leftrightarrow Zn^{2+} + HS^- \quad (4\text{-}1)$$

$$HS^- + H^+ \leftrightarrow H_2S \quad (4\text{-}2)$$

Non-oxidative dissolution of sphalerite (Equation 4-1) is a very slow reaction. For comparison, oxidative dissolution of sphalerite, which is similar to the pyrite oxidative dissolution reaction responsible for rapid Se(IV) removal (Figure 4-3), occurs at rates two orders of magnitude faster than the non-oxidative dissolution reaction described in Equation 4-1 (Crundwell, 2013). Jung et al. (2016) determined that $H_2S_{(aq)}$ and Se(IV) react to produce Se(0) in the following fast, abiotic reaction:

$$HSeO_3^- + H_2S + H^+ \leftrightarrow Se^0 + 2S^0 + 3H_2O \quad (4\text{-}3)$$

The reactions presented in Equations 4-1, 4-2, and 4-3 all consume H^+. While no changes in pH were measured in the 0.7 mg/L Se(IV) batch tests where Se(IV) removal was most evident (Figure 4-4), a measureable increase in pH was observed in the 15 mg/L Se(IV) batch, which showed a greater total Se(IV) removal (Figure B-4). Unfortunately, aqueous S and solid S^0 were not analyzed.

The presence of Se(IV) in the sphalerite sample suggests that, in addition to being reduced to Se(0), Se(IV) was also removed from solution by adsorption or precipitation. Precipitation of Se(IV) was unlikely because the batch test solutions were not supersaturated with $ZnSeO_3$ (Saturation Index $\leq$ -1.2; Seby et al., 2001). Unlike batch tests with the other samples, no measurable Se(IV) removal was observed in the batch tests with sphalerite by day 1. A potential explanation for this observation is the adsorption of dissolved Zn cations to the sphalerite surface, thereby increasing the sphalerite surface charge to allow outer-sphere Se(IV) adsorption. As more sphalerite dissolved, the Zn concentration in solution increased, which may have caused the Zn density on the sphalerite to increase proportionately, allowing for increased Se(IV) adsorption with time. This is consistent with the observation that sorption of Se(IV) on the surfaces of clay (Charlet et al., 2007) and calcite (Chakraborty et al., 2010) is enhanced by the presence of sorbed Fe(II) cations. The hypothesized mechanisms of Se(IV) reduction and adsorption could be tested by conducting XANES analysis for S and EXAFS analyses on sphalerite samples tested with Se(IV) solutions. In summary, both Se(IV) adsorption and reduction to Se(0) in the sphalerite batch tests were limited by the dissolution of sphalerite, which is a very slow process under reducing, circumneutral

conditions (Crundwell, 2013). As such, Se sequestration by sphalerite is not likely to be a major geochemical process in water-saturated, anoxic coal waste rock.

4.5.2 Se Sequestration by Waste Rock

Waste rock did not remove Se(VI) from solution, similar to the observations made for pyrite and sphalerite. The absence of Se(VI) reduction in the waste rock batch tests was attributed to the relatively small amount of siderite (~1% of the solid phase) available to develop the reducing conditions necessary for Se(VI) reduction. The Elk Valley waste rock dumps have solid to solution ratios ~1000 times greater than the batch tests in this study. As such, the dumps have more siderite available for reaction than the siderite batch tests and, thus, abiotic Se(VI) reduction may occur within the dumps. If abiotic Se(VI) reduction by siderite in waste rock does occur, however, it is not expected to be large relative to biotic Se(VI) reduction. In non-sterile batch tests containing waste rock and a 0.39 mg/L Se(VI) solution in the same proportions as this study, all Se(VI) was reduced to Se(IV) in less than 6 d (Figure 3-9). This was more than 6 times the rate calculated in the abiotic 1.0 mg/L Se(VI) batch tests with pure siderite (Table 4).

The concentrations of Se in the 0.7 and 15 mg/L Se(IV) batch tests with waste rock followed the same trends as that of the 15 mg/L Se(IV) batch tests with siderite, suggesting similar Se(IV) removal mechanisms (Figure 4-2a). The combination of Se(IV) adsorption and subsequent reduction to Se(0) by a pseudo-zero order reaction can describe the data from all four sets of Se(IV) batch tests with waste rock (Figure 4-6). These two sequestration mechanisms are supported by the results of XANES analysis (Figure 4-8a and Table 4-5) and the desorption batch tests (Figure 9). XANES analysis identified Se(IV) and Se(0) in the waste rock sample tested using the 15 mg/L Se(IV) solution for 60 d. The consistency of the Se desorbed from the 1.3/1, 3.9/1, 1.3/35, and 3.9/59 waste rock sample sets suggest the increased mass of Se sequestered by waste rock between days 1 and 35/59 does not result in an increase in the mass released as a result of desorption (Figure 4-9). The quantity of Se removed from solution by day 1 reflects the Se sequestered as Se(0), which is not affected by the presence of SO_4^{2-} or PO_4^{3-} anions which may compete with Se(IV) anions for adsorption sites but do not oxidize Se solid phases to soluble Se(IV) or Se(VI) (Balistrieri and Chao, 1987).

In the 0.7 and 15 mg/L Se(IV) waste rock batch tests (Figures 4-5b and B6), the Fe concentration increase on day 1 was consistent with that of pyrite and siderite, but to a much lesser extent (Figures 4-3 and 4-1b, respectively). The pH also increased on day 1, suggesting the primary source of the Fe was the dissolution of the carbonate minerals siderite and ankerite ($Ca_{1.1}Mg_{0.5}Fe_{0.4}(CO_3)_2$; 5% of waste rock by weight; Table A-1) rather than the oxidative dissolution of pyrite. The increased Fe concentration after day 29 in the 0.7 mg/L Se(IV) batch tests with waste rock (Figure 4-5b) reflects the generation of reducing conditions similar to those in batch tests with siderite (Figures 4-1a and 4-1b). The similarity in geochemical trends in the siderite and waste rock batch tests and the absence of Se(-I/-II) from the waste rock XANES sample suggest that the Se(IV) removed from solution by waste rock is sequestered primarily by siderite. Removal of Se(IV) by pyrite oxidative dissolution, however, cannot be ruled out. The imprecise SO_4^{2-} measurements cannot be used to definitively show that no SO_4^{2-} was produced in the waste rock batch tests. Furthermore, the production of Se(-I/-II) is the result of fast reduction kinetics rather than the presence of pyrite (Scheinost et al., 2008). In batch tests sampled prior to complete Se(IV) removal by pyrite, Se(0) was the final reduction product (Breynaert et al., 2008). Sequestration of Se by sphalerite in the waste rock sample is assumed to be negligible given the low Se(IV) removal rates of the sphalerite sample relative to siderite, pyrite, and waste rock samples (Figures 4-2a and 4-2b).

The removal of Se(IV) from solution in the 1 d waste rock batch tests was quantified with a K_d of 15.5±0.9 L/kg (Figure 4-7). Although the 1 d batch test results reflect Se sequestration due to multiple mechanisms, the ratio of Se on the waste rock to Se in solution was independent of the initial Se(IV) concentration over the range of Se(IV) concentrations tested. The effectiveness of this K_d at representing Se removal from solution after relatively short contact times with waste rock is consistent with findings of Fevrier et al. (2007), who quantified Se immobilization in calcareous silty clay soils by multiple mechanisms with a single K_d. The value of K_d for sterile soils tested by Fevrier et al. (2007) was 15.8±1.2 L/kg, which is very similar to the K_d determined for waste rock.

Following the first day, sequestration of Se(IV) by waste rock is attributed to the reduction of Se(IV) to Se(0). Although the rate of reduction in any single set of batch tests appears independent of the Se(IV) concentration in solution, the reduction rate was different in each set of batch tests.

A correlation between the reaction rate and the initial Se(IV) concentration is evident (Table 4-4). The apparent dependence of the reaction rate on the initial Se(IV) concentration, but not the intermediate Se(IV) concentrations, may be attributed to the previously described two-stage Se(IV) sequestration mechanism. An increase in the initial Se(IV) concentration in solution will yield an increase in the amount of Se(IV) adsorbed to the siderite and pyrite. If adsorbed Se(IV), rather than aqueous Se(IV), is reduced, an increase in adsorbed Se(IV) will increase the amount of Se(IV) available for reduction, thus increasing the reduction rate. Conducting additional batch tests could be useful in determining the validity of this correlation. Confirmation of the hypothesised mechanism may require time-resolved Se redox speciation analysis of the Se sequestered by waste rock.

The range of Se(IV) reduction rates for waste rock is narrow (Table 4-4). Although the rate-determining factors for Se(IV) reduction by waste rock were not positively identified, these reduction rates should be useful in the design of larger scale experiments and engineered saturated zones in coal waste rock dumps. In non-sterile batch tests (Figure 3-9), complete removal of Se from batch tests containing 0.39 mg/L Se(VI) was achieved in less than 20 d. Assuming all Se(VI) was reduced instantaneously and ~10% of Se(IV) was removed from solution by adsorption (calculated using K_d = 15.5 L/kg), the Se(IV) reduction rate in the non-sterile batch tests was determined to be >0.23 μM/d (>0.018 mg/L·d). This rate is faster than the reduction rate calculated for the 0.7 mg/L Se(IV) batch tests with waste rock even though the initial Se(IV) concentration was lower (0.39 mg/L). In this case, Se(IV) reduction can likely be attributed to both biotic and abiotic processes. As such, biotic reduction of Se(IV) should be quantified over a range of Se(IV) concentrations using the same methods used to define abiotic Se(IV) reduction in the current study.

4.5.3 Desorption of Sequestered Se

The desorption batch tests were used to quantify the fraction of the waste rock-sequestered Se that was reversibly adsorbed. The consistency of the mass of Se(IV) desorbed from the 1.3/1 and 3.9/1 sample sets with that of the 1.3/35 and 3.9/59 sample sets suggests that adsorption of Se(IV) to the waste rock was limited to day 1 of the batch tests (Figure 4-9). Given that reduction to Se(0) was the dominant Se sequestration mechanism after day 1, the fraction of sequestered Se that could be desorbed from the waste rock in the absence of oxidizing agents decreased greatly between day 1 and day 59 (Figure B-7 and Table B-2). The irreversibly sequestered fraction accounted for 85-

99.8% of the total sequestered Se in the 59 d batch test samples. The total amount of desorbable Se(IV) was less in the 2.3/59 samples than in the 2.3/1 samples despite the 2.3/59 samples having a much higher Se content (Table B-2). This decrease is attributed to the reduction of reversibly adsorbed Se(IV) to Se(0) and is consistent with the suggested mechanism that adsorbed Se(IV) is reduced to the more stable Se(0) over time. The absence of this trend in the 3.9/59 and 1.3/35 sample sets is likely due to the lower Se removal rates in the 3.9 mg/L and 1.3 mg/L Se(IV) batch tests (Figure 4-6). The transition from adsorbed Se(IV) to Se(0) reflects an increase in irreversibly sequestered Se on the waste rock and suggests that long-term Se sequestration can occur in anoxic coal waste rock dumps

The desorption batch tests using PO_4^{3-} and SO_4^{2-} solutions were conducted on waste rock that sequestered Se under identical conditions, yet the PO_4^{3-} solution yielded 2 times as much desorbed Se(IV) from the 1.3/35 sample set than the SO_4^{2-} solution (Figure B-7). The increased desorption is attributed to PO_4^{3-} being a stronger binding anion than SO_4^{2-} (Balistrieri and Chao, 1987). The difference in Se(IV) desorption of Se(IV) from sample sets 2.3/59 and 3.9/59 by the two solutions was, however, less than the standard deviation of the measurements. This inconsistency is attributed to the small number of tests conducted and may be remedied by conducting additional desorption batch tests. Given that the fraction of sequestered Se desorbed in the PO_4^{3-} desorption tests represents the total reversibly-adsorbed Se(IV) content of the waste rock samples (Wright and Parker, 2003), Se(IV) desorbed by PO_4^{3-} but not SO_4^{2-} may represent a fraction of Se(IV) that remains immobilized on waste rock in the presence of high SO_4^{2-}, Se(IV)-depleted groundwater, which is characteristic of environments impacted by sulfide oxidation, such as the Elk Valley waste rock dumps. Water discharging from WLC is characterized by high SO_4^{2-} concentrations (in excess of 1000 mg/L at the rock drain) and negligible PO_4^{3-} concentrations (Szmigielski, 2015). The potential presence of strongly-adsorbed Se(IV) on the waste rock samples should be further investigated using a method more suitable for Se(IV) extraction, such as the method described in Wright and Parker (2003).

4.6 Summary and Conclusions

Laboratory batch tests were conducted to identify the abiotic mechanisms of Se sequestration by coal waste rock under water-saturated, anoxic conditions. Abiotic Se(VI) reduction occurred in

batch tests with siderite, but at a rate much slower than the non-sterile batch tests (Figure 3-9), suggesting that Se(VI) reduction will be dominated by biotic processes in anoxic coal waste rock. No Se(VI) removal was observed in batch tests with pyrite or sphalerite. The extent and rate of removal of Se(IV) from solution by the mineral and waste rock samples was in the order of pyrite > siderite > waste rock > sphalerite. The mechanisms for removal via pyrite were Se(IV) adsorption to pyrite and reduction to Se(0) and Se(-I/-II) by the reducing agent S_2^{2-}. Siderite removed Se(IV) from solution by a combination of adsorption and reduction to Se(0) by the reducing agent Fe(II). In the siderite tests, the immediate removal of Se(IV) from solution compared to the delayed reduction of Se(VI) suggests that adsorbed Se(IV), rather than aqueous Se(IV), was reduced by siderite. This mechanism is most likely responsible for the long-term reduction trends observed in the waste rock batch tests. The slow rates of Se removal in the sphalerite batch tests compared to that of the other samples suggest that it is unlikely that sphalerite present in the waste rock is responsible for significant Se sequestration.

Waste rock did not remove Se(VI) from solution. Removal of Se(IV) from solution by waste rock occurred in two stages: the removal within the first day was attributed to a combination of adsorption and reduction to Se(0) by pyrite and siderite; removal after the first day was attributed primarily to reduction of Se(IV) to Se(0) by siderite. Day 1 sequestration was quantified using a linear sorption isotherm and longer-term sequestration was quantified with a range of pseudo-zero order (constant) reaction rates. Our data suggests that the rate of Se(IV) reduction may be dependent on the amount of Se(IV) adsorbed to the waste rock. The rates of abiotic reduction of Se(IV) are comparable to the reduction rates inferred from non-sterile (abiotic and biotic processes) batch tests presented in Figure 3-9. As such, abiotic reduction could have a significant positive impact on the sequestration of Se in anoxic waste rock. In addition to the quantity of Se sequestered by waste rock, the mechanism by which Se is sequestered has implications on the stability of the sequestered Se. The Se sequestered as Se(0) will not be desorbed and remobilized by Se-depleted water or competitive-binding anions. Approximately 33% of the Se sequestered during the first day of the sorption batch tests was desorbed in subsequent desorption batch tests. Between 0.1% and 15% of the Se sequestered in the 35 and 59 d sorption batch tests was desorbed. This decrease in the mass of Se that could be desorbed was attributed to sustained abiotic Se(IV) reduction. The findings of this study suggest that Se(IV) can be sequestered in anoxic zones of

waste rock dumps. If this condition was widespread within the Elk Valley waste rock dumps, it could lead to decreases in Se loading to surface water receiving dump effluent.

5 Summary and Conclusions

Waste rock dumps at coal mines in the Elk Valley have been identified as the primary source of Se in the Elk River. When Se(-I/-II)-containing minerals in the waste rock are oxidized, Se is mobilized as soluble Se(IV) and Se(VI) oxyanions, which can be transported out of the waste rock dumps in discharging groundwater and surface waters. Previous studies (Bianchin et al., 2013; Kennedy et al., 2015) have shown that Se(VI) can be sequestered in anoxic coal waste materials but they did not study the mechanisms that sequestered the Se. This study investigated the potential for Se sequestration in coal waste rock under anoxic conditions by abiotic and biotic processes. The hypotheses of this study were that (1) Se(IV) and (2) Se(VI) could be removed from solution by a coal waste rock sample under anoxic conditions via (a) biotic mechanisms and (b) abiotic mechanisms. The overarching objectives of this thesis were to:

1. develop anoxic, abiotic laboratory procedures for batch testing;
2. assess the potential for adsorption, abiotic reduction, and biotic reduction of Se(IV) and Se(VI) in anoxic coal waste rock from the Elk Valley;
3. determine which, if any, of the Fe(II)-bearing or sulfide minerals known to be present in coal waste rock (siderite, pyrite, and sphalerite) can remove Se(IV) and Se(VI) from solution under anoxic conditions;
4. quantify abiotic Se(IV) sequestration in one coal waste rock sample using a sorption isotherm and reduction rates; and
5. determine the fraction of waste rock-sequestered Se that is susceptible to desorption.

The anoxic, abiotic laboratory procedures that were developed in this study made it possible to differentiate abiotic Se sequestration from biotic Se sequestration. Biotic processes were excluded from the batch tests by sterilizing the batch test materials using a combination of syringe-filtration, ^{60}Co gamma irradiation, and autoclave sterilization. Multiple, identical batch tests were conducted so that each one could be sacrificially sampled once, thus eliminating the risk of contaminating the batch tests during sampling. These procedures made it possible for the remaining four objectives

to be addressed. They may of value to other researchers interested in isolating abiotic reaction mechanisms from complicated biogeochemical systems.

Microbial and geochemical experiments were used to address the second thesis objective and to test the thesis hypotheses. It was determined that Se(IV) and Se(VI) can be reduced to Se(0), an insoluble phase of Se, by bacteria in the coal waste rock that were affiliated with the genera *Pseudomonas* and *Erwinia*. Bacterial isolates present in the drain water sample that were affiliated with the genus *Arthrobacter* were only able to reduce Se(IV) to Se(0). In abiotic batch tests with waste rock, Se(VI) was not removed from solution. Conversely, Se(IV) was removed by adsorption to mineral surfaces and reduction to Se(0). In summary, the evidence supports hypotheses (1a), (1b), and (2a), but does not support hypothesis (2b). Although, Se(VI) could not be removed from solution by the waste rock under anoxic conditions via abiotic reaction mechanisms, it was determined that aqueous Se(VI) biotically reduced to aqueous Se(IV) could be sequestered by anoxic coal waste rock via biotic and abiotic reaction mechanisms. As such, abiotic mechanisms of Se(IV) sequestration are likely to be important to Se sequestration in anoxic coal waste rock.

Further geochemical testing in support of Objective 2 determined that abiotically sequestered Se was associated with Fe, thus adsorption and/or abiotic reduction of Se(IV) was attributed primarily to Fe-based minerals. To better understand the specific adsorption and reduction mechanisms, as well as satisfy Objective 3, additional geochemical testing was conducted on the waste rock sample and the minerals siderite, pyrite, and sphalerite. All samples removed Se(IV) from solution but only siderite removed Se(VI) from solution. The extent and rate of removal of Se(IV) from solution by the mineral and waste rock samples was in the order of pyrite > siderite > waste rock > sphalerite. The waste rock sample removed Se(IV) from solution in two stages: day 1 removal was attributed to adsorption and reduction by pyrite and siderite; longer-term (up to 91 d), constant-rate removal was attributed to reduction to Se(0) by siderite.

The fourth objective of this thesis was to quantify abiotic Se(IV) sequestration by the waste rock sample under anoxic, water-saturated conditions. The removal of Se(IV) from solution in the 1 d waste rock batch tests was quantified with a K_d of 15.5±0.9 L/kg. Although the 1 d batch test results reflect Se sequestration due to multiple mechanisms, the ratio of Se on the waste rock to Se in solution was independent of the initial Se(IV) concentration over the range of Se(IV)

concentrations tested. Longer-term Se(IV) reduction to Se(0) was quantified using pseudo-zero order (constant rate) reduction rates between 0.063 and 0.55 μM/d. These rates are similar to the biotic Se(IV) reduction rate calculated in this thesis. Further, the rates and value of K_d presented here describe the Se sequestration behaviour for one small waste rock sample and may not reflect Se sequestration behaviour in actual anoxic, coal waste rock dumps.

Desorption batch testing showed that approximately one third of Se sequestered by waste rock in 1 d batch tests could be desorbed by Se(IV)-free water. This fraction decreased with time (Objective 5) because Se sequestered by waste rock after the initial adsorption was reduced to Se(0) and, thus, could not be desorbed by Se-depleted water or competitive anions, such as SO_4^{2-} or PO_4^{3-}. In addition to providing evidence for the aforementioned abiotic Se sequestration mechanisms, the findings of the desorption batch tests show how the transition from adsorbed Se(IV) to Se(0) reflects an increase in irreversibly sequestered Se on the waste rock and suggests that long-term Se sequestration can occur in anoxic coal waste rock dumps.

5.1 Recommendations for Future Work

Several suggestions for additional research and testing to address data gaps in some of the aforementioned reaction mechanisms and to support the implementation of anoxic zones in coal waste rock dumps were presented in Chapters 3 and 4. These included:

a) The research conducted in this thesis was conducted on one waste rock sample. Testing should be conducted on more samples and at larger scales to gain a better quantitative understanding of Se sequestration in actual anoxic, coal waste rock dumps.
b) Reduction of Se(VI) in the non-sterile, anoxic batch tests did not occur until the NO_3^- in solution had been consumed. As such, reduction rates for oxidants, such as NO_3^- and O_2, in anoxic coal waste rock will impact Se(VI) reduction in the waste rock and, thus, should be quantified. Further, non-sterile batch tests should be conducted on more waste rock samples to determine if they contain bacteria that can remove NO_3^- and O_2 from solution faster than those in this study or reduce Se(VI) in the presence of other oxidants.
c) There was Se(IV) and Se(0) present in the sphalerite sample that was collected from batch tests with the 15 mg/L Se(IV) solution and analyzed by XANES, suggesting that sphalerite removed Se(IV) from solution by a combination of adsorption and reduction. Given that

there was negligible Se(IV) removal from solution on day 1 of the batch tests, it was hypothesized that Se(IV) did not adsorb directly to the sphalerite but rather to Zn cations sorbed on the sphalerite surface. This hypothesis could be tested conducting XANES analysis for S and EXAFS analyses on sphalerite samples tested with Se(IV) solutions. These analyses could also test the hypothesis that Se(IV) reacts with H_2S to produce Se(0) and S^0.

d) In abiotic batch tests, waste rock removed Se(IV) from solution at a constant rate, suggesting that the Se(IV) reduction reaction was not dependent on the Se(IV) concentration in solution. There was an apparent correlation, however, between the Se(IV) reduction rate and initial Se(IV) concentration. A potential explanation for this correlation is that the reaction rate is dependent on the content of adsorbed Se(IV) on the waste rock surface. This correlation could be confirmed by conducting additional batch tests at different Se(IV) concentrations. Confirmation of this hypothesised mechanism may require time-resolved Se redox speciation analysis of the Se sequestered by waste rock.

e) One set of non-sterile batch tests were conducted to determine whether biotic Se(VI) reduction can occur in anoxic coal waste rock. Additional non-sterile batch tests should be conducted to determine the biotic Se(VI) and Se(IV) reduction rates.

f) Desorption batch testing was conducted in three sets of three samples. This small number of samples was not sufficient to determine whether PO_4^{3-} anions mobilize more adsorbed Se(IV) than the SO_4^{2-} anions mobilized. Adsorbed Se(IV) mobilized by the PO_4^{3-} solution but not the SO_4^{2-} solution represents a fraction of sequestered Se(IV) that is unlikely to be desorbed from anoxic, WLC waste rock. Water discharging from WLC is characterized by high SO_4^{2-} concentrations and negligible PO_4^{3-} concentrations. Desorption testing by established extraction methods, such as Wright and Parker (2003), may allow for this potential form of sequestered Se to be distinguished from the fraction of Se(IV) that can be desorbed by Se-depleted water.

References

Appelo, C., Postma, D., 2005. Geochemistry, groundwater and pollution, second edition. A.A. Balkema Publishers, Amsterdam, the Netherlands.

Badaut, V., Schlegel, M.L., Descostes, M., Moutiers, G., 2012. In situ time-resolved X-ray near-edge absorption spectroscopy of selenite reduction by siderite. Environmental Science and Technology 46, 10820–10826.

Baik, M.H., Lee, S.Y., Jeong, J., 2013. Sorption and reduction of selenite on chlorite surfaces in the presence of Fe(II) ions. Journal of Environmental Radioactivity 126, 209–215.

Baldwin, S., Mirjafari, P., Rezahdebashi, M., Subedi, G., Taylor, J., 2015. Start-up of a passive remediation bioreactor for sulfate and selenium removal from mine tailings water, in: 10th International Conference on Acid Rock Drainage. pp. 1224–1234.

Balistrieri, L., Chao, T., 1987. Selenium Adsorption by Goethite. Soil Science Society of America Journal 51, 1145–1151.

Bar-Yosef, B., Meek, D., 1987. Selenium Sorption By Kaolinite and Montmorillonite. Soil Science 144, 11–19.

Barbour, S.L., Hendry, M.J., Carey, S.K., 2016. High-Resolution Profiling of the Stable Isotopes of Water in Unsaturated Coal Waste Rock. Journal of Hydrology 534, 616–629.

Beatty, J., Russo, G., 2014. Ambient water quality guidelines for Selenium Technical Report Update. British Columbia Ministry of Environment, Victoria, BC.

Bebie, J., Schoonen, M., Fuhrmann, M., Strongin, D., 1998. Surface charge development on transition metal sulfides: an electrokinetic study. Geochimica et Cosmochimica Acta 62, 633–642.

Bianchin, M., Martin, A., Adams, J., 2013. In-Situ Immobilization of Selenium within the Saturated Zones of Backfilled Pits at Coal-Mine Operations, in: 37th Annual British Columbia Mine Reclamation Symposium. Vancouver, BC, 16-19 September 2013, pp. 1–16.

Biswas, A., Hendry, M.J., Essilfie-Dughan, J., 2016. Geochemistry of arsenic in low sulfide-high carbonate coal waste rock, Elk Valley, British Columbia, Canada. Science of the Total Environment 579, 396–408.

Bondici, V.F., Lawrence, J.R., Khan, N.H., Hill, J.E., Yergeau, E., Wolfaardt, G.M., Warner, J., Korber, D.R., 2013. Microbial communities in low permeability, high pH uranium mine tailings: characterization and potential effects. Journal of Applied Microbiology 114, 1671–1686.

Bostick, B.C., Fendorf, S., Manning, B.A., 2003. Arsenite adsorption on galena (PbS) and sphalerite (ZnS). Geochimica et Cosmochimica Acta 67, 895–907.

Breynaert, E., Bruggeman, C., Maes, A., 2008. XANES-EXAFS analysis of se solid-phase reaction products formed upon contacting Se(IV) with FeS2 and FeS. Environmental Science & Technology 42, 3595–3601.

Bruggeman, C., Maes, A., Vancluysen, J., Vandemussele, P., 2005. Selenite reduction in Boom clay: Effect of FeS2, clay minerals and dissolved organic matter. Environmental Pollution 137, 209–221.

Bruggeman, C., Vancluysen, J., Maes, A., 2002. New selenium solution speciation method by ion chromatography + gamma counting and its application to FeS2-controlled reducing conditions. Radiochimica Acta 90, 629–635.

Burton, G.A., Giddings, T.H., DeBrine, P., Fall, R., 1987. High incidence of selenite-resistant bacteria from a site polluted with selenium. Applied and Environmental Microbiology 53, 185–188.

Chakraborty, S., Bardelli, F., Charlet, L., 2010. Reactivities of Fe(II) on calcite: selenium reduction. Environmental Science & Technology 44, 1288–1294.

Charlet, L., Kang, M., Bardelli, F., Kirsch, R., Géhin, A., Grenèche, J.-M., Chen, F., 2012.

Nanocomposite pyrite-greigite reactivity toward Se(IV)/Se(VI). Environmental Science & Technology 46, 4869–4876.

Charlet, L., Scheinost, A.C., Tournassat, C., Greneche, J., Géhin, A., Fernández-Martınez, A., Coudert, S., Tisserand, D., Brendle, J., 2007. Electron transfer at the mineral/water interface: Selenium reduction by ferrous iron sorbed on clay. Geochimica et Cosmochimica Acta 71, 5731–5749.

Charlet, L., Wersin, P., Stumm, W., 1990. Surface charge of MnCO3 and FeC03. Geochimica et Cosmochimica Acta 54, 2329–2336.

Chen, Y.-W., Truong, H.-Y.T., Belzile, N., 2009. Abiotic formation of elemental selenium and role of iron oxide surfaces. Chemosphere 74, 1079–1084.

Cole, J.R., Wang, Q., Cardenas, E., Fish, J., Chai, B., Farris, R.J., Mcgarrell, D.M., Marsh, T., Garrity, G.M., Tiedje, J.M., 2009. The Ribosomal Database Project: improved alignments and new tools for rRNA analysis. Nucleic Acids Research 37, D141–D145.

Couture, R., Charlet, L., Markelova, E., Madé, B., Parsons, C.T., 2015. On–Off Mobilization of Contaminants in Soils during Redox Oscillations. Environmental Science & Technology 49, 3015–3023.

Crundwell, F.K., 2013. The dissolution and leaching of minerals: Mechanisms, myths and misunderstandings. Hydrometallurgy 139, 132–148.

Curti, E., Aimoz, L., Kitamura, A., 2013. Selenium uptake onto natural pyrite. Journal of Radioanalytical and Nuclear Chemistry 295, 1655–1665.

Day, S., Kennedy, C., Pumphrey, J., 2012. Interpretation of Selenium Release from Coal Mine Waste Rock Dumps, Southeastern British Columbia, Canada, in: 9th International Conference on Acid Rock Drainage. pp. 1678–1689.

Dessouki, T.C.E., Ryan, A., 2010. Canada-British Columbia Water Quality Monitoring Agreement: Water Quality Assessment of the Kootenay, Elk and St. Mary River. B.C. Ministry of Environment and Environment Canada 1–47.

Diener, A., Neumann, T., Kramar, U., Schild, D., 2012. Structure of selenium incorporated in pyrite and mackinawite as determined by XAFS analyses. Journal of Contaminant Hydrology 133, 30–39.

Duc, M., Lefevre, G., Fedoroff, M., Jeanjean, J., Rouchaud, J.C., Monteil-Rivera, F., Dumonceau, J., Milonjic, S., 2003. Sorption of selenium anionic species on apatites and iron oxides from aqueous solutions. Journal of Environmental Radioactivity 70, 61–72.

Dungan, R.S., Frankenberger, W.T., 1999. Microbial Transformations of Selenium and the Bioremediation of Seleniferous Environments. Bioremediation Journal 3, 171–188.

Eschbach, M., Möbitz, H., Rompf, A., Jahn, D., 2003. Members of the genus Arthrobacter grow anaerobically using nitrate ammonification and fermentative processes: Anaerobic adaptation of aerobic bacteria abundant in soil. FEMS Microbiology Letters 223, 227–230.

Essilfie-Dughan, J., Hendry, M.J., Dynes, J.J., Hu, Y., Biswas, A., Barbour, S.L., Day, S., 2017. Geochemical and mineralogical characterization of sulfur and iron in coal waste rock, Elk Valley, British Columbia, Canada. Science of The Total Environment 586, 753–769.

Fernández-Martínez, A., Charlet, L., 2009. Selenium environmental cycling and bioavailability: A structural chemist point of view. Reviews in Environmental Science and Biotechnology 8, 81–110.

Février, L., Martin-Garin, A., Leclerc, E., 2007. Variation of the distribution coefficient (Kd) of selenium in soils under various microbial states. Journal of Environmental Radioactivity 97, 189–205.

Finck, N., Dardenne, K., 2016. Interaction of selenite with reduced Fe and/or S species: An XRD and XAS study. Journal of Contaminant Hydrology 188, 44–51.

Garbisu, C., Ishii, T., Leighton, T., Buchanan, B., 1996. Bacterial reduction of selenite to elemental selenium. Chemical Geology 132, 199–204.

Goodarzi, F., Grieve, D.A., Sanei, H., Gentzis, T., Goodarzi, N.N., 2009. Geochemistry of coals from the Elk Valley coalfield, British Columbia, Canada. International Journal of Coal Geology 77, 246–259.

Han, D.S., Batchelor, B., Abdel-Wahab, A., 2012. Sorption of selenium(IV) and selenium(VI) onto synthetic pyrite (FeS2): spectroscopic and microscopic analyses. Journal of colloid and interface science 368, 496–504.

Hay, M.B., Leone, G., Partey, F., Wilking, B., 2016. Selenium attenuation via reductive precipitation in unsaturated waste rock as a control on groundwater impacts in the Idaho Phosphate Patch. Applied Geochemistry 74, 176–193.

Hayes, K.F., Roe, A.L., Brown, G.E., Hodgson, K.O., Leckie, J.O., Parks, G.A., 1987. In Situ X-ray Absorption Study of Surface Complexes: Selenium Oxyanions on α-FeOOH. Science 238, 783–786.

Hendry, M.J., Biswas, A., Essilfie-Dughan, J., Chen, N., Day, S.J., Barbour, S.L., 2015. Reservoirs of Selenium in Coal Waste Rock: Elk Valley, British Columbia, Canada. Environmental Science & Technology 49, 8228–8236.

Herbel, M., Johnson, T., Oremland, R., Bullen, T., 2000. Fractionation of selenium isotopes during bacterial respiratory reduction of selenium oxyanions. Geochimica et Cosmochimica Acta 64, 3701–3709.

Hockin, S., Gadd, G.M., 2006. Removal of selenate from sulfate-containing media by sulfate-reducing bacterial biofilms. Environmental Microbiology 8, 816–826.

Hunter, W.J., Manter, D.K., 2009. Reduction of selenite to elemental red selenium by Pseudomonas sp. Strain CA5. Current Microbiology 58, 493–498.

Ike, M., Takahashi, K., Fujita, T., Kashiwa, M., Fujita, M., 2000. Selenate reduction by bacteria isolated from aquatic environment free from selenium contamination. Water Research 34, 3019–3025.

Jenner, G.A., Longerich, H.P., Jackson, S.E., Fryer, B.J., 1990. ICP-MS - A powerful tool for high-precision trace-element analysis in Earth sciences: Evidence from analysis of selected U.S.G.S. reference samples. Chemical Geology 83, 133–148.

Jung, B., Safan, A., Batchelor, B., Abdel-Wahab, A., 2016. Spectroscopic study of Se(IV) removal from water by reductive precipitation using sulfide. Chemosphere 163, 351–358.

Kang, M., Chen, F., Wu, S., Yang, Y., Bruggeman, C., Charlet, L., 2011. Effect of pH on aqueous Se(IV) reduction by pyrite. Environmental Science & Technology 45, 2704–2710.

Kang, M., Ma, B., Bardelli, F., Chen, F., Liu, C., Zheng, Z., Wu, S., Charlet, L., 2013. Interaction of aqueous Se(IV)/Se(VI) with FeSe/FeSe2: Implication to Se redox process. Journal of hazardous materials 248–249, 20–28.

Keller, R., Holzapfel, W., Schulz, H., 1977. Effect of pressure on the atom positions in Se and Te. Physical Review B 16, 4404–4412.

Kelly, S.D., Hesterberg, D., Ravel, B., 2008. Analysis of soils and minerals using X-ray absorption spectroscopy, in: Methods of Soil Analysis Part 5—Mineralogical Methods. Soil Science Society of America, Madison, WI, pp. 387–463.

Kennedy, C., Day, S., Mackie, D., Pesonen, N., 2015. Biogeochemical Selenium Sequestration in Unsaturated Coal Reject Piles, in: 10th International Conference on Acid Rock Drainage. pp. 107–117.

Knotek-Smith, H.M., Crawford, D.L., Möller, G., Henson, R.A., 2006. Microbial studies of a selenium-contaminated mine site and potential for on-site remediation. Journal of Industrial Microbiology & Biotechnology 33, 897–913.

Kuroda, M., Notaguchi, E., Sato, A., Yoshioka, M., Hasegawa, A., Kagami, T., Narita, T., Yamashita, M., Sei, K., Soda, S., Ike, M., 2011. Characterization of Pseudomonas stutzeri NT-I capable of removing soluble selenium from the aqueous phase under aerobic conditions. Journal of Bioscience and Bioengineering 112, 259–264.

Langmuir, D., 1997. Aqueous Environmental Geochemistry. Prentice-Hall, Upper Saddle River, NJ.

Lemly, A., 2004. Aquatic selenium pollution is a global environmental safety issue. Ecotoxicology and Environmental Safety 59, 44–56.

Lenz, M., Hullebusch, E.D. Van, Hommes, G., Corvini, P.F.X., Lens, P.N.L., 2008. Selenate removal in methanogenic and sulfate-reducing upflow anaerobic sludge bed reactors. Water Research 42, 2184–2194.

Lenz, M., Lens, P.N.L., 2009. The essential toxin: the changing perception of selenium in environmental sciences. The Science of the Total Environment 407, 3620–3633.

Lortie, L., Gould, W.D., Rajan, S., McCready, R.G., Cheng, K.J., 1992. Reduction of Selenate and Selenite to Elemental Selenium by a Pseudomonas stutzeri Isolate. Applied and Environmental Microbiology 58, 4042–4044.

Luek, A., Brock, C., Rowan, D.J., Rasmussen, J.B., 2014. A Simplified Anaerobic Bioreactor for the Treatment of Selenium-Laden Discharges from Non-acidic, End-Pit Lakes. Mine Water and the Environment 33, 295–306.

Lussier, C., Veiga, V., Baldwin, S., 2003. The geochemistry of selenium associated with coal waste in the Elk River Valley, Canada. Environmental Geology 44, 905–913.

Macy, J.M., Michel, T.A., Kirsch, D.G., 1989. Selenate reduction by a Pseudomonas species: a new mode of anaerobic respiration. FEMS Microbiology Letters 52, 195–198.

Mahmood, F.N., Barbour, S.L., Hendry, M.J., Kennedy, C., 2017. Nitrate release from Coal Waste Rock Dumps in the Elk Valley, British Columbia, Canada. Science of the Total Environment In revisio.

Maiers, D.T., Wichlacz, P.L., Thompson, D.L., Bruhn, D.F., 1988. Selenate reduction by bacteria from a selenium-rich environment. Applied and Environmental Microbiology 54, 2591–2593.

Martin, A.J., Simpson, S., Fawcett, S., Wiramanaden, C.I.E., Pickering, I.J., Belzile, N., Chen, Y.-W., London, J., Wallschläger, D., 2011. Biogeochemical mechanisms of selenium exchange between water and sediments in two contrasting lentic environments. Environmental Science & Technology 45, 2605–2612.

Masscheleyn, P.H., Delaune, R.D., Patrick, W.H., 1990. Transformations of Selenium As Affected by Sediment Oxidation-Reduction Potential and pH. Environmental Science & Technology 24, 91–96.

McDonald, L.E., Strosher, M.M., 1998. Selenium Mobilization from Surface Coal Mining in the Elk River Basin, British Columbia: A Survey of Water, Sediment and Biota, Proceedings of the 24th Annual British Columbia Mine Reclamation Symposium. The Technical and

Research Committee on Reclamation, Cranbrook, BC.

Myneni, S.C., 1997. Abiotic Selenium Redox Transformations in the Presence of Fe(II,III) Oxides. Science 278, 1106–1109.

Naveau, A., Monteil-Rivera, F., Guillon, E., Dumonceau, J., 2007. Interactions of aqueous selenium (-II) and (IV) with metallic sulfide surfaces. Environmental Science & Technology 41, 5376–5382.

Neal, R., Sposito, G., Holtzclaw, K., Traina, S., 1987a. Selenite Adsorption on Alluvial Soils: I. Soil Composition and pH Effects. Soil Science Society of America Journal 51, 1161–1165.

Neal, R., Sposito, G., Holtzclaw, K., Traina, S., 1987b. Selenite Adsorption on Alluvial Soils: II. Solution Composition Effects. Soil Science Society of America Journal1 51, 1165–1169.

Oremland, R.S., Herbel, M.J., Blum, J.S., Langley, S., Beveridge, T.J., Ajayan, P.M., Sutto, T., Ellis, A. V, Curran, S., 2004. Structural and spectral features of selenium nanospheres produced by Se-respiring bacteria. Applied and Environmental Microbiology 70, 52–60.

Oremland, R.S., Hollibaugh, J.T., Maest, A.S., Presser, T.S., Miller, L.G., Culbertson, C.W., 1989. Selenate reduction to elemental selenium by anaerobic bacteria in sediments and culture: biogeochemical significance of a novel, sulfate-independent respiration. Applied and Environmental Microbiology 55, 2333–2343.

Oremland, R.S., Steinberg, N.A., Maest, A.S., Miller, L.G., Holllbaugh, J.T., 1990. Measurement of in Situ Rates of Selenate Removal by Dissimilatory Bacterial Reduction in Sediments. Environmental Science & Technology 24, 1157–1164.

Palmer, M., Bernhardt, E., Schlesinger, W., Eshleman, K., Foufoula- Georgiou, E., Hendryx, M., Lemly, A., Likens, G., Loucks, O., Power, M., White, P., Wilcock, P., 2010. Mountaintop Mining Consequences. Science 327, 148–149.

Parkhurst, D.L., Appelo, C. a J., 1999. User's Guide To PHREEQC (version 2)— a Computer Program for Speciation, Batch-Reaction, One-Dimensional Transport, and Inverse Geochemical Calculations. US Department of the Interior, US Geological Survey Water-Reso, 326.

Parmentier, M., Ollivier, P., Joulian, C., Albrecht, A., Hadi, J., Greneche, J.M., Pauwels, H., 2014. Enhanced heterotrophic denitrification in clay media: The role of mineral electron donors. Chemical Geology 390, 87–99.

Peak, D., Sparks, D., 2002. Mechanisms of Selenate Adsorption on Iron Oxides and Hydroxides. Environmental Science & Technology 36, 1460–1466.

Picardal, F., 2012. Abiotic and Microbial Interactions during Anaerobic Transformations of Fe(II) and NOx. Frontiers in Microbiology 3, 1–7.

Pickering, I.J., Brown, Jr., G.E., Tokunagas, T.K., 1995. Quantitative Speciation of Selenium in Soils Using X-ray Absorption Spectroscopy. Environmental Science & Technology 29, 2456–2459.

Price, W., 2009. Prediction manual for drainage chemistry from sulphidic geologic materials, Mend Report 1.20.1. Smithers, BC.

Ravel, B., Newville, M., 2005. ATHENA, ARTEMIS, HEPHAESTUS: Data analysis for X-ray absorption spectroscopy using IFEFFIT. Journal of Synchrotron Radiation 12, 537–541.

Rovira, M., Giménez, J., Martínez, M., Martínez-Lladó, X., de Pablo, J., Martí, V., Duro, L., 2008. Sorption of selenium(IV) and selenium(VI) onto natural iron oxides: goethite and hematite. Journal of Hazardous Materials 150, 279–284.

Schabert, M.S., 2016. The Application of Push-Pull Testing to Define Biogeochemical Controls on Selenium and Nitrate Attenuation in Saturated Coal Waste Rock. University of Saskatchewan.

Scheinost, A.C., Charlet, L., 2008. Selenite reduction by mackinawite, magnetite and siderite: XAS characterization of nanosized redox products. Environmental Science & Technology 42, 1984–1989.

Scheinost, A.C., Kirsch, R., Banerjee, D., Fernandez-Martinez, A., Zaenker, H., Funke, H., Charlet, L., 2008. X-ray absorption and photoelectron spectroscopy investigation of selenite reduction by FeII-bearing minerals. Journal of Contaminant Hydrology 102, 228–245.

Seby, F., Potin-Gautier, M., Giffaut, E., Borge, G., Donard, O.F.X., 2001. A critical review of thermodynamic data for selenium species at 25 C. Chemical Geology 171, 173–194.

Staicu, L.C., Ackerson, C.J., Cornelis, P., Ye, L., Berendsen, R.L., Hunter, W.J., Noblitt, S.D., Henry, C.S., Cappa, J.J., Montenieri, R.L., Wong, A.O., Musilova, L., Sura-de Jong, M., van Hullebusch, E.D., Lens, P.N.L., Reynolds, R.J.B., Pilon-Smits, E.A.H., 2015. Pseudomonas moraviensis subsp. stanleyae, a bacterial endophyte of hyperaccumulator Stanleya pinnata, is capable of efficient selenite reduction to elemental selenium under aerobic conditions. Journal of Applied Microbiology 119, 400–410.

Steinberg, N., Oremland, R., 1990. Dissimilatory selenate reduction potentials in a diversity of sediment types. Applied and Environmental Microbiology 56, 3550–3557.

Steinberg, N., Switzer Blum, J., Hochstein, L., Oremland, R., 1992. Nitrate is a Preferred Electron Acceptor for Growth of Freshwater Selenate-Respiring Bacteria. Applied and Environmental Microbiology 58, 426–428.

Stolz, J., Basu, P., Santini, J.M., Oremland, R., 2006. Arsenic and selenium in microbial metabolism. Annual review of microbiology 60, 107–130.

Stolz, J., Oremland, R., 1999. Bacterial respiration of arsenic and selenium. FEMS Microbiology Reviews 23, 615–627.

Su, C., Suarez, D., 2000. Selenate and selenite sorption on iron oxides an infrared and electrophoretic study. Soil Science Society of America Journal 64, 101–111.

Swanson, S., 2010. The Way Forward: A Strategic Plan for the Management of Selenium at Teck Coal Operations. The Strategic Advisory Panel on Selenium Management. Report prepared for Teck Coal Limited, Calgary, AB.

Switzer Blum, J., Stolz, J., Oren, A., Oremland, R., 2001. Selenihalanaerobacter shriftii gen. nov., sp. nov., a halophilic anaerobe from Dead Sea sediments that respires selenate. Archives of microbiology 175, 208–219.

Szmigielski, J.T., 2015. Characterizing a Groundwater System Downgradient of a Coal Mine Waste Rock Dump, Elk Valley, British Columbia, Canada. University of Saskatchewan.

Tachi, Y., Shibutani, T., Sato, H., Yui, M., 1998. Sorption and diffusion behavior of selenium in tuff. Journal of Contaminant Hydrology 35, 77–89.

Tamura, K., Peterson, D., Peterson, N., Stecher, G., Nei, M., Kumar, S., 2011. MEGA5: Molecular evolutionary genetics analysis using maximum likelihood, evolutionary distance, and maximum parsimony methods. Molecular Biology and Evolution 28, 2731–2739.

Teck Resources Limited, 2014. Elk Valley Water Quality Plan. Report to British Columbia Minister of Environment. Available for download from http://www.teck.com/media/2015-Water-elk_valley_water_quality_plan_T3.2.3.2.pdf.

Teck Resources Limited, 2016. Permit 107517 Environmental Monitoring Committee: 2016 Public Report.

Tonietto, G.B., Godoy, J.M., Oliveira, A.C., De Souza, M. V., 2010. Simultaneous speciation of arsenic (As(III), MMA, DMA, and As(V)) and selenium (Se(IV), Se(VI), and SeCN-) in petroleum refinery aqueous streams. Analytical and Bioanalytical Chemistry 397, 1755–1761.

Villeneuve, S.A., Barbour, S.L., Hendry, M.J., Carey, S.K., 2017. Estimates of water and solute release from a coal waste rock dump in the Elk Valley, British Columbia, Canada. Science of the Total Environment 601–602, 543–555.

Weerasooriya, R., Tobschall, H.J., 2005. Pyrite–water interactions: Effects of pH and pFe on surface charge. Colloids and Surfaces A: Physicochemical and Engineering Aspects 264, 68–74.

Wellen, C.C., Shatilla, N.J., Carey, S.K., 2015. Regional scale selenium loading associated with surface coal mining, Elk Valley, British Columbia, Canada. Science of The Total Environment 532, 791–802.

White, A., Benson, S., Yee, A., Wollenberg, H., Flexser, S., 1991. Groundwater Contamination at the Kesterson Reservoir, California: 2. Geochemical Parameters Influencing Selenium Mobility. Water Resources Research 27, 1085–1098.

Wright, M.T., Parker, D.R., 2003. Critical Evaluation of the Ability of Sequential Extraction

Procedures To Quantify Discrete Forms of Selenium in Sediments and Soils. Environmental Science 37, 4709–4716.

Yamamoto, M., Endo, M., Ujihira, K., 1984. Distribution of selenium between galena and sphalerite. Chemical geology 42, 243–248.

Yang, S.I., 2011. Biotransformation and Interactions of Selenium with Mixed and Pure Culture Biofilms. M.Sc. Thesis. Department of Geological Sciences, University of Saskatchewan.

Yang, S.I., George, G.N., Lawrence, J.R., Kaminskyj, S.G.W., Dynes, J.J., Lai, B., Pickering, I.J., 2016. Multispecies Biofilms Transform Selenium Oxyanions into Elemental Selenium Particles: Studies Using Combined Synchrotron X-ray Fluorescence Imaging and Scanning Transmission X-ray Microscopy. Environmental Science & Technology 50, 10343–10350.

Yllera De Llano, A., Bidoglio, G., Avogadro, A., Gibson, P.N., Rivas Romero, P., 1996. Redox reactions and transport of selenium through fractured granite. Journal of Contaminant Hydrology 21, 129–139.

Zhao, Y., 2014. Genoics of Erwinia amylovora and Related Erwinia Species Associated with Pome Fruit Trees, in: Gross, D.C., Lichens-Park, A., Kole, C. (Eds.), Genomics of Plant-Associated Bacteria. Springer, pp. 1–36.

Ziemkiewicz, P.F., O'Neal, M., Lovett, R.J., 2011. Selenium Leaching Kinetics and In situ Control. Mine Water and the Environment 30, 141–150.

Appendix A: Characterization of Waste Rock and Mineral Samples

X-ray Diffraction

Powder X-ray Diffraction (XRD) was conducted to determine the mineral composition of the West Line Creek waste rock sample tested in this thesis. The PANanalytical Empyrean X-ray diffractometer used to conduct XRD has a limit of detection around 1% by weight. The XRD pattern collected is presented in Figure A-1. The mineral components were identified and quantified using XPert Highscore Plus software (Table A-1). The carbonate minerals, siderite ($FeCO_3$) and ankerite ($CaMg_{0.5}Fe_{0.5}(CO_3)_2$), have key diffraction peaks at 37.6° and 36.0°, respectively (Drits et al., 2005; Sherman, 2009). Dissolution of these two minerals is the main source of Fe and Mn in the batch tests conducted in Chapter 3 of the thesis. The majority of the peaks in the waste rock diffraction pattern are due to the quartz and clay mineral components, which did not impact the batch test solutions.

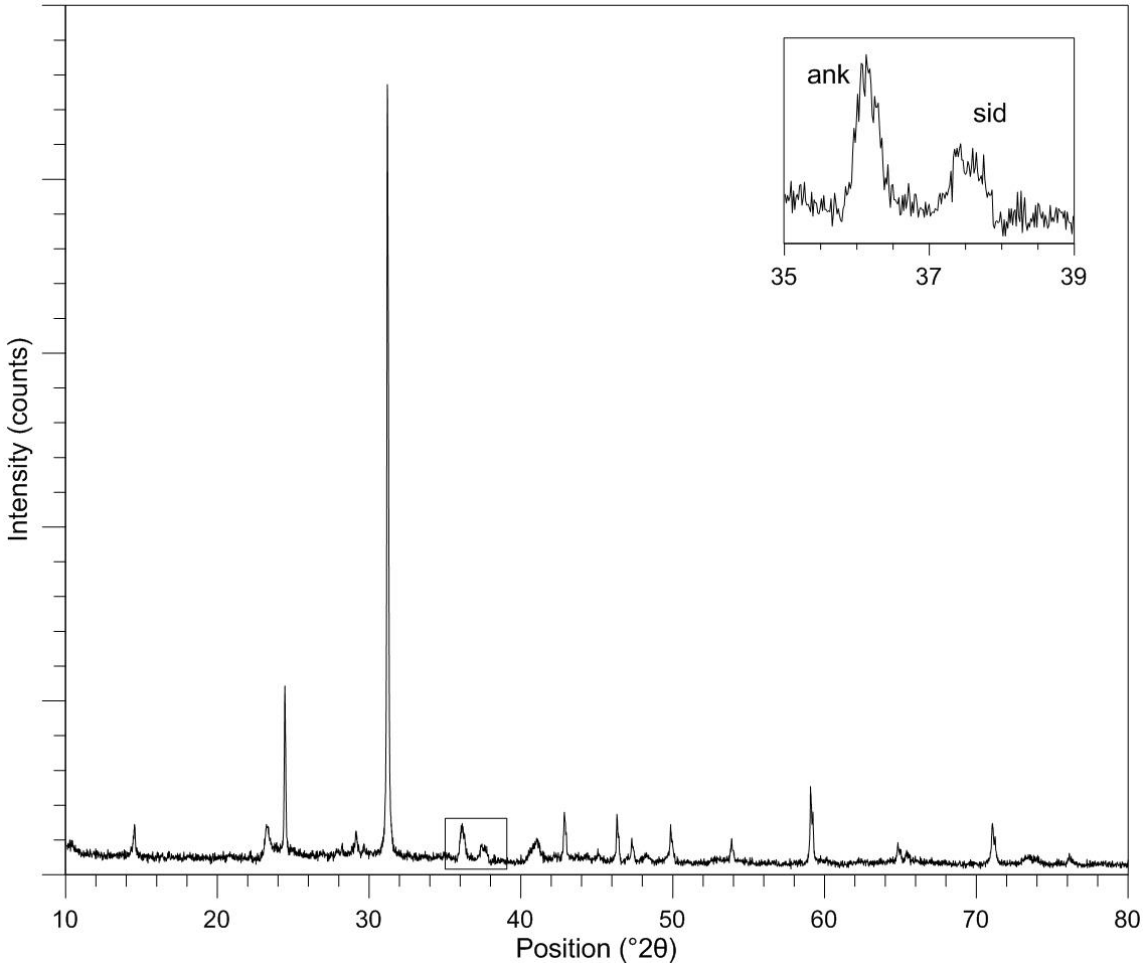

Figure A-1: XRD pattern (Co Kα) for solid waste rock sample.

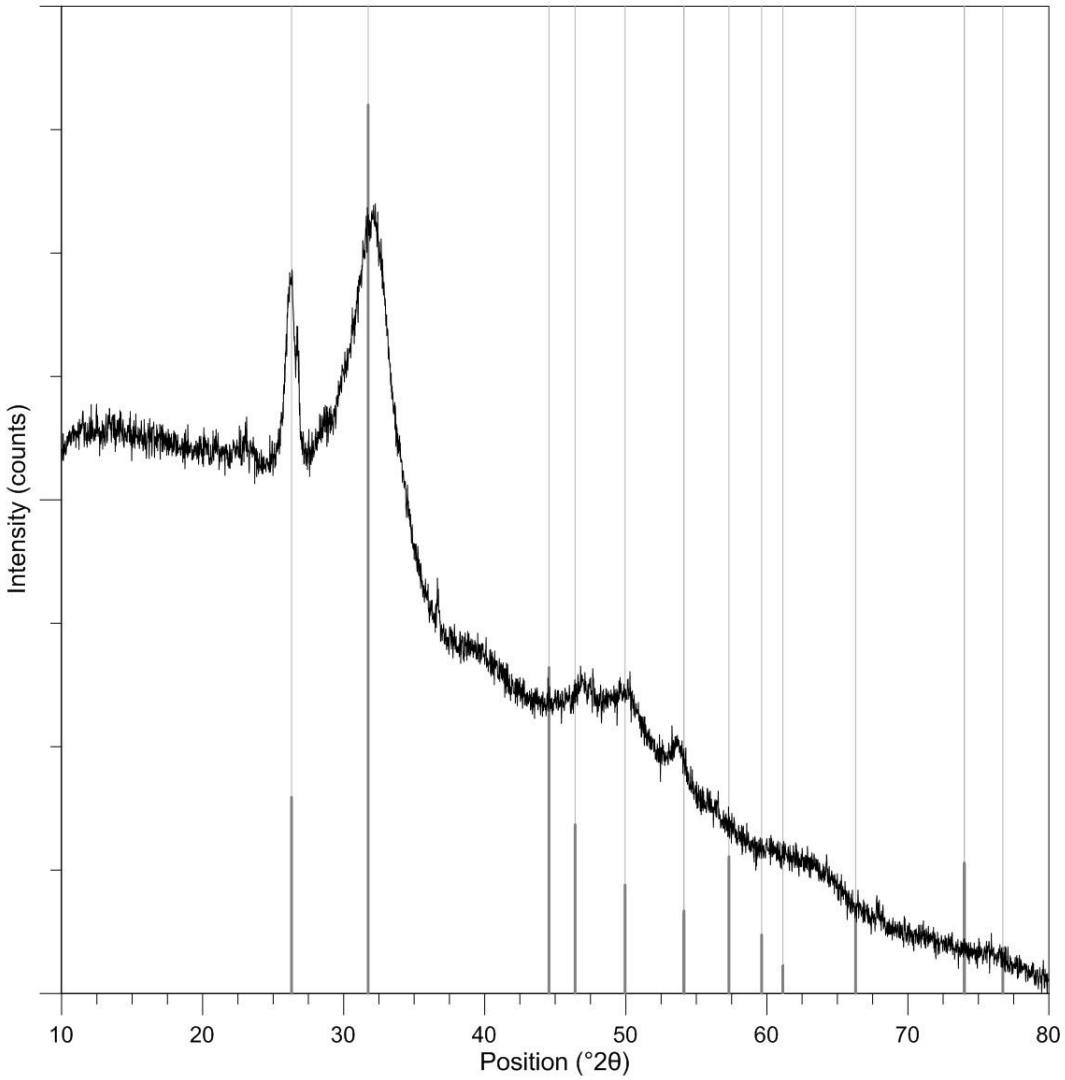

Figure A-2: XRD pattern (Cu Kα) for red precipitate isolated from broth media. The grey stick pattern is the Se(0) diffraction pattern measured by Keller et al. (1977).

Table A-1: Minerals Present in the waste rock sample as measured by XRD.

Mineral	**Concentration (% by mass)**
Clinichlore	35
Illite	35
Quartz	23
Ankerite	5
Siderite	1
Montmorillinite	1

Electron Microprobe Wavelength Dispersive Spectroscopy

Electron Microprobe Wavelength Dispersive Spectroscopy (WDS) was conducted on the waste rock sample to determine the elements present in carbonate minerals siderite and ankerite using JEOL 8600 Superprobe electron microprobe analyzer. Samples were polished to 0.3 µm and coated with 0.02 µm carbon prior to WDS. The detection limit for Se is approximately 100 mg/kg. The results are presented in Table A-2.

Table A-2: Cation weight percent and ratio in ankerite and siderite in waste rock sample as measured by WDS.

Mineral phase	No. of point analyses	Element	Weight Percent					Mean Cation Ratio
			Min	Max	Median	Mean	Std. Dev.	
Siderite	26	Ca	0.087	3.870	1.217	1.400	0.903	0.031
		Mg	0.072	8.160	3.550	3.934	2.787	0.087
		Fe	29.510	54.830	36.955	39.258	7.131	0.869
		Mn	0.118	2.626	0.543	0.600	0.508	0.013
		Zn	0	1.456	0.029	0.122	0.306	0.003
Ankerite	23	Ca	13.250	25.800	21.720	21.590	2.705	1.105
		Mg	4.460	11.670	9.090	8.940	1.594	0.458
		Fe	5.620	10.750	8.650	8.386	1.292	0.429
		Mn	0.045	0.249	0.168	0.155	0.063	0.008
		Zn	0	0.057	0	0.009	0.016	0.000

Confirmation of mineral stability during sterilization

The solid waste rock sample was sterilized by a combination of 30 kGy $^{60}C0$ gamma irradiation and two cycles of autoclaving (30 m, dry, 121°C, 120 kPa) 24 h apart. The solids were kept in sealed bottles during autoclaving to minimize oxidation of the reduced minerals of interest, namely pyrite, siderite, and sphalerite. To address this concern, pure-phase minerals were ground and sterilized by the same processes and characterized to confirm that they were not oxidized. Details of the minerals are presented in Table A-3. The minerals were characterized by XRD (Figure A-3) and Raman Spectroscopy (Figure A-4). Raman Spectroscopy was conducted at 50x magnification using excitation wavelengths of 514 nm for pyrite and sphalerite and 785 nm for siderite. Nearly

all major peaks in the XRD patterns and Raman spectra between the initial and sterilized solids match up, providing confidence that reduced minerals were not oxidized.

Table A-3: Minerals characterized before and after sterilization procedures.

Sample/Mineral	Ideal Formula	BET surface area (m^2/g)	Source
Siderite	$FeCO_3$	0.52	Ward's Science - Mt. St. Hilaire, Quebec
Pyrite	FeS_2	0.35	Sigma Aldrich - synthetic
Sphalerite	ZnS	0.13	University of Saskatchewan Minerals Collection - Specimen no. 2621-N2

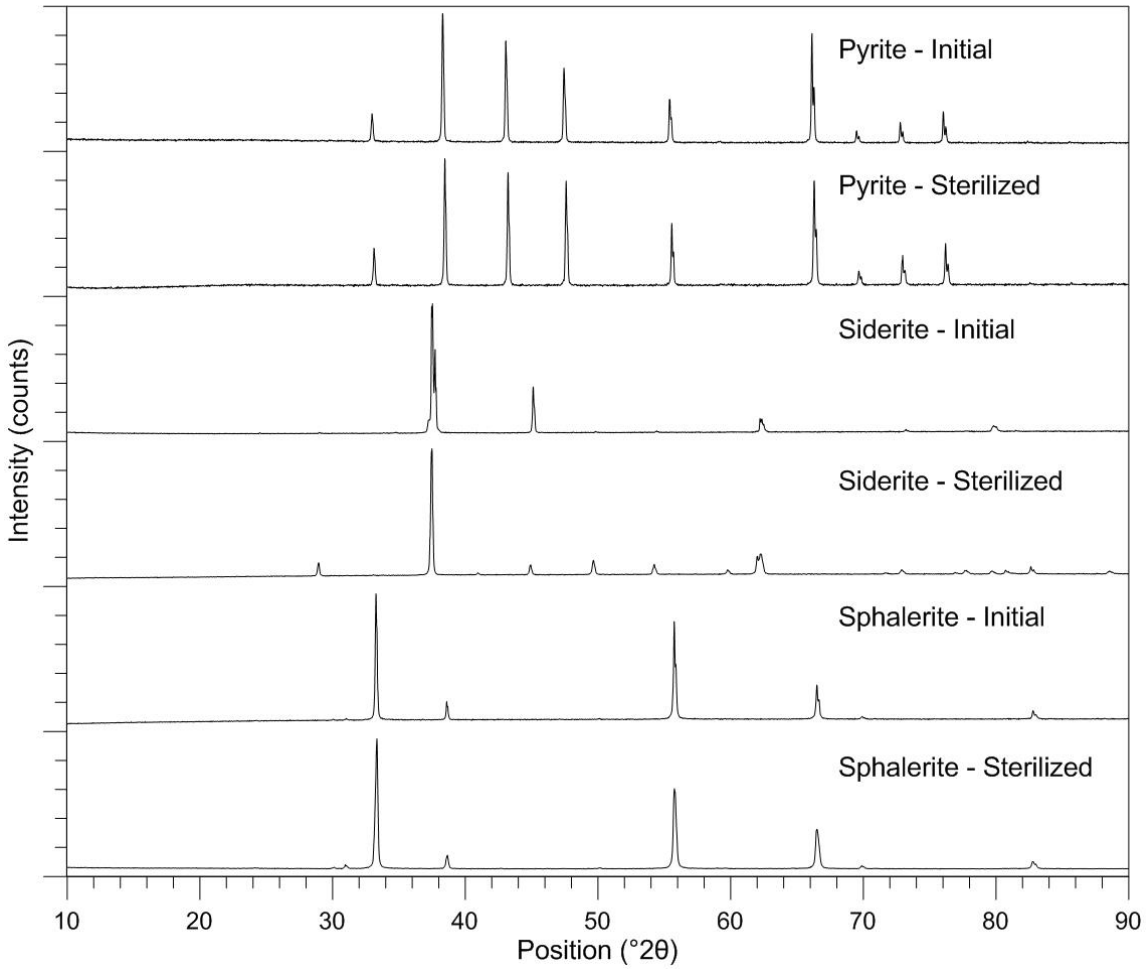

Figure A-3: XRD patterns (Co Kα) for initial and sterilized minerals.

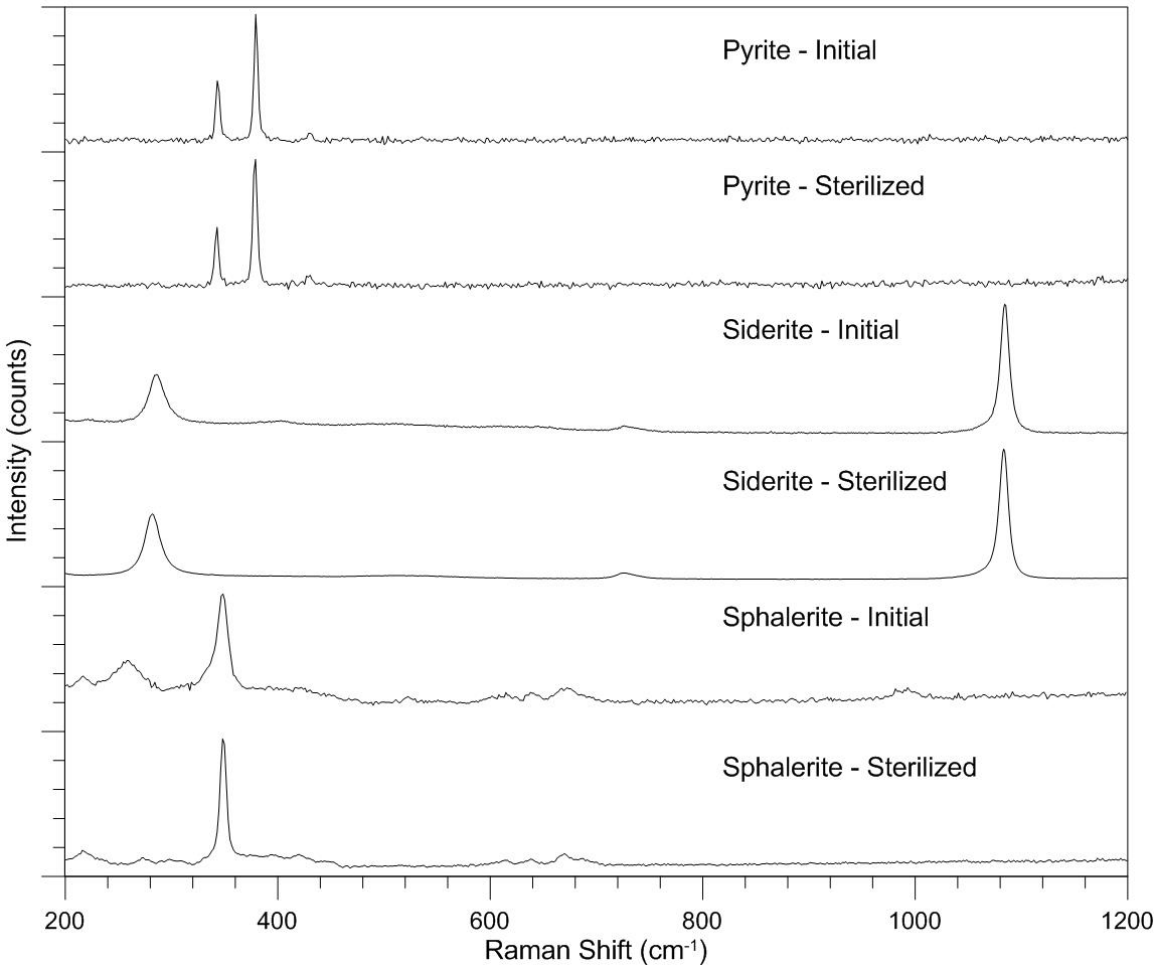

Figure A-4: Raman spectra for initial and sterilized minerals.

Discussion sample specific surface area

The siderite sample tested in this study had a specific surface area of 0.34 m^2/g, which corresponds to a mean particle size of ~3 μm (assuming a density of 3.9 g/cm^3). This is consistent with the siderite samples tested by Badaut et al. (2012) and Scheinost et al. (2008), which had mean particle sizes of 1 to 10 μm and 3 μm, respectively.

The specific surface area of pyrite samples tested in batch tests similar those in this study ranged from 0.03 to 15.9 m^2/g (Breynaert et al. 2008; Bruggeman et al., 2005; Curti et al., 2013; Han et al., 2012; Kang et al., 2011; Naveau et al., 2007). The pyrite sample tested in this study had a specific surface area of 0.52 m^2/g, which fits well within the bounds of this range.

Much less research has been conducted using sphalerite as an adsorbent or reductant as compared to siderite and pyrite. Bostick et al. (2003) and Sun et al. (1991) conducted tests using synthetic and natural sphalerite samples with specific surface areas of 2.93 and 0.7 m^2/g, respectively. The specific surface area of the natural sphalerite sample used in this study was 0.13 m^2/g, which is lower than both of these samples but is within one order of magnitude of the other natural sample.

References

Badaut, V., Schlegel, M.L., Descostes, M., Moutiers, G., 2012. In situ time-resolved X-ray near-edge absorption spectroscopy of selenite reduction by siderite. Environmental Science and Technology 46, 10820–10826.

Bostick, B.C., Fendorf, S., Manning, B.A., 2003. Arsenite adsorption on galena (PbS) and sphalerite (ZnS). Geochimica et Cosmochimica Acta 67, 895–907.

Breynaert, E., Bruggeman, C., Maes, A., 2008. XANES-EXAFS analysis of se solid-phase reaction products formed upon contacting Se(IV) with FeS2 and FeS. Environmental Science & Technology 42, 3595–3601.

Bruggeman, C., Maes, A., Vancluysen, J., Vandemussele, P., 2005. Selenite reduction in Boom clay: Effect of FeS2, clay minerals and dissolved organic matter. Environmental Pollution 137, 209–221.

Curti, E., Aimoz, L., Kitamura, A., 2013. Selenium uptake onto natural pyrite. Journal of Radioanalytical and Nuclear Chemistry 295, 1655–1665.

Drits, V.A., McCarty, D.K., Sakharov, B., Milliken, K.L., 2005. New insight into structural and compositional variability in some ancient excess-Ca dolomite. Canadian Mineralogist 43, 1255–1290.

Han, D.S., Batchelor, B., Abdel-Wahab, A., 2012. Sorption of selenium(IV) and selenium(VI) onto synthetic pyrite (FeS2): spectroscopic and microscopic analyses. Journal of colloid and interface science 368, 496–504.

Kang, M., Chen, F., Wu, S., Yang, Y., Bruggeman, C., Charlet, L., 2011. Effect of pH on aqueous Se(IV) reduction by pyrite. Environmental Science & Technology 45, 2704–2710.

Keller, R., Holzapfel, W., Schulz, H., 1977. Effect of pressure on the atom positions in Se and Te. Keller, R., Holzapfel, W., Schulz, H., 1977.

Naveau, A., Monteil-Rivera, F., Guillon, E., Dumonceau, J., 2007. Interactions of aqueous selenium (-II) and (IV) with metallic sulfide surfaces. Environmental Science & Technology

41, 5376–5382.

Scheinost, A.C., Charlet, L., 2008. Selenite reduction by mackinawite, magnetite and siderite: XAS characterization of nanosized redox products. Environmental Science & Technology 42, 1984–1989.

Sherman, D., 2009. Electronic Structures of Siderite (FeCO3) and Rhodochrosite (MnCO3): Oxygen K-edge Spectroscopy and Hybrid Density Functional Theory. American Mineralogist 94, 2009.

Sun Z., Forsling W., Ronngren L. and Sjoberg S. (1991) Surface reactions in aqueous metal sulfide systems. 1. Fundamental surface reactions of hydrous PbS and ZnS. International Journal of Mineral Processing 33, 83–93.

Appendix B: Additional Figures and Tables for Chapter 4 Experiments

There are seven figures and two tables in Appendix B. They correspond to experiments conducted in support of the manuscript in Chapter 4 but could not be included in the manuscript due to word and space constraints. They are provided here for completeness.

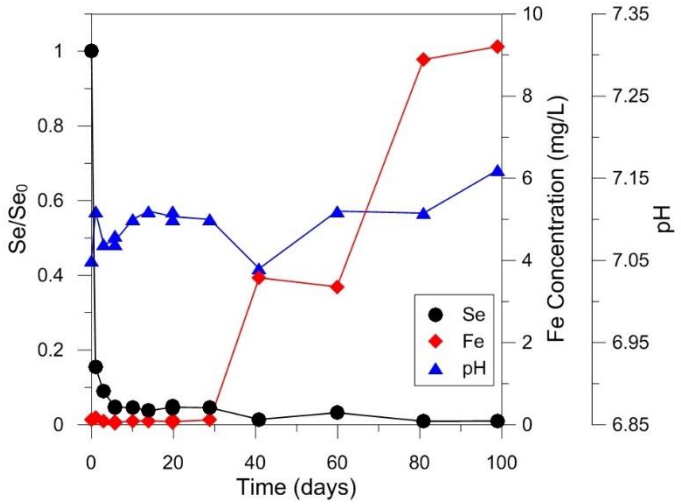

Figure B-1: Relative Se concentrations (black circles), Fe concentrations (red diamonds), and pH (blue triangles) in sterile batch testing using a 0.7 mg/L Se(IV) solution with siderite.

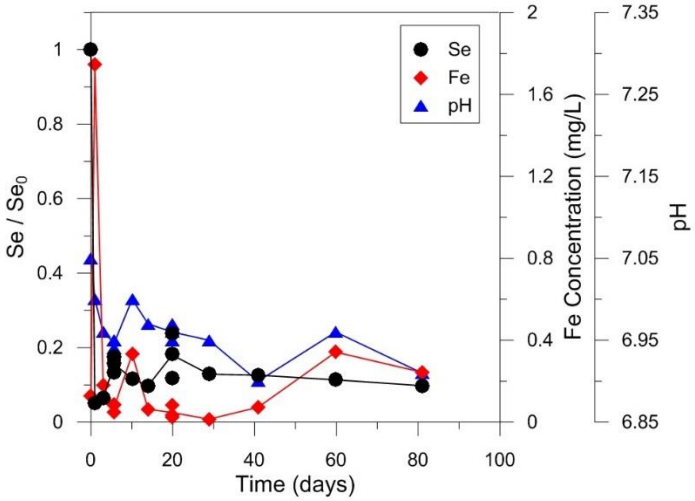

Figure B-2: Relative Se concentrations (black circles), Fe concentrations (red diamonds), and pH (blue triangles) in sterile batch testing using a 0.7 mg/L Se(IV) solution with pyrite.

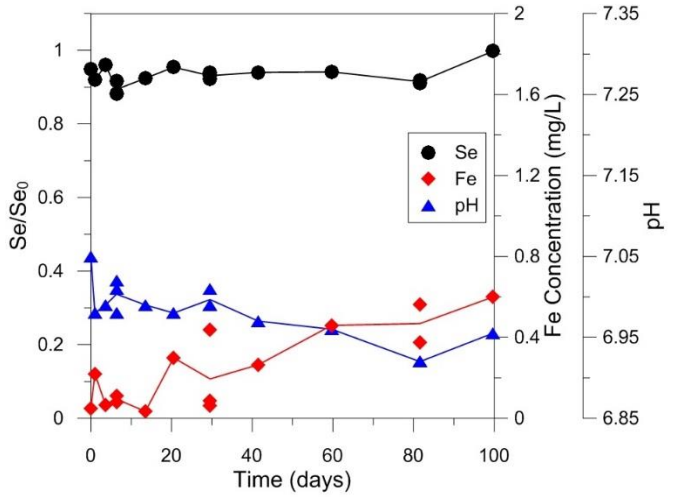

Figure B-3: Relative Se concentrations (black circles), Fe concentrations (red diamonds), and pH (blue triangles) in sterile batch testing using a 1.0 mg/L Se(VI) solution with pyrite.

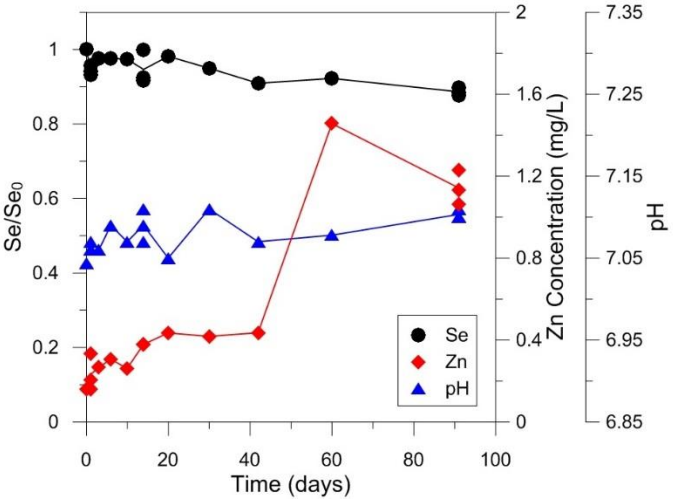

Figure B-4: Relative Se concentrations (black circles), Zn concentrations (red diamonds), and pH (blue triangles) in sterile batch testing using a 15 mg/L Se(IV) solution with sphalerite. The Zn concentrations on days 60 and 91 are believed to be erroneous as similar increases in concentration were noted in all samples (including pyrite and siderite batch test samples) measured on those days.

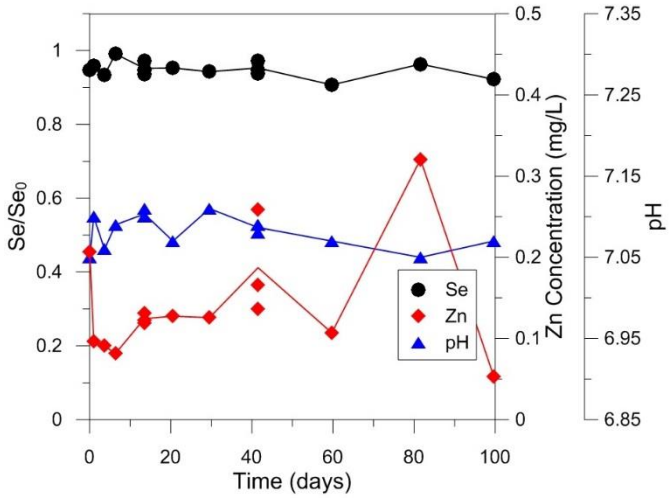

Figure B-5: Relative Se concentrations (black circles), Fe concentrations (red diamonds), and pH (blue triangles) in sterile batch testing using a 1.0 mg/L Se(VI) solution with sphalerite.

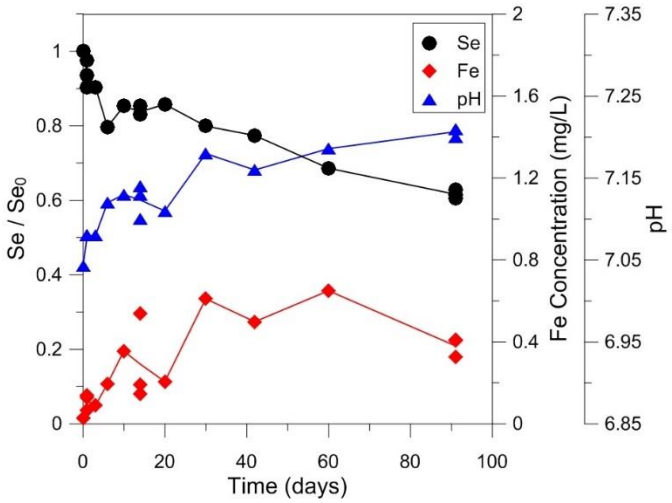

Figure B-6: Relative Se concentrations (black circles), Fe concentrations (red diamonds), and pH (blue triangles) in sterile batch testing using a 15 mg/L Se(IV) solution with waste rock.

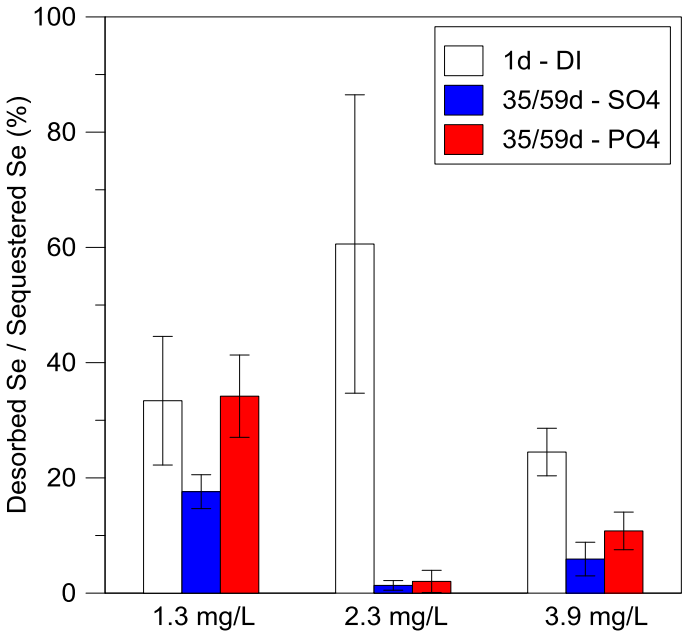

Figure B-7: Percentage of sequestered Se desorbed in desorption batch tests. Error bars represent one standard deviation (n = 3).

Table B-1: Results of HPLC-ICP-MS analyses.

Sample	ICP-MS	HPLC-ICP-MS		Fraction of Se as
	Total Se	Se(IV)	Se(VI)	Se(IV)
1.0 mg/L Se(VI)	0.98	0	0.95	0
Pyrite, day 4	0.96	0	0.94	0
Pyrite, day 21	0.95	0	0.93	0
Pyrite, day 100	0.99	0	0.91	0
Siderite, day 4	0.97	0	0.96	0
Siderite, day 21	0.90	0	0.96	0
Siderite, day 100	0.09	0	0.08	0
Siderite, day 100-2	0.09	0	0.05	0
Sphalerite, day 4	0.93	0	0.93	0
Sphalerite, day 21	0.95	0	0.95	0
Sphalerite, day 100	0.91	0	0.86	0
Waste rock, day 4	0.91	0	0.96	0
Waste rock, day 21	0.94	0	0.46	0
Waste rock, day 100	0.92	0	0.82	0
0.7 mg/L Se(IV)	0.69	0.71	0	1
Pyrite, day 3	0.04	0	0.05	0
Pyrite, day 20	0.08	0.01	0.07	0.10
Pyrite, day 20-2	0.13	0.04	0.08	0.34
Pyrite, day 81	0.06	0	0.09	0
Siderite, day 3	0.06	0.05	0.01	0.79
Siderite, day 20	0.03	0.00	0.02	0.11
Siderite, day 20-2	0.03	0.00	0.02	0.22
Siderite, day 81	0.01	0	0	-
Sphalerite, day 3	0.66	0.70	0	1
Sphalerite, day 20	0.57	0.44	0	1
Sphalerite, day 81	0.49	0.43	0	1
Waste rock, day 3	0.41	0.42	0.025	0.95
Waste rock, day 20	0.25	0.10	0.016	0.86
Waste rock, day 81	0.05	0.01	0.034	0.28

Table B-1: Results of HPLC-ICP-MS analyses.

Sample	ICP-MS	HPLC-ICP-MS		Fraction of Se as
	Total Se	Se(IV)	Se(VI)	Se(IV)
15 mg/L Se(IV)	14.65	6.63	0	1
Pyrite, day 3	0.01	0.00	0	-
Pyrite, day 3-2	0.01	0.00	0	-
Siderite, day 3	11.92	5.95	0	1
Siderite, day 3-2	11.76	5.30	0	1
Siderite, day 20	9.64	1.39	0	1
Siderite, day 20-2	9.57	1.87	0	1
Siderite, day 60	2.77	2.78	0	1
Siderite, day 60-2	2.20	0.97	0	1
Sphalerite, day 3	14.53	7.83	0	1
Sphalerite, day 20	14.61	2.16	0	1
Sphalerite, day 60	14.00	7.37	0	1
Sphalerite, day 60-2	13.66	6.35	0	1
Waste rock, day 3	13.46	6.14	0	1
Waste rock, day 20	12.77	2.13	0	1
Waste rock, day 60	11.36	5.93	0	1
Waste rock, day 60-2	9.93	4.19	0	1
1.3 mg/L Se(IV)	1.27	1.44	0	1
Waste rock, day 1	1.15	1.27	0	1
Waste rock, day 35	0.89	0.02	0	1
Waste rock, day 35-2	0.95	0.03	0	1
3.9 mg/L Se(IV)	3.84	2.05	0	1
Waste rock, day 59	2.54	0.79	0	1
Waste rock, day 59-2	2.13	1.57	0.07	0.96
2.3 mg/L Se(IV)	2.47	0.82	0	1
Waste rock, day 59	0.28	0.10	0.01	0.90
Waste rock, day 59-2	0.32	0.09	0	0.97
4.5 mg/L Se(IV)	4.50	5.07	0	1
Waste rock, day 1	4.16	4.28	0	1
2.3 mg/L Se(IV)	2.28	2.61	0	1
Waste rock, day 1	2.17	2.40	0	1
0.2 mg/L Se(IV)	0.20	0.23	0	1
Waste rock, day 1	0.19	0.21	0	1

Table B-1: Results of HPLC-ICP-MS analyses.

Sample	ICP-MS	HPLC-ICP-MS		Fraction of Se as
	Total Se	Se(IV)	Se(VI)	Se(IV)
DI + 1.3/1	0.05	1.32	0	1
SO4 + 1.3/35	0.12	0.91	0.03	0.97
PO4 + 1.3/35	0.13	0.00	0.00	1
DI + 3.9/1	0.14	0.14	0	1
DI + 3.9/1-2	0.14	0.14	0	1
SO4 + 3.9/59	0.12	0.11	0	1
SO4 + 3.9/59-2	0.12	0.09	0	1
PO4 + 3.9/59	0.16	0.09	0	1
PO4 + 3.9/59-2	0.22	0.14	0	1
DI + 2.3/1	0.09	0.11	0	1
DI + 2.3/1-2	0.14	0.14	0	1
SO4 + 2.3/59	0.05	0.02	0	1
SO4 + 2.3/59-2	0.03	0.01	0	1
PO4 + 2.3/59	0.01	0	0	-
PO4 + 2.3/59-2	0.07	0.06	0	1

Table B-2: Numerical results of desorption batch tests.

Sample	Age (d)	$Se(IV)_i$ (mg/L)	$Se(IV)_f$ (mg/L)	Solid Se (mg/kg)	Desorp. Sol.	Se Desorbed (mg/kg)	Fraction Desorbed[1]	Slope of Desorption Line (L/kg)
1.3/1-a	1	1.27	1.15	16.0	DI	4.8	0.30	4.3
1.3/1-b	1	1.27	1.11	20.9	DI	5.2	0.25	4.9
1.3/1-c	1	1.27	1.17	13.6	DI	6.2	0.46	5.6
1.3/35-a	35	1.27	0.89	50.3	SO4	9.1	0.18	11.4
1.3/35-b	35	1.27	0.97	39.3	SO4	8.0	0.20	9.0
1.3/35-c	35	1.27	0.96	41.5	SO4	6.0	0.14	6.8
1.3/35-d	35	1.27	1.00	35.2	PO4	13.2	0.38	14.8
1.3/35-e	35	1.27	0.99	36.5	PO4	14.2	0.39	16.3
1.3/35-f	35	1.27	0.91	47.5	PO4	12.3	0.26	15.3
2.3/1-a	1	2.33	2.22	13.7	DI	12.1	0.88	5.7
2.3/1-b	1	2.33	1.94	51.0	DI	18.8	0.37	10.5
2.3/1-c	1	2.33	2.02	40.6	DI	23.0	0.57	12.5
2.3/59-a	59	2.33	0.28	272.9	SO4	6.2	0.02	26.7
2.3/59-b	59	2.33	0.14	291.5	SO4	3.2	0.01	28.2
2.3/59-c	59	2.33	0.07	300.8	SO4	2.0	0.01	35.9
2.3/59-d	59	2.33	0.02	307.7	PO4	0.7	0.00	58.3
2.3/59-e	59	2.33	0.52	241.1	PO4	9.8	0.04	22.1
2.3/59-f	59	2.33	0.42	254.5	PO4	4.6	0.02	12.0
3.9/1-a	1	3.92	3.42	66.1	DI	18.8	0.29	5.7
3.9/1-b	1	3.92	3.34	77.9	DI	19.2	0.25	6.0
3.9/1-c	1	3.92	3.20	95.4	DI	19.3	0.20	6.3
3.9/59-a	59	3.92	2.54	184.3	SO4	15.5	0.08	6.4
3.9/59-b	59	3.92	2.12	239.8	SO4	15.8	0.07	7.9
3.9/59-c	59	3.92	0.94	397.9	SO4	10.8	0.03	12.6
3.9/59-d	59	3.92	2.11	240.7	PO4	21.5	0.09	11.0
3.9/59-e	59	3.92	2.44	197.1	PO4	28.7	0.15	12.9
3.9/59-f	59	3.92	2.08	245.6	PO4	21.9	0.09	11.4

[1] Presented in Figure B-7